

Construction of cucurbit[*n*]uril-based supramolecular frameworks *via* host-guest inclusion and functional properties thereof

Kai Chen^{*a}, Zi-Yi Hua^a, Jiang-Lin Zhao^{*c}, Carl Redshaw^d, and Zhu Tao^{*b}

^a Collaborative Innovation Center of Atmospheric Environment and Equipment Technology, Jiangsu Key Laboratory of Atmospheric Environment Monitoring and Pollution Control, School of Environmental Science and Engineering, Nanjing University of Information Science & Technology, 210044, Nanjing, China. E-mail: kaichen85@nuist.edu.cn

^b Key Laboratory of Macrocyclic and Supramolecular Chemistry of Guizhou Province, Guizhou University, 550025, Guiyang, China. E-mail: gzutao@263.net

^c Center for Precision Medicine, Zhuhai Institute of Advanced Technology, Chinese Academy of Sciences, Zhuhai 519080, Guangdong, China. E-mail: zhaojianglin1314@163.com

^d Plastics Collaboratory, Department of Chemistry, University of Hull, Hull HU6 7RX, UK.

Abstract

Frameworks utilizing cucurbit[*n*]uril-based chemistry build on the rapid developments in the fields of metal-organic frameworks (MOFs), covalent-organic frameworks (COFs) and supramolecular organic frameworks (SOFs), and as porous materials have found broad applications in heterogeneous catalysis, adsorption and ion exchange as well as other fields. Cucurbit[*n*]urils (Q[*n*]s) are suitable as the basic building blocks used for the construction of new Q[*n*]-based frameworks due to their special structural characteristics including the positive electrostatic potential of the outer surface, the negative portal carbonyl groups and the near neutral potential of the cavity. Herein, summaries of cucurbit[*n*]uril-based supramolecular frameworks assembled through outer surface interactions and cucurbit[*n*]uril/metal ion complex-based frameworks are discussed, and this is followed by a review of Q[*n*]-based frameworks assembled using the structural characteristics associated with the cavity of Q[*n*]s, *i.e.* host-guest inclusion chemistry. These assembled Q[*n*]-based frameworks can be catalogued as 1) simple host-guest inclusion complexes, 2) host-guest inclusion supramolecular polymers, 3) host-guest exclusion complexes or polymers and 4) coordination products of the host-guest inclusion complexes with metal ions. The design and construction of Q[*n*]-based frameworks

via host–guest inclusion chemistry will undoubtedly enrich this new research direction in Q[*n*] chemistry, and will lead to multiple new applications.

Keywords: cucurbit[*n*]uril, host-guest inclusion, Q[*n*]-based frameworks, outer surface interactions

Contents

1. Introduction

2. Q[n]-based supramolecular organic frameworks constructed through host-guest inclusion complexes

2.1 Q[n]-based supramolecular organic frameworks constructed by simple host-guest inclusion complexes

2.2 Q[n]-based supramolecular organic frameworks constructed by host-guest inclusion supramolecular polymers

2.3 Q[n]-based supramolecular organic frameworks constructed by host-guest exclusion complexes

2.4 Q[n]-based frameworks constructed by coordination of host-guest inclusion complexes with metal ions

2.4.1 Q[n]-based frameworks constructed by 1D guest@Q[n]/Mⁿ⁺polyrotaxanes

2.4.2 Q[n]-based frameworks constructed by 2D guest@Q[n]/Mⁿ⁺polyrotaxanes

2.4.3 Q[n]-based frameworks constructed by 3D guest@Q[n]/Mⁿ⁺polyrotaxanes

3 Potential applications of guest@Q[n]-based frameworks

3.1 Adsorption characteristics

3.1.1 Exchange

3.1.2 Selective adsorption and release

3.1.3 Sensor

3.2 Catalysis

3.3 Bioapplications

4 Conclusion

1. Introduction

Supramolecular frameworks are found in many fields, including zeolites,^[1-7] coordination networks,^[8,9] metal-organic frameworks (MOFs)^[10-17] and coordination polymers,^[18-22] organic frameworks, including covalent-organic frameworks (COFs)^[23-26] and porous organic polymers,^[27-31] as well as some supramolecular polymers.^[32-37] In general, metal ions interact

with ligands to form simple complexes rather than MOF type systems, however, some of these simple complexes can be further assembled via supramolecular interactions to form supramolecular coordination frameworks.^[38-40] On the other hand, different organic molecules interact with each other via supramolecular interactions, such as interlocked and host–guest interactions, to form supramolecular organic frameworks (SOFs).^[32-34,41,42]

To construct these inorganic, organic or supramolecular frameworks, it is important to select the appropriate building blocks, which can be used to construct various frameworks with periodicity and porous characteristics via coordination, covalent and supramolecular interactions. These frameworks present different functions and have been applied in areas such as adsorption, absorption, release, delivery, identification, sensing and catalysis.^[43-56]

For two decades, our group has been exploring cucurbit[*n*]urils (Q[*n*]s), a kind of macrocyclic compound formed by *n* glycolurils linked through 2*n* methylene units.^[57] Based on an in-depth understanding of the three structural characteristics of Q[*n*]s, namely, the neutral cavity, the negative electrostatic potential carbonyl portals and the positive electrostatic potential of the outer surface, as well as an increased understanding of these interactions in Q[*n*]-based host–guest chemistry,^[58-65] Q[*n*]-based coordination chemistry^[66-69] and Q[*n*]-based outer surface interaction chemistry (please refer to the calculation results of electrostatic potential on the surface of the representative Q[6] in the middle column of [Figure 1](#)),^[70,71] respectively, we believe that Q[*n*]s are ideal as basic building blocks for the construction of Q[*n*]-based frameworks. Firstly, Q[*n*]s possesses a rigid structure, which can easily form periodic multi-channel frameworks. Secondly, there are various kinds of Q[*n*]s, including Q[*n*]s of different sizes (Q[4]-Q[15]),^[72-79] different (alkyl)-substituted Q[*n*]s^[80-92] and various Q[*n*]-analogues.^[93-96] These different kinds of Q[*n*]s can be constructed to form various Q[*n*]-based frameworks. Thirdly, the three intrinsic structural properties of Q[*n*]s described above,^[70,71] allow Q[*n*]s to be used to construct a variety of Q[*n*]-based frameworks. These include various Q[*n*]-based supramolecular frameworks (QSFs) formed by virtue of the electrostatic

interactions of the outer surface of Q[n]s or the outer surface interactions of Q[n]s (OSIQ, Figure 1a-1d),^[70,71] and various Q[n]-based coordination frameworks by virtue of the interactions formed between the negative electrostatic potential of the carbonyl oxygen atoms of Q[n]s and various metal cations and positively charged species.^[66-69] In addition, various Q[n]-based SOFs are formed by virtue of the Q[n] cavity and inclusion of various guest molecules, *i.e.* Q[n]-based host-guest inclusion.^[58-65] We have recently comprehensively summarized Q[n]-based supramolecular frameworks driven by OSIQ^[70,71], Q[n]-based coordination frameworks driven by the coordination of Q[n]s to metal ions,^[97] and the interaction of Q[n]s with guest molecules, respectively. Thus, we have summarized the Q[n]-based frameworks related to two of the three structural characteristics of Q[n]s: the positive electrostatic potential of the outer surface and the negative electrostatic potential of two-carbonyl portals.

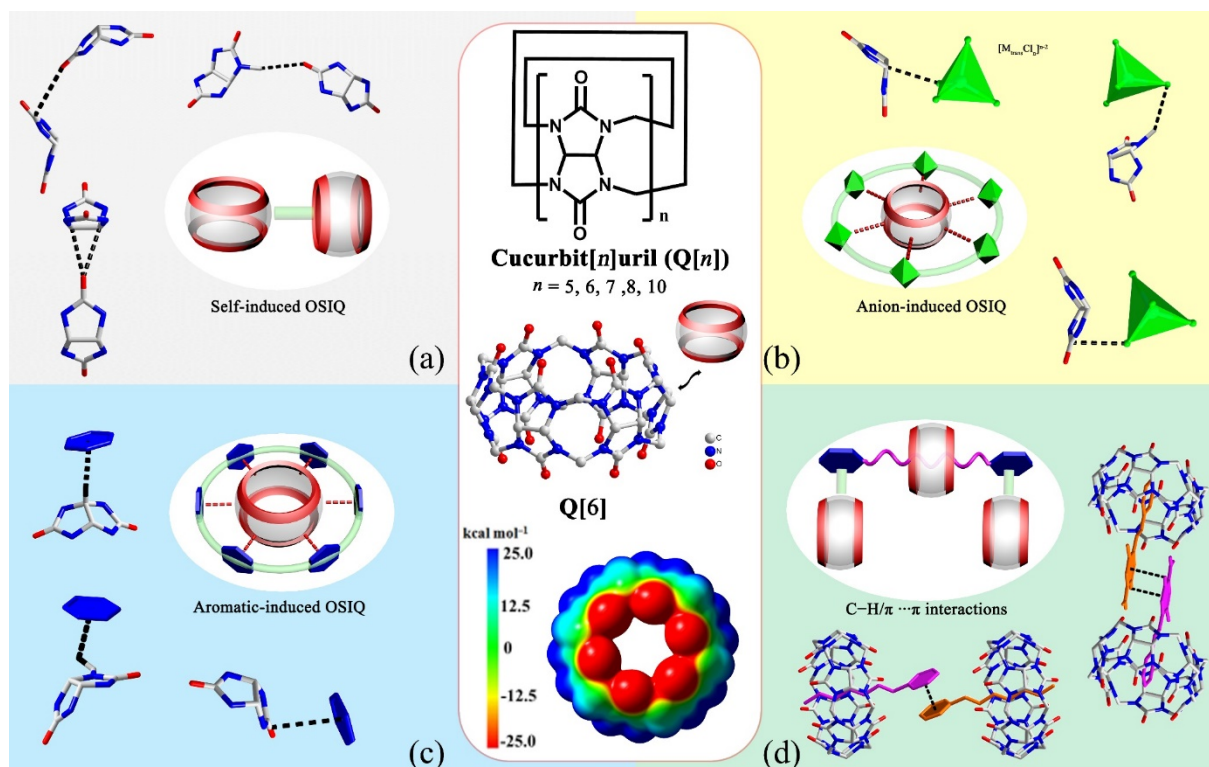


Figure 1. (middle column) The structures of Q[n]s and electrostatic potential map (ESP) obtained for a representative Q[6]. The ESP is mapped on the electron density isosurfaces (0.001 e/au³) of the cucurbit[n]urils at the B3LYP/6-311G (d, p) level of theory using Gaussian09 software. The representative (a) self-induced OSIQs; (b) anion-induced OSIQs; (c) aromatic-induced OSIQs; (d) $\pi \cdots \pi$ stacking and C-H \cdots π interactions.

Since 2013, Li *et al.* have reported a number of novel two-dimensional (2D) and three-dimensional (3D) water soluble supramolecular frameworks based on the interaction of Q[8] with special guest molecules.^[98-108] The driving force is derived from host–guest inclusion, typically supramolecular interactions, and so these Q[*n*]-based frameworks are classed as supramolecular organic frameworks (SOFs). Initially, we thought that these Q[*n*]-based SOFs were restricted to Q[8] and a number of very special guest molecules, and that the scope of this area may be relatively narrow, despite the elegant structures adopted and novel properties. Therefore, we intended to incorporate these findings into our summary of the Q[*n*]-based supramolecular frameworks driven by OSIQ. However, when we started to summarize the relevant literature, we were somewhat surprised to find that reports describing Q[*n*]-based supramolecular frameworks driven by host–guest interactions were comparable in number to those driven by OSIQ or coordination chemistry. As a consequence, summarizing Q[*n*]-based frameworks driven by Q[*n*]-based host–guest interactions is a meaningful exercise that will inform and impact upon other areas.

It should be noted that, as with the other two types of Q[*n*]-base frameworks, the formation of these frameworks can often be accompanied by other auxiliary driving forces, namely the OSIQs and coordination interactions. Therefore, we will discuss such systems with this in mind.

2. Q[*n*]-based supramolecular organic frameworks constructed through host-guest inclusion complexes

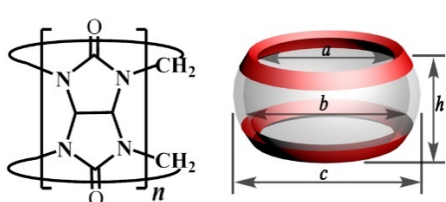
As mentioned above, research on Q[*n*]s can be divided into Q[*n*]-based host-guest chemistry,^[58-65] Q[*n*]-based coordination chemistry,^[66-69] and Q[*n*]-based outer surface interaction chemistry^[70,71] according to the three structural characteristics of Q[*n*]s, that is, the neutral electrostatic potential cavity, the negative electrostatic potential two carbonyl portals and the positive electrostatic potential outer surface, respectively. However, the investigation of Q[*n*]-based frameworks has closely linked these three seemingly independent characteristics.

Previous reviews have summarized work on Q[n]-based frameworks driven by the OSIQ^[71] and those constructed by Q[n]-Mⁿ⁺-based complexes,^[97] respectively. Herein, we will focus on studies on Q[n]-based frameworks, which are primarily driven by host-guest inclusion chemistry and are supplemented by other forms of interactions, such as the OSIQs, coordination and other supramolecular interactions.

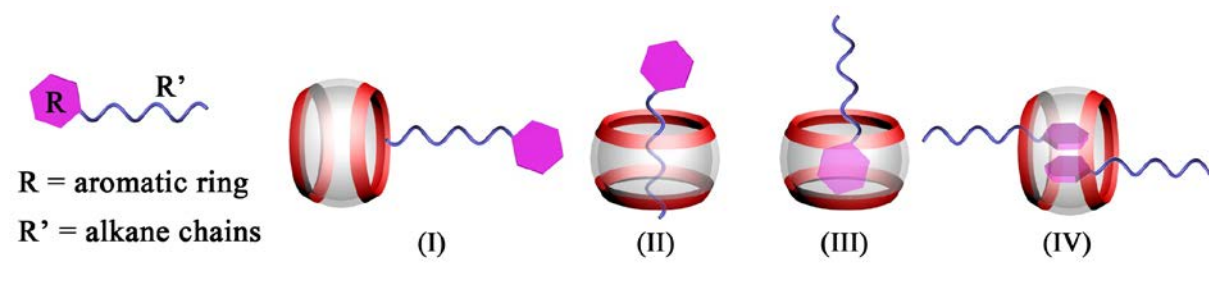
Among the three structural characteristics of Q[n]s, host-guest inclusion chemistry related to the cavity has generated the most interest and has become a central theme of Q[n]-chemistry^[58-65]. For Q[n]-based frameworks driven by host-guest inclusion, not only are host-guest inclusion or exclusion complexes required, but also such complexes must further assemble into frameworks. According to the type of host-guest complexes used, the construction of Q[n]-based frameworks can be catalogued as follows: (1) simple host-guest inclusion complexes; (2) host-guest inclusion supramolecular polymers; (3) host-guest exclusion complexes or polymers and (4) coordination products of the host-guest inclusion complexes with metal ions.

According to the Q[n]'s cavity size, the smallest cucurbituril, namely Q[5], can only bind the guest at the portals of the Q[5] forming so-called exclusion compounds; Q[6] can encapsulate an aliphatic chain in the cavity; the larger cavity of Q[7] or Q[8] can bind bulkier groups other than simple aliphatic chains, such as phenyl, naphthyl and larger aromatic rings, thus allowing for the formation of host-guest inclusion complexes^[76] (Table 1).

Table 1. Structural Parameters for uncomplexed Q[5] - Q[8] and Q[n] host-guest inclusion and exclusion complexes.^[76]

	Q[n]	Q[5]	Q[6]	Q[7]	Q[8]
	$a/\text{\AA}$	2.4	3.9	5.4	6.9
	$b/\text{\AA}$	4.4	5.8	7.3	8.8
	$c/\text{\AA}$	13.4	14.4	16.0	17.5
	$h/\text{\AA}$	2.9	2.9	2.9	2.9
	cavity volume V/ \AA^3	82	164	279	479
	guest@Q[n]	I	II	II, III, VI	

host- guest inclusion or exclusion compounds	The type of guest	-	R=phenyl.	R = phenyl; naphthyl; or larger moieties.
--	-------------------	---	-----------	---



2.1. Q[n]-based supramolecular organic frameworks constructed by simple host-guest inclusion complexes

In 2010, we investigated the host–guest interactions of a symmetrical $\alpha,\alpha',\delta,\delta'$ -tetramethylcucurbit[6]uril (TMeQ[6]) with the hydrochloride salts of three isomers: *N,N'*-bis(4-pyridylmethyl)-1,6-hexanediamine (C6N4), *N,N'*-bis(3-pyridyl-methyl)-1,6-hexanediamine (C6N3), and *N,N'*-bis(2-pyridylmethyl)-1,6-hexanediamine (C6N2) (Figure 2a). The experimental results revealed that the cavity of the TMeQ[6] preferred to include the hexyl moiety of C6N4 or C6N3 and form equilibrium pseudorotaxane shaped inclusion complexes C6N4@TMeQ[6] and C6N3@TMeQ[6], as shown in Figure 2b and c), while the two pyridylmethyl moieties of C6N2 form an equilibrium dumbbell shaped inclusion complex C6N2@TMeQ[6], as shown in Figure 2d.^[109] When reviewing the crystal structures assembled by these three TMeQ[6]-based host-guest inclusion complexes, it was interesting to find that they all had frameworks with different channels and holes (Figures 2h-j). Considering that all the components are organic, these frameworks can be classified as SOFs. How did the TMeQ[6]-based host–guest inclusion complexes construct these SOFs? What are the driving forces that result in the formation of such SOFs? Figures 2e-g show the detailed interactions for the C6N4@TMeQ[6], C6N3@TMeQ[6] and C6N2@TMeQ[6] inclusion complexes in the

three frameworks, respectively. For C₆N₄@TMeQ[6], the protruding pyridyl moieties of the C₆N₄@TMeQ[6] inclusion complex interact with the protruding pyridyl moieties of adjacent C₆N₄@TMeQ[6] inclusion complexes via $\pi\cdots\pi$ stacking. Moreover, typical OSIQs or dipole interactions can be observed between two adjacent TMeQ[6] molecules. These include electrostatic negative potential portal carbonyl oxygens of a TMeQ[6] molecule interacting with the electrostatic positive potential outer surface of adjacent TMeQ[6] molecules. Other interactions involve the portal carbonyl oxygen atoms of the TMeQ[6] molecule and methine units, bridged methylene units, and the portal carbonyl carbon atoms of adjacent TMeQ[6] molecules. In order to distinguish from the other type of OSIQs, the dipole interaction occurring in the adjacent Q[*n*] molecules was defined as a self-induced OSIQ. [Figure 1a](#) shows the representative self-induced OSIQs that exist between the adjacent Q[*n*] molecules, which basically involve dipole interactions.

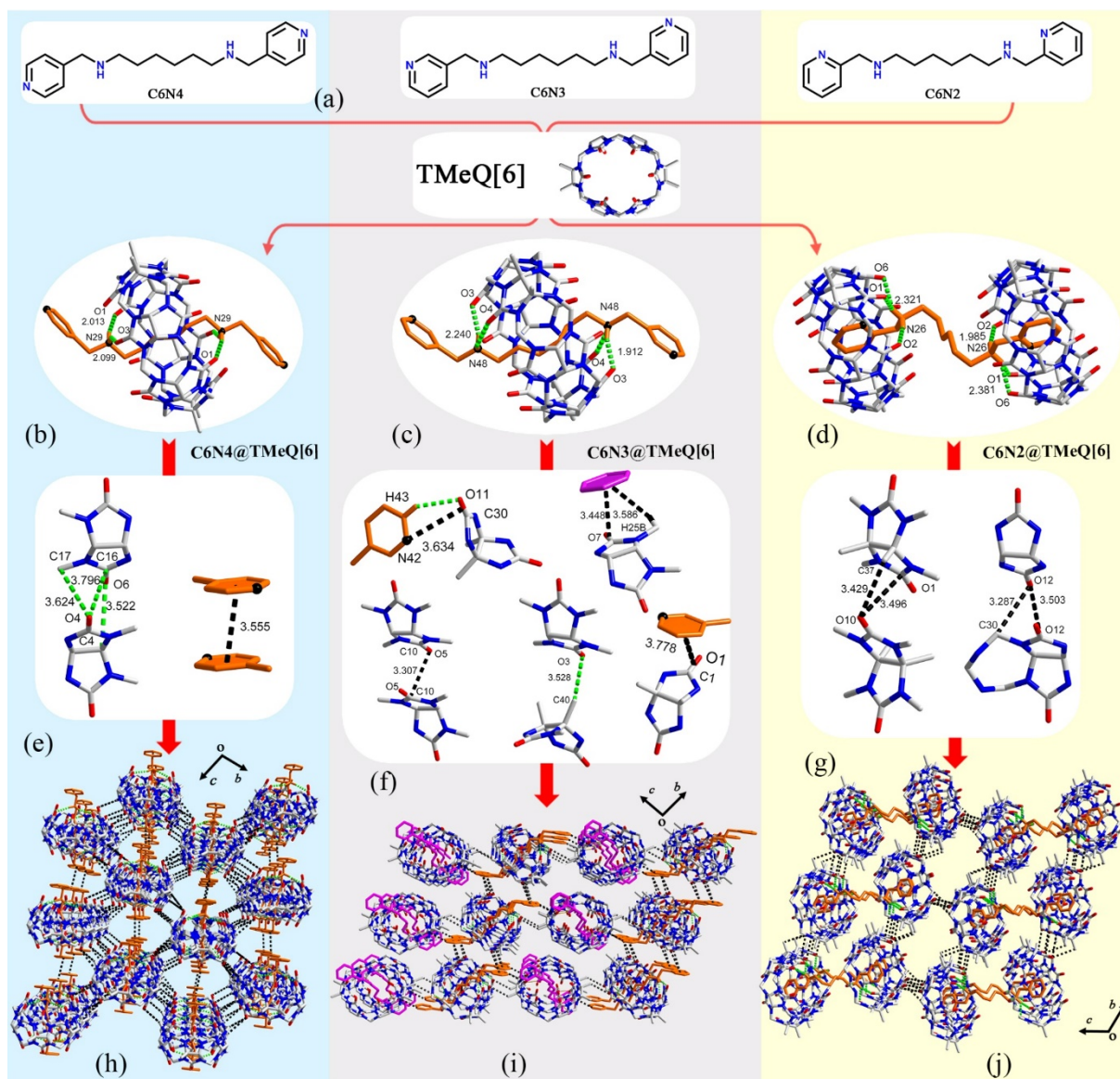


Figure 2. The structures of (a) C6N4, C6N3 and C6N2; (b-d) the inclusion complexes of C6N4@TMeQ[6], C6N3@TMeQ[6] and C6N2@TMeQ[6]; (e-g) detailed supramolecular interactions formed among the neighboring inclusion complexes of C6N4@TMeQ[6], C6N3@TMeQ[6] and C6N2@TMeQ[6], respectively; (h-j) frameworks constructed by the inclusion complexes of C6N4@TMeQ[6], C6N3@TMeQ[6] and C6N2@TMeQ[6], respectively.

For C6N3@TMeQ[6], the protruding pyridyl moieties of the C6N3@TMeQ[6] inclusion complex interact with the outer surface of adjacent TMeQ[6] molecules via π interactions formed between the pyridyl moieties with portal carbonyl units. There are also C-H \cdots π interactions formed between the pyridyl moieties with the waist methine, bridged methylene and substituted methyl units, which are defined as aromatic-induced OSIQ first proposed by Chen and coworkers in 2004^[110] (Figure 2f). Figure 1c shows the representative aromatic-

induced OSIQs that exist between the aromatic moiety and the outer surface of the adjacent Q[n] molecules. Besides aromatic-induced OSIQs, self-induced OSIQs exist among the adjacent TMeQ[6] molecules in this SOF (Figure 2f).

For C₆N₂@TMeQ[6], the two pyridyl moieties of a C₆N₂ are included by two TMeQ[6] molecules, respectively, resulting in the formation of a dumbbell-like inclusion complex (Figure 2d). In the framework constructed by the dumbbell-like inclusion complexes, the self-induced OSIQ can be observed between any two adjacent TMeQ[6] molecules. Also present are dipole interactions formed between the portal carbonyl oxygen atoms of the TMeQ[6] molecule and the substituted methyl, bridged methylene and portal carbonyl carbon atoms of adjacent TMeQ[6] molecules. It should be noted that generally, there are a large number of water and protoned water molecules in Q[n]-based supramolecular frameworks, which interact with the portal carbonyl oxygen atoms via hydrogen bonding and can form a hydrogen bonded network. This can act as an auxiliary interaction during the formation of these Q[n]-based frameworks and supramolecular assemblies.

We have described three TMeQ[6]-based inclusion complexes prepared using three isomers (C₆N₄, C₆N₃ and C₆N₂) and their coresponding SOFs constructed from the C₆N₄@TMeQ[6], C₆N₃@TMeQ[6] and C₆N₂@TMeQ[6], respectively. Moreover, we have introduced two kinds of OSIQ, abbreviated as self-induced and aromatic-induced OSIQs, which are derived from adjacent Q[n] molecules and aromatic moieties, respectively. We will use this terminology to describe the examples that follow.

In 2012, Ramamurthy *et al.* utilized a cucurbit[8]uril (Q[8]) template effect to stereoselectively synthesize an organic olefin photodimer.^[111] The symmetry of the butadiene monomers influences the relative arrangement of the monomers in the Q[8]-based host-guest inclusion complexes leading to the observed product selectivity. However, on analysis of the crystal structure of the inclusion complex of Q[8] and a butadiene monomer, 4Bpbd·2HCl (Figures 3a, b), it is evident that a chain made up of the 4Bpbd·2HCl@Q[8] complexes via $\pi\cdots\pi$

stacking between the two pyridyl moieties of two adjacent 4Bpbd·2HCl guest molecules is present (Figure 3c). Also, hydrogen bonding interactions form between the protonated pyridyl nitrogen and portal carbonyl oxygen atoms. A SOF was formed and furthermore, a 3D SOF was constructed from the one-dimensional (1D) supramolecular chains (Figure 3d). What driving forces made the 4Bpbd·2HCl@Q[8]-based supramolecular chains pile up? One can see each supramolecular chain is surrounded by four identical supramolecular chains (Figure 3d). In order to understand the interaction or the driving forces between the central supramolecular chain and the four surrounding supramolecular chains, we more closely investigated these interactions (Figure 3e). Close inspection revealed that the interaction between the central Q[8] molecule and the four surrounding Q[8] molecules belongs to self-induced OSIQ. This includes dipole interactions formed between the portal carbonyl oxygen atoms of the Q[8] molecule and the bridged methylene units and portal carbonyl carbon atoms of the adjacent Q[8] molecules, respectively.

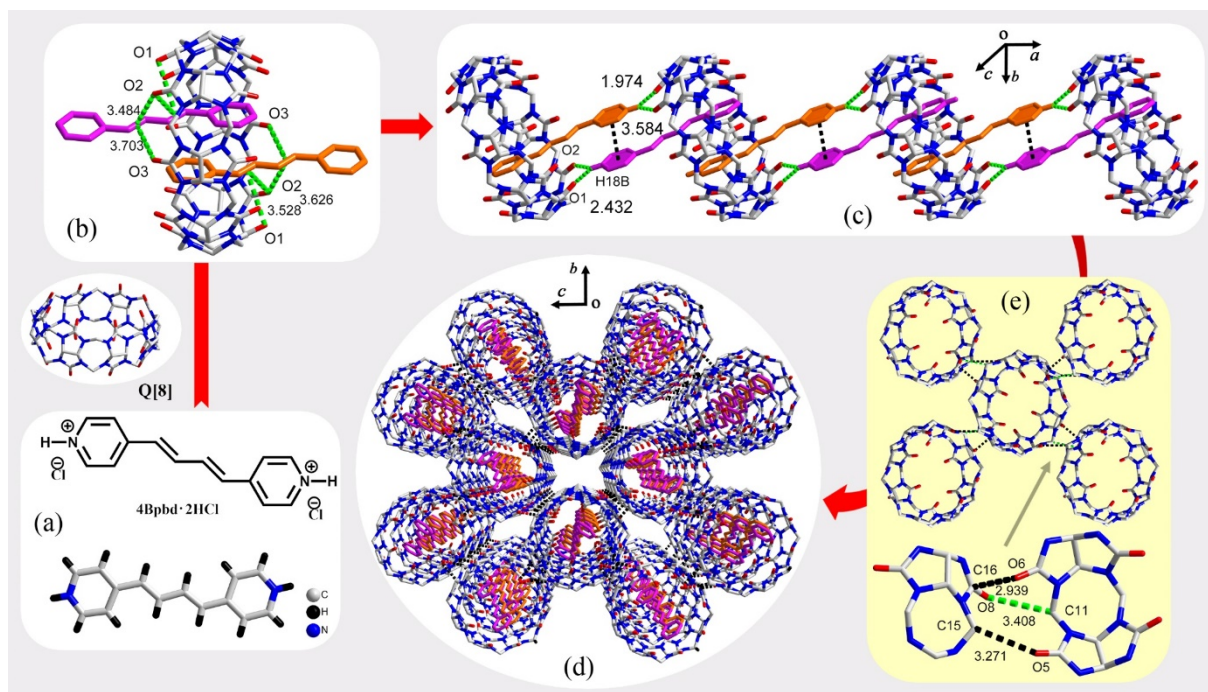


Figure 3. The structures of the (a) 4Bpbd·2HCl guest molecule and (b) inclusion complexes of 4Bpbd·2HCl@Q[8]; (c) detailed supramolecular interactions formed in the 4Bpbd·2HCl@Q[8]-based 1D supramolecular chain; (d) 3D SOF constructed by the 4Bpbd·2HCl@Q[8]-based 1D supramolecular chains; (e) detailed self-induced OSIQ formed between the central chain and four surrounding chains.

In 2012, we investigated the host-guest interaction of cucurbit[*n*]urils (*n*=7 and 8; Q[7] and Q[8]) and TMeQ[6] with the hydrochloride salts of 2,4-diaminoazobenzene (g·HCl, [Figure 4a](#)), respectively, both in solution and in the solid state.^[112] The ¹H NMR spectra and single crystal X-ray structures of the inclusion complexes (g·HCl@Q[*n*]) showed that the phenyl moiety of the guest molecule had inserted into the host cavity. Moreover, the crystal structures of g·HCl@TMeQ[6] and g·HCl@Q[8] ([Figures 4b,e](#)) showed framework characteristics. [Figure 4d](#) shows the g·HCl@TMeQ[6]-based 3D SOF, in which $\pi\cdots\pi$ stacking is evident between two protruding 2,4-diaminoazo moieties of adjacent g·HCl@TMeQ[6] inclusion complexes and the hydrogen bonding between the amine units on the diaminoazo moieties and portal carbonyl oxygen atoms of adjacent TMeQ[6]. These supramolecular interactions could be the driving forces resulting in the formation of the g·HCl@TMeQ[6] inclusion complex pair. Self-induced OSIQ is likely the main driving force resulting in the g·HCl@TMeQ[6]-based 3D SOF ([Figure 4d](#)). The system includes dipole interactions between portal carbonyl oxygen atoms of the TMeQ[6] molecule and the methine units, bridged methylene units, portal carbonyl carbon atoms of adjacent TMeQ[6] molecules, respectively ([Figure 4c right](#)). Analysis of the SOF constructed using the g·HCl@Q[8]-based inclusion complex ([Figure 4e](#)) reveals it is similar to the 4Bpbd·2HCl@Q[8]-based framework shown in [Figure 3](#). For example, the g·HCl@Q[8]-based 3D SOF has numerous g·HCl@Q[8]-based 1D supramolecular chains and each chain is made up of the g·HCl@Q[8] complexes via C-H $\cdots\pi$ stacking between the two protruding 2,4-diaminoazo moieties from the two adjacent g·HCl@Q[8] complexes. Moreover, there are hydrogen bonds formed between the amine unit on the diaminoazo moiety and the portal carbonyl oxygen atoms of an adjacent Q[8] molecule. Self-induced OSIQ, as shown in [Figure 4g](#), is the main driving force resulting in the formation of the g·HCl@Q[8]-based 3D SOF ([Figure 4h](#)).

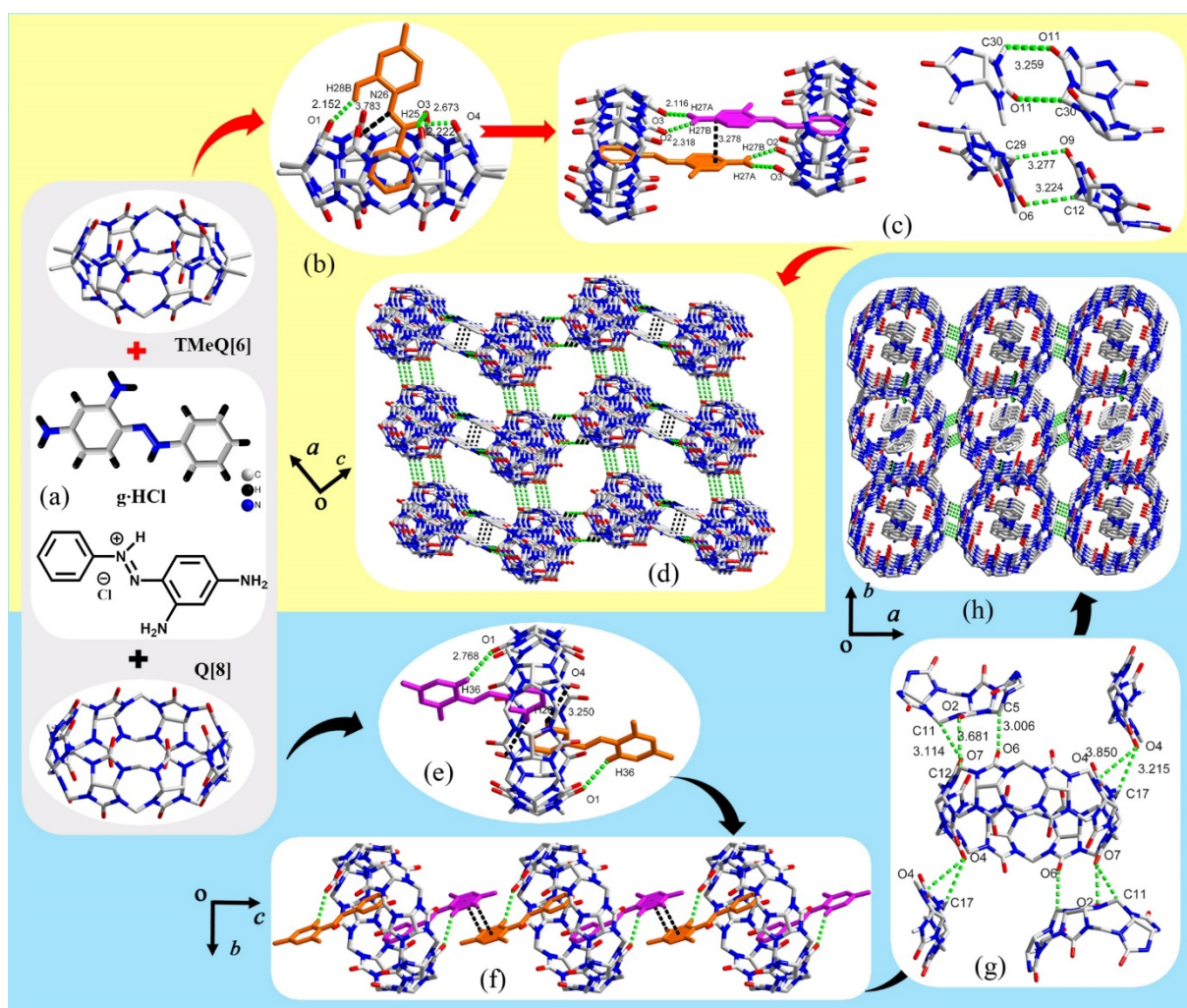


Figure 4. The structure of (a) the g-HCl guest molecule and (b) inclusion complexes of g-HCl@TMQ[6]; (c) supramolecular interactions formed in the 3D SOF; (d) 3D SOF constructed by the g-HCl@TMQ[6] inclusion complexes; (e) inclusion complexes of g-HCl@Q[8]; (f) supramolecular interactions formed in the g-HCl@Q[8]-based 1D supramolecular chain; (g) self-induced OSIQ formed between the central chain and four surrounding chains; (h) g-HCl@Q[8]-based 3D SOF.

In 2013, Stoddart *et al.* demonstrated the homophilic and heterophilic binding nature of the *N,N'*-dimethyl-2,9-diazaperopyrenium dication (MP^{2+} , Figure 5a) within Q[8].^[113] They obtained solid state $(MP^{2+})_2@Q[8]$ inclusion complexes grown from an aqueous solution of equimolar amounts of $MP \cdot 2Cl$ and Q[8] (MP^{2+} , Figure 5b). Single crystal structure analysis revealed that the 2D SOF constructed by empty Q[8] molecules co-crystallized with the 1:2 $(MP^{2+})_2@Q[8]$ inclusion complexes (Figure 5c). Close inspection revealed the detailed interactions formed among the species in the 2D SOFs included 1) $\pi \cdots \pi$ stacking formed

between the two protruding pyridyl moieties of adjacent $(MP^{2+})_2@Q[8]$ inclusion complexes resulting in the formation of $(MP^{2+})_2@Q[8]$ -based 1D supramolecular chains (Figure 5d) and 2) self-induced OSIQs between the empty Q[8] molecules and $(MP^{2+})_2@Q[8]$ inclusion complexes (Figure 5e). Each empty Q[8] interacts with four adjacent $(MP^{2+})_2@Q[8]$ inclusion complexes and two adjacent empty Q[8] molecules, and thus the 2D SOF can be viewed as $(MP^{2+})_2@Q[8]$ -based supramolecular chains linked by empty Q[8]-based supramolecular chains (Figure 5c). The $(MP^{2+})_2@Q[8]$ -Q[8]-based 2D SOFs further stack into a 3D SOF (Figures 5g) via an anion-induced OSIQ formed between the Cl^- anions and ClO_4^- anions, and the electrostatics of the outer surface of the Q[8]s in the 2D SOFs (Figure 5f).

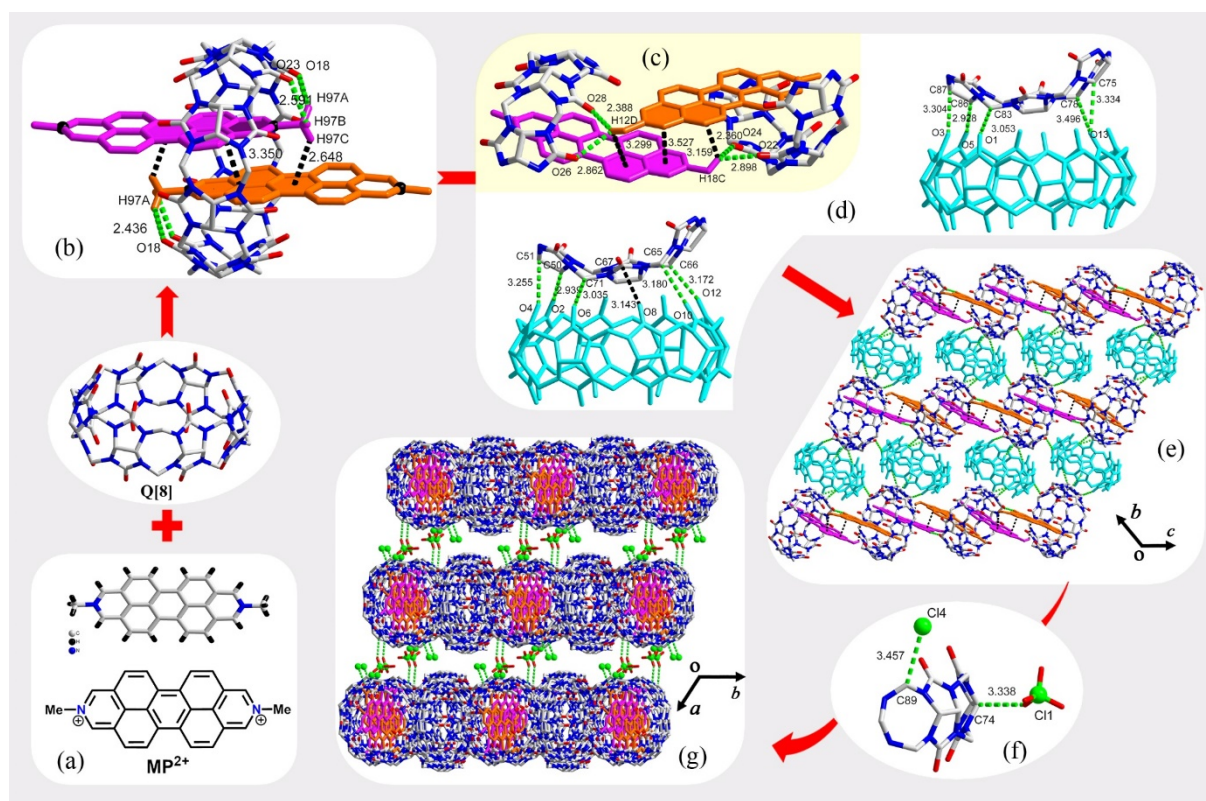


Figure 5. The structures of (a) the MP^{2+} guest molecule and (b) $MP^{2+}@Q[8]$ inclusion complex; (c) $\pi\cdots\pi$ stacking interactions formed between the two protruding pyridyl moieties of the adjacent $(MP^{2+})_2@Q[8]$ inclusion complexes; (d) self-induced OSIQs formed between the empty Q[8] molecules and $(MP^{2+})_2@Q[8]$ inclusion complexes in the 2D SOF; (e) 2D SOF constructed by the empty Q[8] molecules and $(MP^{2+})_2@Q[8]$ inclusion complexes; (f) anion-induced OSIQ; (g) 3D SOF stacked by the 2D SOFs.

In 2013, Su *et al.* attempted to prepared Q[6]-based self-catenated metal-organic rotaxane

frameworks *in-situ* using the *trans/cis*-configuration (1:1) of rotaxanes by taking advantage of a transition metal ion directed synthesis.^[114] However, we found that the two Q[6]/guest pseudorotaxane-based precursors, which were used to synthesize the metal-organic rotaxane frameworks, could also be used to construct SOFs. Figures 6a and b show the structures of the two guest molecules (C6CN4 and C6CA4) and Figures 6c and d show the structures of the two Q[6]-based pseudorotaxane-based inclusion complexes (C6CN4@Q[6] and C6CA4@Q[6]), respectively. Figure 6e shows the 2D SOF constructed by the C6CN4@Q[6] inclusion complexes. The adjacent C6CN4@Q[6] inclusion complexes are arranged perpendicular to each other and create numerous grid holes; the 2D SOFs are stacked into a 3D SOF, in which the Q[6] molecules in adjacent 2D SOFs (shown in orange) cover the grid holes in the 2D SOF (shown in pink, Figure 6i). Figure 6j shows the 3D SOF constructed by the C6CA4@Q[6] inclusion complexes. The 3D SOF can be made by stacking the C6CA4@Q[6]-based monolayer assemblies, as shown in Figure 6f, and the adjacent layers can overlap upon rotating by 94.549°. Each C6CA4@Q[6]-based monolayer assembly is constructed by numerous parallel C6CA4@Q[6]-based 1D supramolecular chains. How are the two 3D SOFs constructed? The key interactions in the two 3D SOFs are highlighted in Figures 6g and h; the interactions basically belong to the OSIQ type. For the C6CN4@Q[6]-based SOF, the key interactions include 1) π interactions formed between the C \equiv N moieties of the included C6CN4 guest molecule and the adjacent portal C=O moieties of the Q[6] molecules. 2) The C–H $\cdots\pi$ interactions formed between the protruding aromatic ring and adjacent methylene units, categorized as aromatic-induced OSIQ and 3) dipole interactions formed between the portal carbonyl oxygen atoms of a Q[6] molecule with the electrostatic portal carbonyl carbon atoms and methylene units of the adjacent Q[6] molecules, categorized as self-induced OSIQ (Figure 6g). For the C6CA4@Q[6]-based SOF, the key interactions are more complicated and include 1) a π interaction formed between the carboxyl C=O moieties of the included C6CA4 guest molecule and the protruding aromatic ring of the adjacent C6CA4@Q[6] and 2) C–H $\cdots\pi$ interactions formed between the

protruding aromatic ring and the C–H units of an adjacent C6CA4@Q[6] molecule. The remaining interactions are typical self-induced OSIQs, including the dipole interactions formed between the portal carbonyl oxygen atoms of a Q[6] molecule and the electrostatic portal carbonyl carbon atoms, methine units and methylene units of adjacent Q[6] molecules (Figure 6h).

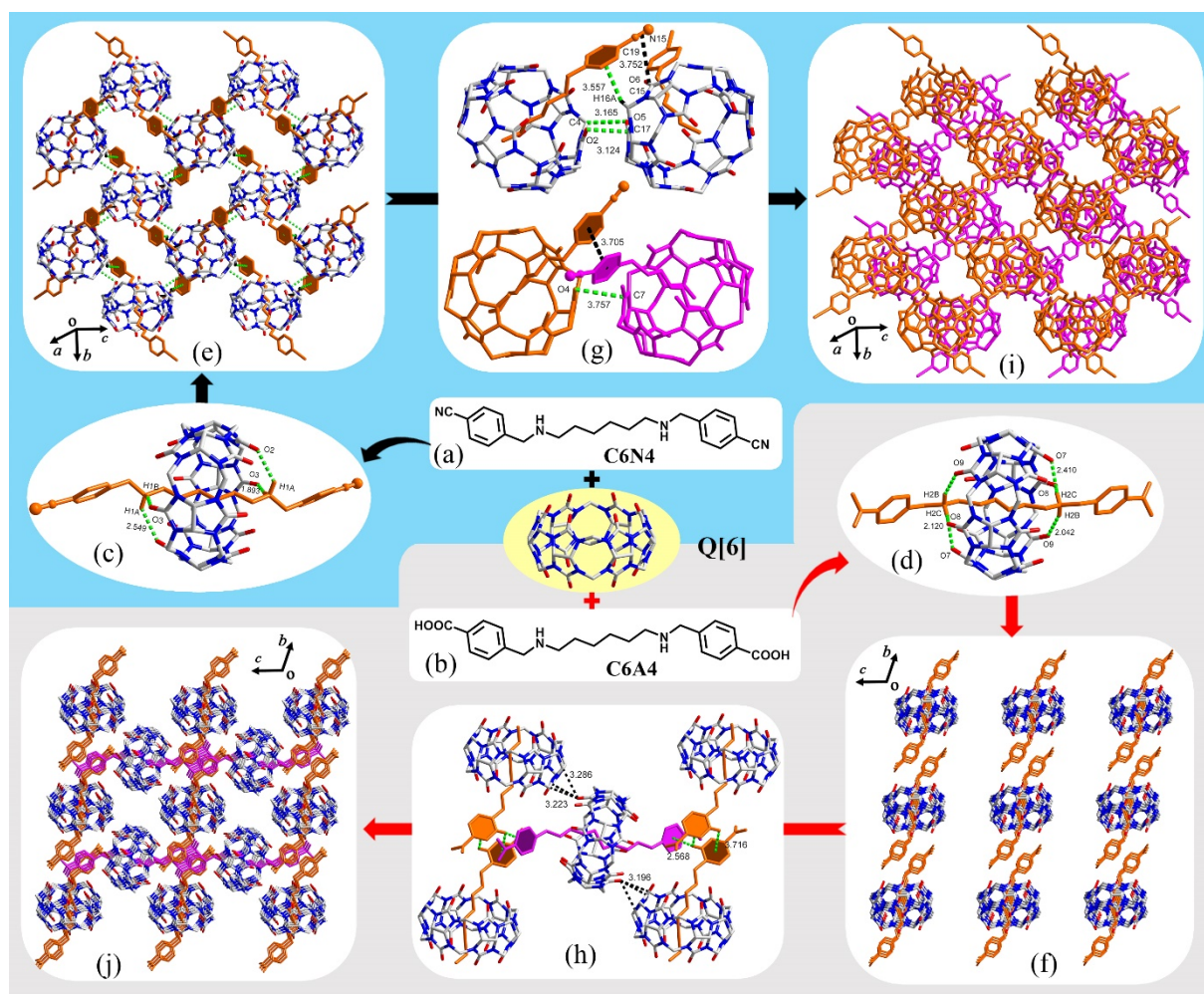


Figure 6. The crystal structures of two guest molecules (a) C6CN4 and (b) C6CA4; the inclusion complexes of Q[6] formed using the two guest molecules: (c) C6CN4@Q[6] and (d) C6CA4@Q[6]; (e) 2D SOF constructed by the C6CN4@Q[6] inclusion complexes; (f) C6CA4@Q[6]-based monolayer assembly; interactions formed in (g) C6CN4@Q[6]-based 3D SOF and (h) C6CA4@Q[6]-based 3D SOF; (i) C6CN4@Q[6]-based 3D SOF formed by stacking the 2D SOFs; (j) C6CA4@Q[6]-based 3D SOF.

In the same year, Danylyuk *et al.* investigated the host-guest interactions of Q[6] with the catecholamine drug, isoprenaline (Figure 7a) in the absence and presence of magnesium ions and obtained two isoprenaline@Q[6]-based SOFs (Figure 7d, f).^[115] Figure 7d exhibits an Mg²⁺-

free isoprenaline@Q[6]-based honeycomb-like 3D SOF, in which the isoprenaline@Q[6] inclusion complex (Figure 7b) was the basic building block, which overlap to create numerous channels. The key interactions resulting in the formation of the 3D SOF are shown in Figure 7c, including the π interactions formed between the portal carbonyl units of the Q[6] molecules and the protruding aromatic ring of the adjacent host-guest inclusion complexes. Others include the C-H $\cdots\pi$ interactions formed between the protruding aromatic ring and methylene units from the adjacent Q[6] molecules, namely, aromatic-induced OSIQs. Moreover, dipole interactions were formed between the portal carbonyl oxygen atom of the Q[6] and portal carbonyl carbon atom, as well as the methylene unit of an adjacent Q[6] molecule in the same six membered building block, *i.e.* self-induced OSIQs. Figure 7f exhibits an isoprenaline@Q[6]-based 3D SOF formed in the presence of Mg²⁺ ions (omitted for clarity). Close inspection revealed that two types of OSIQs exist in the SOF (Figure 7e). Firstly, the self-induced OSIQ of the adjacent Q[6] molecules, such as the dipole interaction formed between the portal carbonyl oxygen atom and the portal carbonyl carbon atom, as well as the methine or methylene unit of an adjacent Q[6] molecule. Secondly, aromatic-induced OSIQs, such as π interactions formed between portal carbonyl units of the Q[6] molecules and the protruding aromatic rings of adjacent host-guest inclusion complexes, as well as C-H $\cdots\pi$ interactions formed between the protruding aromatic rings and adjacent methylene units of adjacent Q[6] molecules.

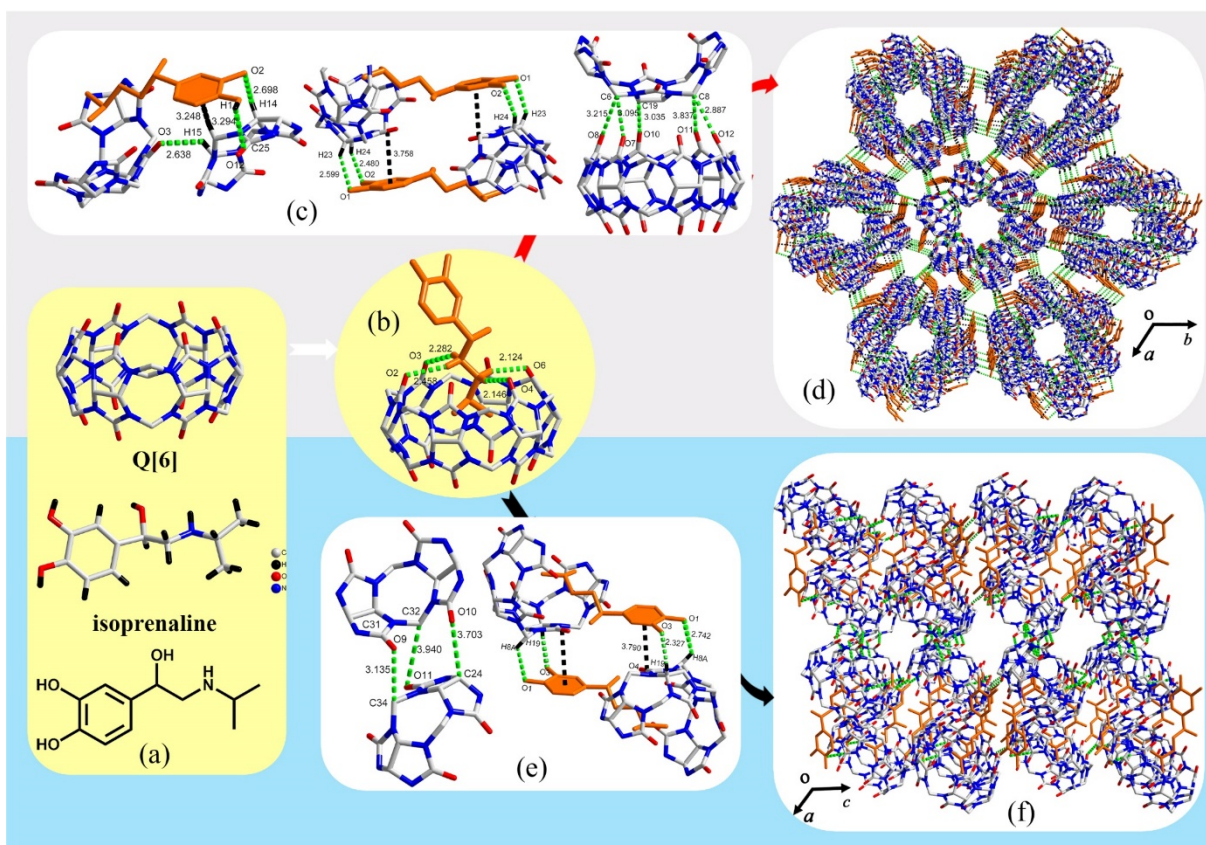


Figure 7. The crystal structures of (a) isoprenaline guest molecule, (b) isoprenaline@Q[6] inclusion complex and (d) key supramolecular interactions formed in the Mg^{2+} -free isoprenaline@Q[6]-based 3D SOF; (d) Mg^{2+} -free isoprenaline@Q[6]-based 3D SOF; (e) key supramolecular interactions formed in the isoprenaline@Q[6]-based 3D SOF with Mg^{2+} ions; (f) isoprenaline@Q[6]-based 3D SOF with the Mg^{2+} ions omitted for clarity.

Lu *et al.* investigated the delivery of triamterene using Q[7]^[116] and obtained two polymorphic single crystals constructed from triamterene@Q[7] inclusion complexes via fast and slow cooling, respectively (Figures 8a and b). The crystal structures showed that both of the polymorphs have similar framework characteristics, constructed from numerous diamond-shaped assemblies (Figures 8g and h). Close inspection reveals that each diamond-shaped assembly is formed from triamterene@Q[7] inclusion complexes constructed via self-induced and aromatic-induced OSIQs (Figures 8e and f). Figures 8c and d show the detailed OSIQs, including the dipole interactions formed between the portal carbonyl oxygen atom of a Q[6] and the portal carbonyl carbon atoms and methine or methylene units of adjacent Q[6]s. Also π interactions are formed between the portal carbonyl units of the Q[6]s and the protruding

aromatic rings of the adjacent host-guest inclusion complexes, and C–H $\cdots\pi$ interactions form between the protruding aromatic ring and methine or methylene units of the adjacent Q[6]s. Moreover, the $\pi\cdots\pi$ stacking interactions formed between two adjacent protruding aromatic rings (3.2–3.4 Å) also play an important role in the construction of the two triamterene@Q[7]-based SOFs.

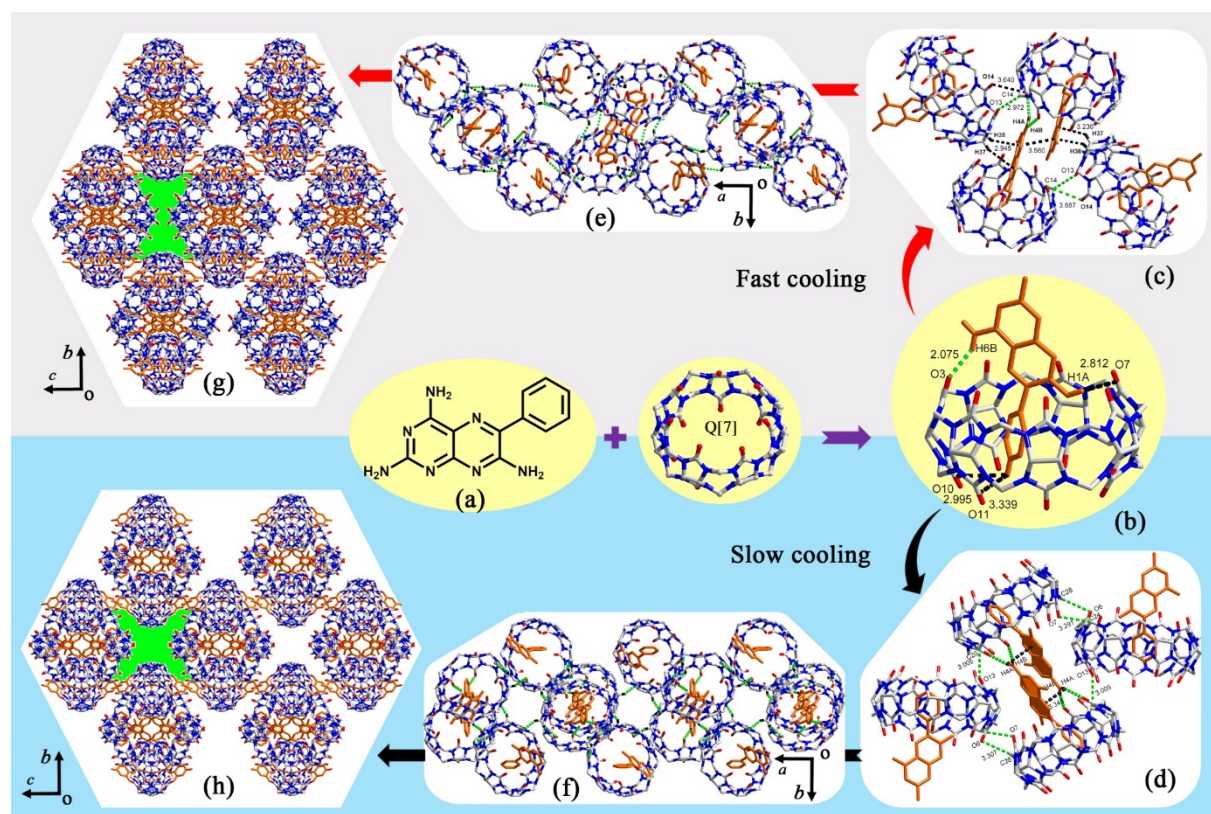


Figure 8. The crystal structures of (a) triamterene guest molecule, (b) triamterene@Q[7] inclusion complex; (c and d) key supramolecular interactions formed in the two SOFs; (e and f) the diamond-shaped assemblies of the two 3D SOFs, respectively; (g and h) triamterene@Q[7]-based 3D SOFs prepared via (c) slow cooling and (d) fast cooling.

In 2014, Sindelar *et al.* reported a novel cucurbit[6]uril (Q[6]) with a substituent solely attached to one methylene bridge, namely mono(2-phenylethyl)cucurbit[6]uril (*mPheQ[6]*, Figure 9a).^[117] This was the first example of such a substituent at the methylene bridge of a Q[6]. Although *mPheQ[6]* exhibited similar host-guest inclusion properties to those of the previously reported Q[6]s, it undergoes solid-state self-assembly to form a cyclic tetramer via host-guest interactions (Figure 9b), as well as self-induced OSIQ. Interactions include the

dipole interaction formed between the portal carbonyl oxygen atoms of the *m*PheQ[6]s and the methine and methylene units of the *m*PheQ[6] molecule, for the latter the substituent was included (Figure 9c). Moreover, the tetramers can further arrange into a porous SOF (Figure 9d), in which the self-induced OSIQs formed between adjacent tetramers are the main driving forces (Figure 9e).

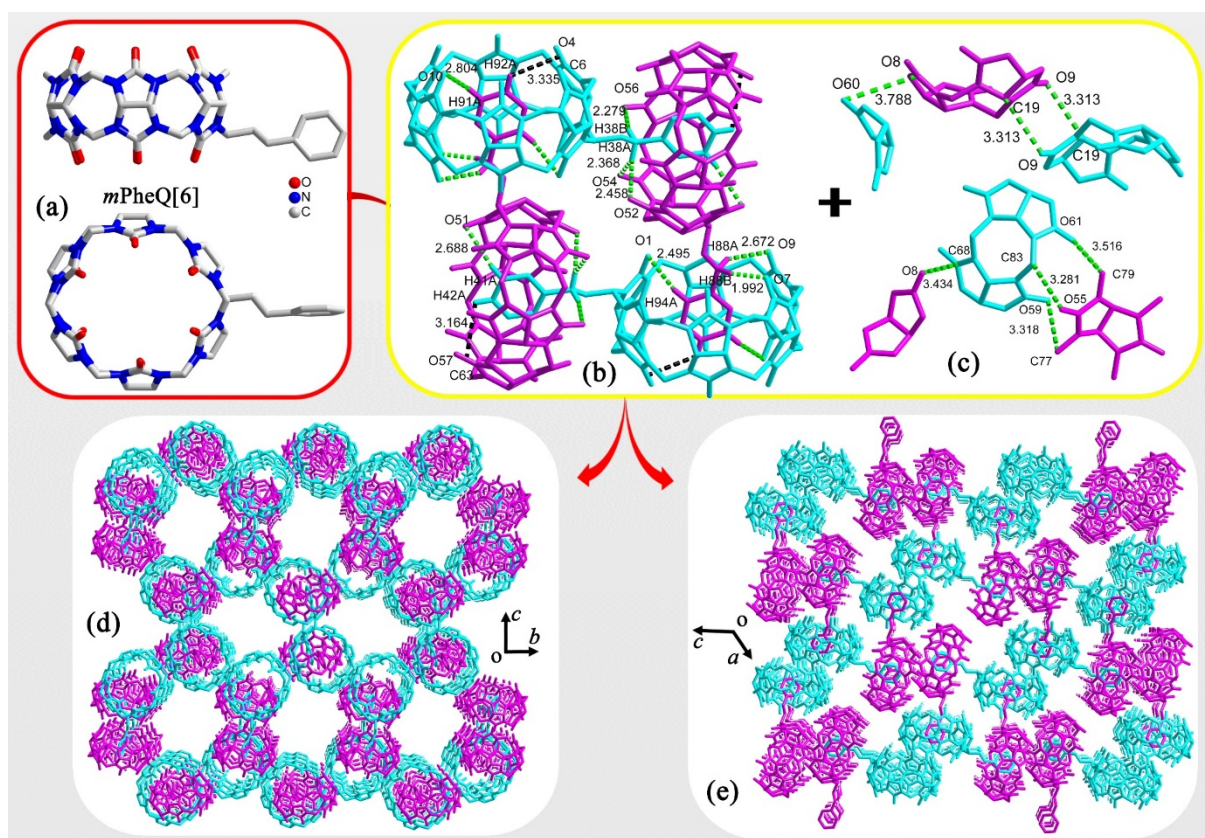


Figure 9. Crystal structures of (a) *m*PheQ[6] and (b) *m*PheQ[6]-based tetramer; (c) key self-induced OSIQs formed in the 3D SOF; (d and e) *m*PheQ[6]-based 3D SOF viewed from different directions.

In 2015, we investigated the interaction of TMeQ[6] with a series of 1, ω -alkyldiammonium guest molecules and found that 1,3-propanediammonium interacted with TMeQ[6] to form an inclusion complex (Figure 10a), which can further arrange into a 3D SOF (Figure 10c).^[118] A three inclusion complex-based trimer appeared to be the 3D SOF building block and the self-induced OSIQs were the main driving force. Interactions included dipole interactions between portal carbonyl oxygen atoms of a TMeQ[6] molecule in the trimer and the portal carbonyl

carbon atoms or methyl, methylene or methine units of adjacent TMeQ[6]s in the trimer.

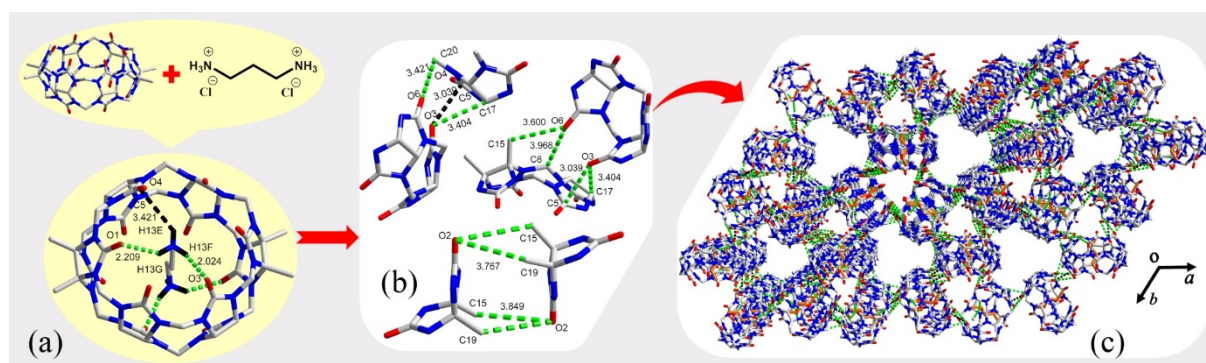


Figure 10. (a) Crystal structure of the 1,3-propanediammonium@TMeQ[6] inclusion complex; (b) detailed self-induced OSIQs formed between the TMeQ[6] molecules in the trimer; (c) 1,3-propanediammonium@TMeQ[6]-based 3D SOFs.

In 2016, Cao *et al.* reported three supramolecular organic frameworks (SOFs), which were constructed from three cucurbit[*n*]uril-based [2]pseudorotaxanes by orthogonal and/or parallel $\pi \cdots \pi$ interactions formed between 4,4'-bipyridin-1-ium units, in addition to the self-induced OSIQ formed between adjacent Q[*n*] molecules in the SOFs.^[119] The three guest molecules were 4,4'-bipyridin-1-ium derivatives (**1-3**), as shown in Figures 11a-c, respectively. The single crystal X-ray structure of the inclusion complex **1**@Q[6] (Figure 11d) exhibited an interwoven 3D SOF (Figure 11f). The **1**@Q[6] pseudorotaxane inclusion complexes interact through orthogonal $\pi \cdots \pi$ stacking interactions formed between protruding 4,4'-bipyridin-1-ium units, as well as self-induced OSIQs formed between adjacent Q[6]s (Figure 11e) to form a rectangular helic channel (Figure 11g). The pseudorotaxane inclusion complexes **2**@Q[6] (Figure 11h) can also form a 3D framework (Figure 11j), in which **2**@Q[6] complexes are linked together through parallel $\pi \cdots \pi$ stacking interactions between protruding 4,4'-bipyridin-1-ium units to form supramolecular chains (Figure 11k). Moreover, there are numerous free Q[6]s, which fall in between the supramolecular chains formed via the self-induced OSIQ of the adjacent bound and unbound Q[6]s as well as the pseudo hydrogen bonds formed between the portal carbonyl oxygen atoms and C-H bonds in the 4,4'-bipyridin-1-ium moieties (Figure 11i). Guest **3** interacts with Q[7] to form the **3**@Q[7] inclusion complex, in which guest **3** is bent due to the

larger cavity of the Q[7] (Figure 11l). Interestingly, it seems that $\pi\cdots\pi$ stacking interactions are the dominant driving force resulting in the formation of the $\mathbf{3}@Q[7]$ -based 3D SOF (Figure 11o). In particular, parallel $\pi\cdots\pi$ stacking interactions result in the formation of an unbound guest $\mathbf{3}$ -based layer (Figure 11n, in pink), whilst numerous $\mathbf{3}@Q[7]$ inclusion complexes are inserted in the unbound $\mathbf{3}$ -based layers via orthogonal $\pi\cdots\pi$ stacking interactions formed between protruding 4,4'-bipyridin-1-ium units of the $\mathbf{3}@Q[7]$ inclusion complexes and 4,4'-bipyridin-1-ium units of the unbound guest molecules ($\mathbf{3}$) to form layers.

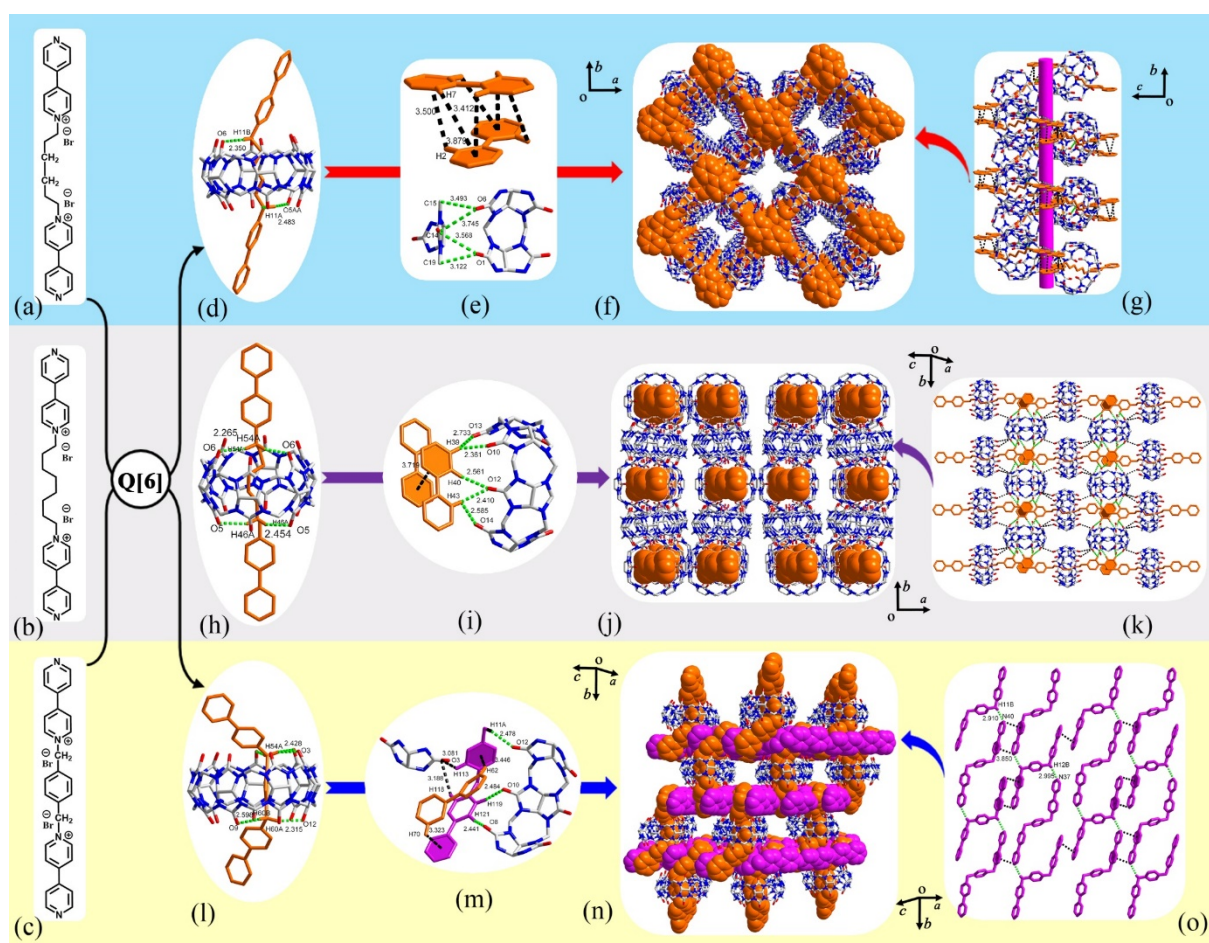


Figure 11. The structures of guest molecules (a) **1**; (b) **2**; (c) **3**; crystal structures of (d) **1@Q[6]** inclusion complex and (e) the non-covalent interaction and self-induced OSIQs; (f) **1@Q[6]**-based 3D SOF; (g) an isolated **1@Q[6]**-based channel; (h) **2@Q[6]** inclusion complex; (i) the non-covalent interaction and self-induced OSIQs; (j) **2@Q[6]**-based 3D SOF viewed along the *c*-axis; (k) **3**-based layer formed via parallel $\pi\cdots\pi$ stacking interactions; (l) **3@Q[7]** inclusion complex; (m) the non-covalent interaction; (n) **3@Q[7]**-based 3D SOF; (o) **3@Q[7]**-based 3D SOF viewed along the *c*-axis, in which the Q[7] molecules are omitted for clarity.

In 2017, we reported a series of host-guest inclusion complexes consisting of Q[6]s with

different long chain guests, which have framework features. For example, the host-guest interactions of 2,2'-(decane-1,10-diyl)-diisoquinolinium with Q[6] lead to the formation of a [2]pseudorotaxane with the Q[6] molecule located over the decyl chain of the guest molecule (Figure 12a).^[120] The neighbouring [2]pseudorotaxane inclusion complexes can arrange into a 2D SOF as shown in Figure 12c. Close inspection revealed that each inclusion complex interacts with six adjacent inclusion complexes via different supramolecular interactions: *viz* $\pi\cdots\pi$ stacking and C-H $\cdots\pi$ interactions with three complexes. For the self induced OSIQs of the remaining three complexes, the interaction distances are in the range 3.034–3.402 Å (Figure 12b). The 2D SOFs can further stack into a [2]pseudorotaxane-based 3D SOF (Figure 12e) via self-induced OSIQs; the interaction distances are in the range 3.332–3.516 Å (Figure 12d).

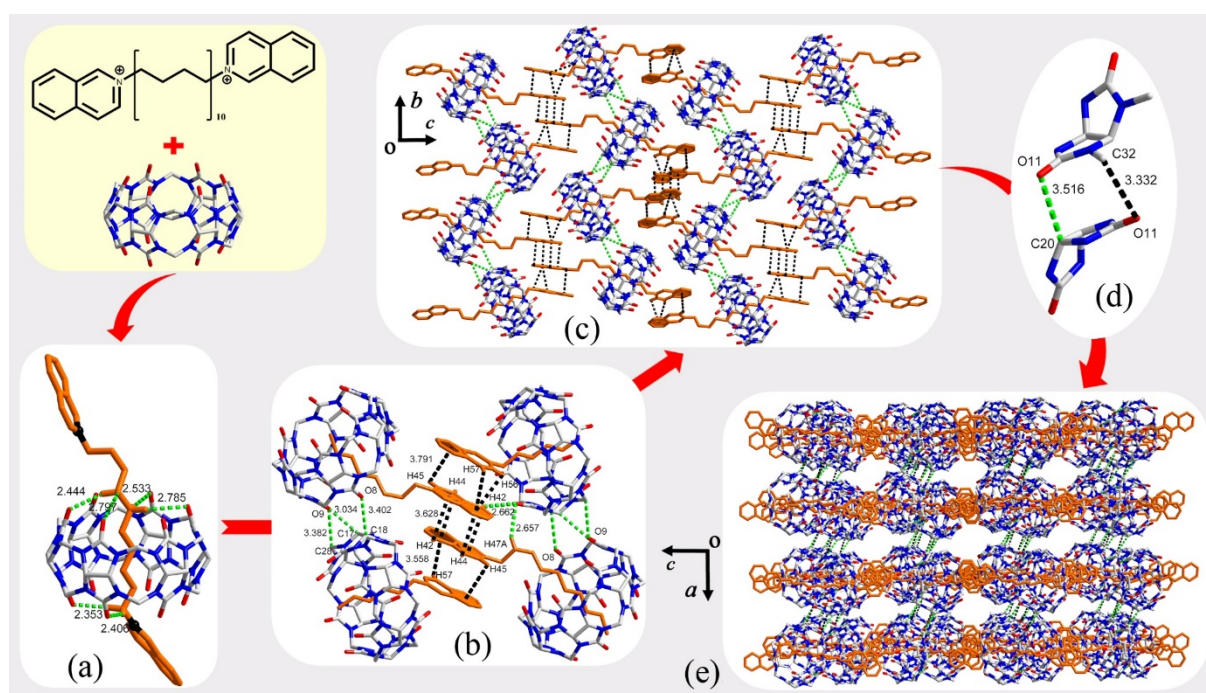


Figure 12. The crystal structure of (a) 2,2'-(decane-1,10-diyl)-diisoquinolinium@Q[6] inclusion complex; (b) supramolecular interactions formed between each complex and four adjacent complexes; (c) 2,2'-(decane-1,10-diyl)-diisoquinolinium@Q[6]-based 2D SOF; (d) self-induced OSIQs formed in the 3D SOF; (e) the diisoquinolinium@Q[6]-based 3D SOF.

Polychloride transition-metal anions ($[M_{\text{trans}}\text{Cl}_4]^{2-}$, $M_{\text{trans}} = \text{Cd}, \text{Zn}, \text{Cu}, \text{Co}, \text{Ni}, \text{etc.}$) as the third species can not only lead to the formation of various Q[n]-based 1D supramolecular coordination polymers^[68], but can also result in the formation of various supramolecular

frameworks constructed from free Q[n]s or simple Q[n]-based host-guest inclusion complexes.^[71] The interaction of Q[6] with a series of 1, ω -alkyldiammonium guest molecules may be the earliest host-guest systems investigated in Q[n]-chemistry. When we re-investigated these host-guest interaction systems in the presence of [CdCl₄]²⁻ as a structure directing agent (formed from CdCl₂ in aqueous HCl solutions), we found that the most significant framework was formed using Q[6] with 1,6-hexyldiammonium as the guest molecule (1,6N2).^[121] Before analyzing this framework, we needed to introduce a third OSIQ, namely the anion-induced OSIQ, which is derived from the ion-dipole interactions formed between anions and the electrostatic (potential positive) portal carbonyl carbon atoms, methine units and methylene units (Figure 1b).

Looking again at the structure of the previously mentioned framework,^[121] Figure 13a reveals the basic building block, whilst Figure 13b shows two basic interactions: the self-induced OSIQ between the adjacent 1,6N2@Q[6] and an anion-induced OSIQ of each C6N2@Q[6] complex with eight adjacent [CdCl₄]²⁻ anions as well as the hydrogen bonding of anionic units of the included guests with the portal carbonyl oxygen atoms of the adjacent 1,6N2@Q[6] complexes. This creates a puckered 10-membered 1,6N2@Q[6] beaded ring without and with [CdCl₄]²⁻ anions (Figure 13c). It is interesting that there is a space present, and this can accommodate one 1,6N2@Q[6], whilst eight [CdCl₄]²⁻ anions surround this 1,6N2@Q[6] complex in the 10-membered “beaded” ring. Further fusing of this accommodated 1,6N2@Q[6] complex can result in another catenated 10-membered “beaded” ring and these two ring systems seem to be independent (Figure 13d). Thus, the 10-membered “beaded” ring can further fuse into a 3D QSF (Figure 13e), which is constructed by two independent 1,6N2@Q[6]-based 3D QSFs (Figures 13f and g) and a [CdCl₄]²⁻ anion-based 3D framework (Figure 13h).

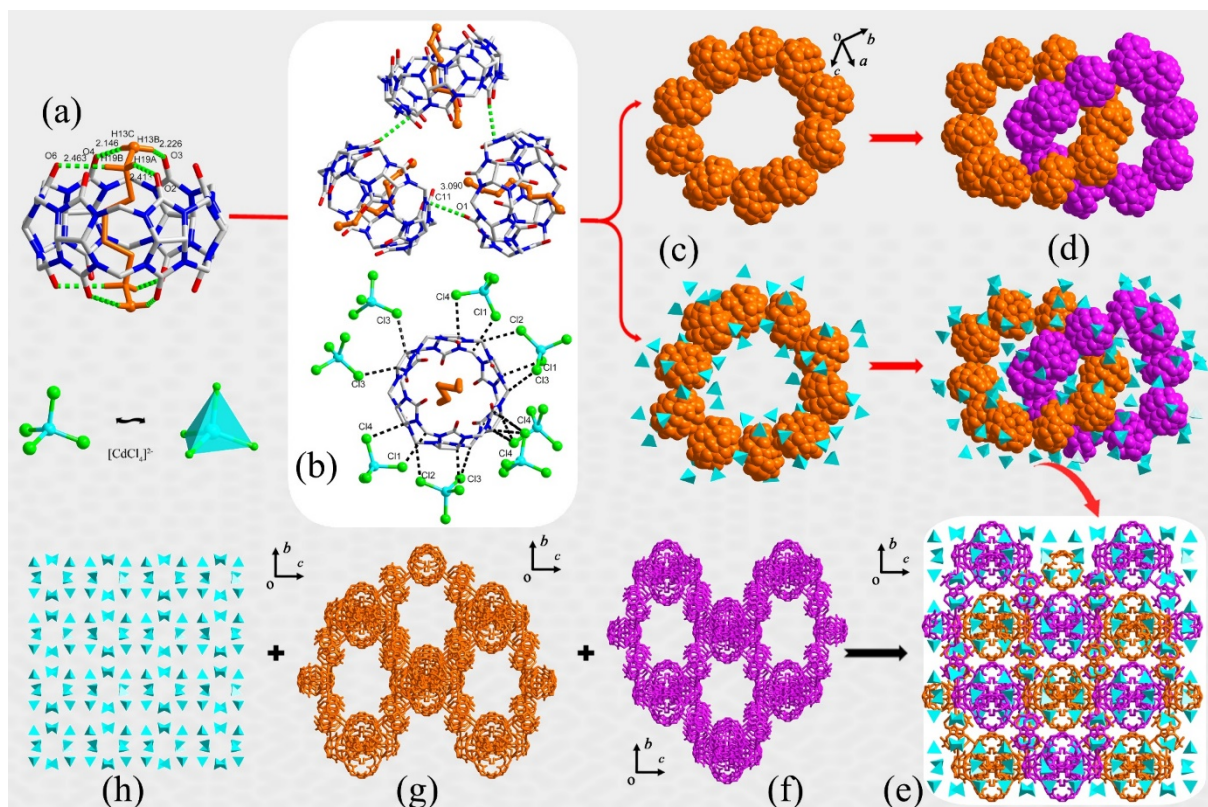


Figure 13. The crystal structure of (a) 1,6N2@Q[6] complex and topologic $[\text{CdCl}_4]^{2-}$ anion; (b) the self-induced OSIQ involving a 1,6N2@Q[6] trimer and anion-induced OSIQ of each 1,6N2@Q[6] complex and eight $[\text{CdCl}_4]^{2-}$ anions; (c) the puckered 10-membered 1,6N2@Q[6] ring without and with adjacent $[\text{CdCl}_4]^{2-}$ anions; (d) the puckered 10-membered 1,6N2@Q[6] ring without and with adjacent $[\text{CdCl}_4]^{2-}$ anions; (e) the 1,6N2@Q[6]/ $[\text{CdCl}_4]^{2-}$ -based supramolecular framework constructed by two independent (f, g) 1,6N2@Q[6]/ $[\text{CdCl}_4]^{2-}$ -based and (h) $[\text{CdCl}_4]^{2-}$ -based frameworks.

If we now look at the solid-state structure of the inclusion complex (1,6N2@Q[6]) without $[\text{CdCl}_4]^{2-}$ anions, but prepared under the same conditions, the crystal structure analysis shows that the interaction of Q[6] with 1,6N2 (Figure 14a) in the aqueous HCl solution also forms the 1,6N2@Q[6] inclusion complex (Figure 14b). Also, the 1,6N2@Q[6] complex stacks into a 1,6N2@Q[6]-based 3D framework (Figure 14d and e), which is made up of numerous 1,6N2@Q[6]-based chains, whereas the neighbouring 1,6N2@Q[6]s in the chain, which are 5.45 Å apart, seem to be isolated (Figure 14f). Close inspection reveals that each 1,6N2@Q[6] complex is holed by 1,6N2@Q[6]s complexes from four adjacent chains *via* self-induced OSIQ (Figure 14c). Thus, a comparison of the two 1,6N2@Q[6]-based 3D frameworks revealed that

the presence and absence of $[\text{CdCl}_4]^{2-}$ anions can result in the formation of entirely different QSFs. The extra anion-induced OSIQ play an important role which links two independent 1,6N2@Q[6]-based 3D frameworks.

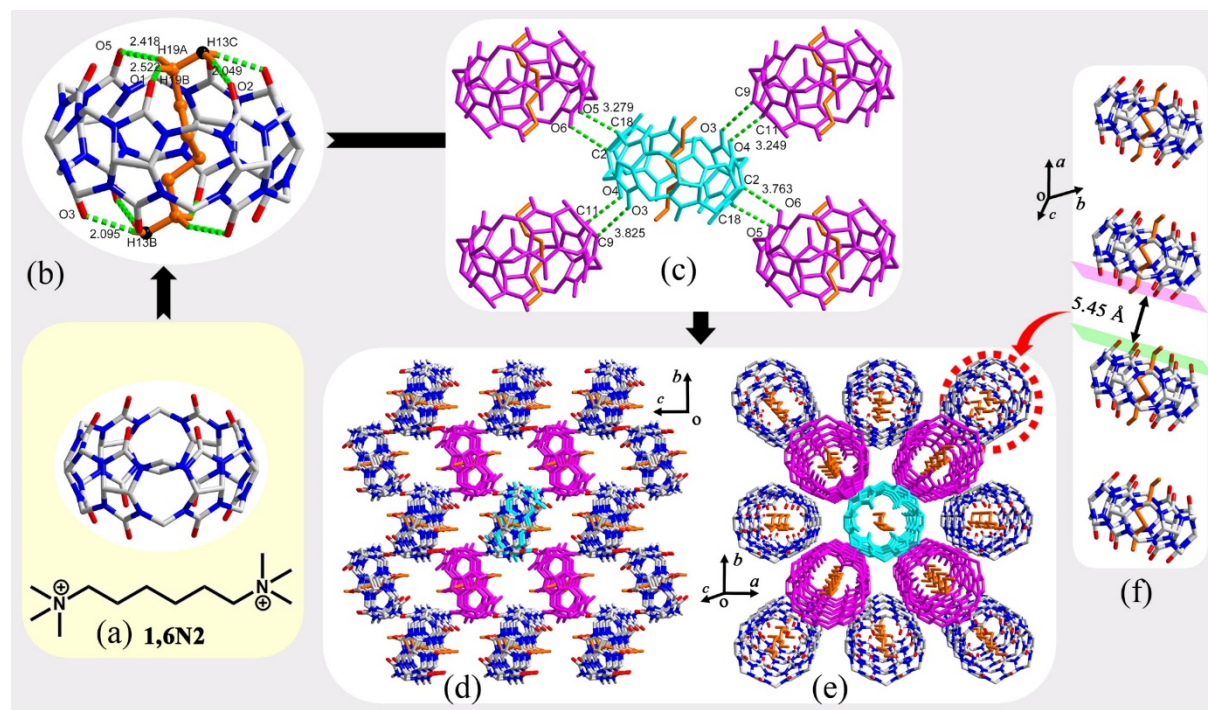


Figure 14. (a) Structure of 1,6N2; (b) crystal structure of the 1,6N2@Q[6] inclusion complex; (c) self-induced OSIQs formed between the central 1,6N2@Q[6] inclusion complex and the adjacent 1,6N2@Q[6] inclusion complexes from four adjacent chains (the H atoms, free Cl^- anions and free water molecules are omitted for clarity); (d and e) the 1,6N2@Q[6]-based 3D framework constructed from numerous 1D chains; (f) the 1,6N2@Q[6]-based 1D chain.

When we investigated the interaction of an unsymmetric butyl viologen guest molecule (BV^+ , Figure 15a) with Q[6], we obtained the SOF constructed from the inclusion complex of *para*-dicyclohexanocucurbit[6]uril ($\text{Cy}_2\text{Q}[6]$) with the BV^+ guest ($\text{BV}^+@ \text{Cy}_2\text{Q}[6]$).^[122] Interestingly, the $\text{Cy}_2\text{Q}[6]$ host includes the butyl moieties of two unsymmetrical BV^+ guest molecules to form a symmetrical 1:2 host–guest inclusion complex (Figure 15b). X-ray diffraction analysis revealed that adjacent $\text{BV}^+@ \text{Cy}_2\text{Q}[6]$ complexes interact via $\pi \cdots \pi$ stacking of the protruding viologen moieties of the included BV^+ guests to form supramolecular chains and adjacent $\text{BV}^+@ \text{Cy}_2\text{Q}[6]$ -based chains interact via self-induced OSIQs to form a $\text{BV}^+@ \text{Cy}_2\text{Q}[6]$ -based 2D framework with numerous parallelogram holes (Figure 15c). Each

parallelogram hole in the 2D framework contains a pair of protruding $\pi\cdots\pi$ stacked viologen moieties from the other vertically inserted 2D frameworks (Figure 15d) and the neighbouring $\text{Cy}_2\text{Q}[6]$ molecules in different $\text{BV}^+\text{@Cy}_2\text{Q}[6]$ -based 2D frameworks (Figure 15f) via self-induced OSIQs (Figure 15e). Thus, the combination of all the above-mentioned supramolecular interactions results in the formation of the $\text{BV}^+\text{@Cy}_2\text{Q}[6]$ -based 3D framework (Figure 15g).

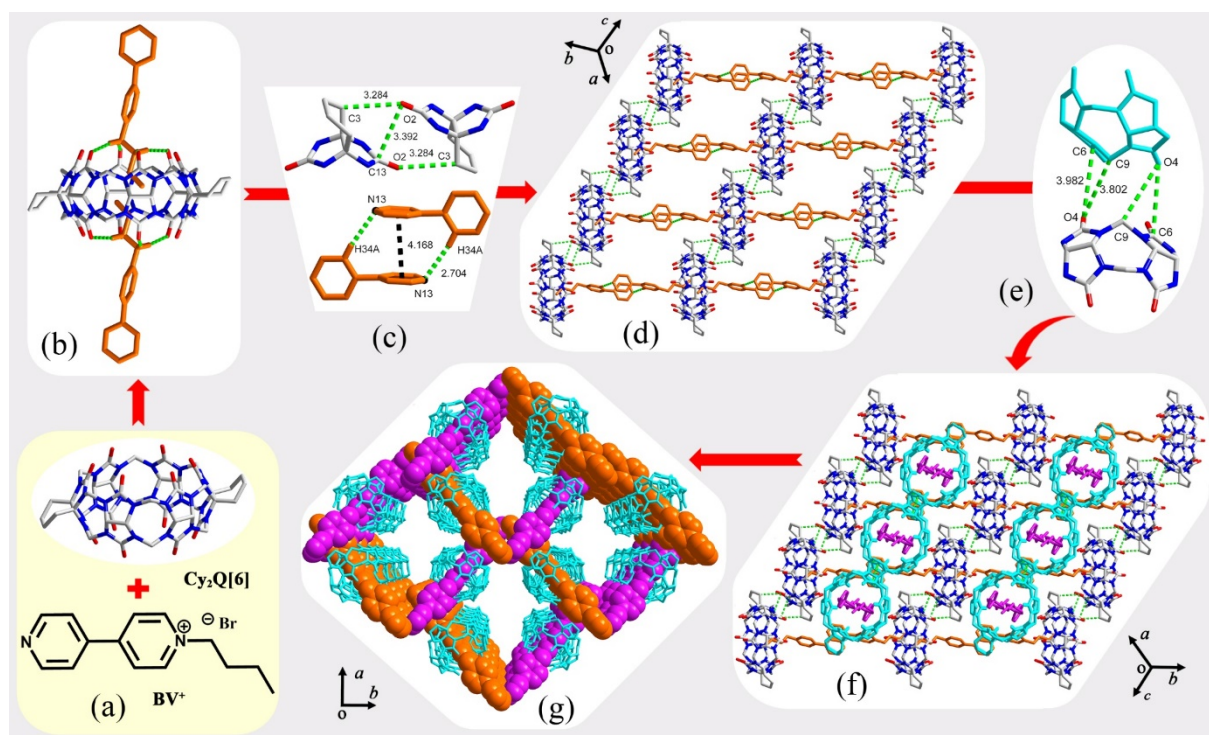


Figure 15. (a) Structure of BV^+ ; (b) crystal structure of the $\text{BV}^+\text{@Cy}_2\text{Q}[6]$ inclusion complex; (c) the non-covalent interaction and self-induced OSIQs; (d) the $\text{BV}^+\text{@Cy}_2\text{Q}[6]$ -based 2D framework with parallelogram holes; (e) interactions formed between the vertically inserted $\text{BV}^+\text{@Cy}_2\text{Q}[6]$ -based 2D frameworks; (f) the vertically inserted $\text{BV}^+\text{@Cy}_2\text{Q}[6]$ -based 2D frameworks; (g) the $\text{BV}^+\text{@Cy}_2\text{Q}[6]$ -based 3D framework.

When the alkyl group is longer, such as a hexyl group, the interactions formed between the hexyl viologen bromide guest (HV^+ , Figure 16a) and the $\text{Q}[6]$ host in the presence of $[\text{CdCl}_4]^{2-}$ yielded an unsymmetrical $\text{HV}^+\text{@Q}[6]$ inclusion complex. Here, the hexyl moiety is included in the cavity and the viologen moiety of the HV^+ guest is located at the portal of the host and every two $\text{HV}^+\text{@Q}[6]$ complexes form a pair via parallel $\pi\cdots\pi$ interactions formed between protruding viologen moieties as well as hydrogen bonds formed between protonated pyridine nitrogen atoms and portal carbonyl oxygen atoms (Figure 16b).^[123] X-ray diffraction analysis revealed

that in addition to the HV⁺@Q[6] complex pairs, there are free Q[6] molecules surrounded by [CdCl₄]²⁻ anions through anion-induced OSIQs (Figure 16c down). Meanwhile, the HV⁺@Q[6] pairs and free Q[6] molecules are linked by the [CdCl₄]²⁻ anions via anion-induced OSIQs. Moreover, the Q[6] molecules in the HV⁺@Q[6] pairs and free Q[6] molecules can interact via self-induced OSIQs (Figure 16c top). Thus, a combination of all these supramolecular interactions, the HV⁺@Q[6] pairs, free Q[6] molecules, and [CdCl₄]²⁻ anions can form a 3D supramolecular framework with numerous different channels (Figure 16d).

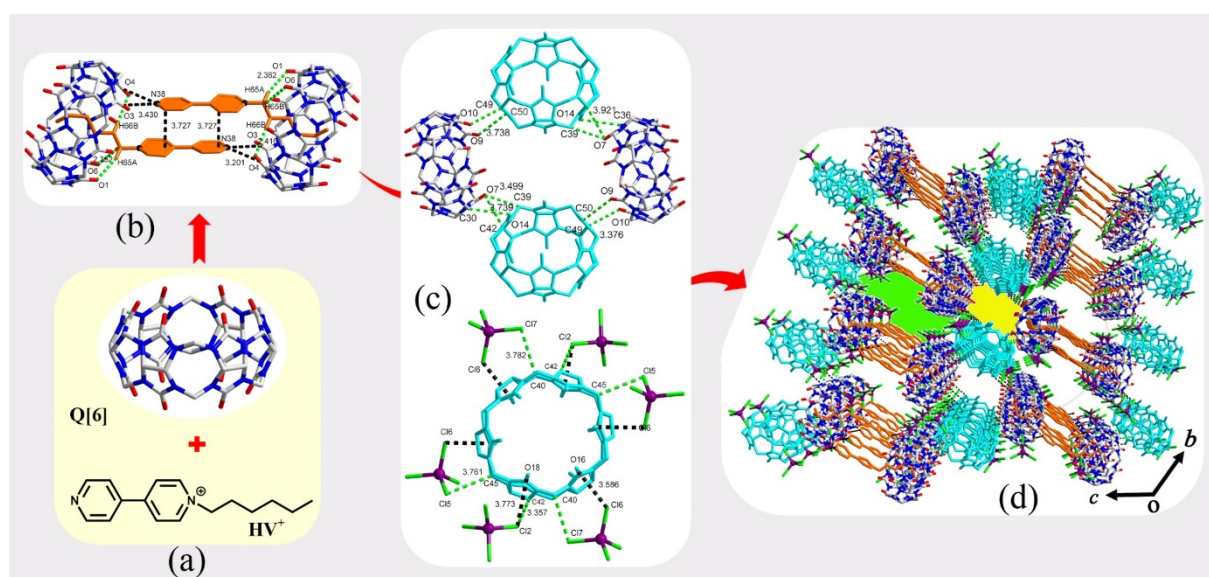


Figure 16. (a) Structure of HV⁺, (b) crystal structure of the HV⁺@Q[6] inclusion complex; (c) interactions formed among the HV⁺@Q[6] inclusion complexes, free Q[6] molecules and [CdCl₄]²⁻ anions; (d) the 3D framework constructed by the HV⁺@Q[6] inclusion complexes, free Q[6] molecules and [CdCl₄]²⁻ anions.

In 2018, we decided to investigate the use of an inverted Q[6] (*i*Q[6]). Such an *i*Q[6] contains an inverted glycoluril unit and places two methine protons within the cavity and therefore possesses a smaller cavity than does Q[6]. Investigation of the interaction of *i*Q[6] with a series of symmetrical viologens bearing aliphatic substituents,^[124] found that in the case of the dibutyl viologen guest (DBV²⁺, Figure 17a) a dumbbell-like DBV²⁺@*i*Q[6] inclusion complex formed in the presence of [CdCl₄]²⁻ anions (Figure 17b). Single crystal X-ray diffraction analysis revealed that a 3D framework was constructed by DBV²⁺@*i*Q[6] inclusion

complexes and $[\text{CdCl}_4]^{2-}$ anions via supramolecular interactions (Figure 17g). It is interesting that this $\text{DBV}^{2+}@i\text{Q}[6]-[\text{CdCl}_4]^{2-}$ -based 3D framework can be fully expressed in horticultural language. Firstly, the 3D framework can be regarded as a 3D multi-layered flower wall (Figure 17g right). Secondly, each $\text{DBV}^{2+}@i\text{Q}[6]-[\text{CdCl}_4]^{2-}$ -based 2D honeycomb-like framework layer along the c -axis (Figure 17e) resembles honeycombed flowerpots aligned in neat rows, with each flowerpot containing a brown $i\text{Q}[6]$ “soil” through anion-induced OSIQs. One end of the DBV^{2+} “limb” inserts into the $i\text{Q}[6]$ “soil” via host-guest inclusion and the other end of the DBV^{2+} “limb” holds a red $i\text{Q}[6]$ “flower” via host-guest inclusion (referring to Figure 17d). The layer-to-layer interactions are mainly anion-induced OSIQs formed between the $[\text{CdCl}_4]^{2-}$ anions and red $i\text{Q}[6]$ “flowers” and self-induced OSIQs formed between the brown $i\text{Q}[6]$ “soil” and red $i\text{Q}[6]$ “flowers”.

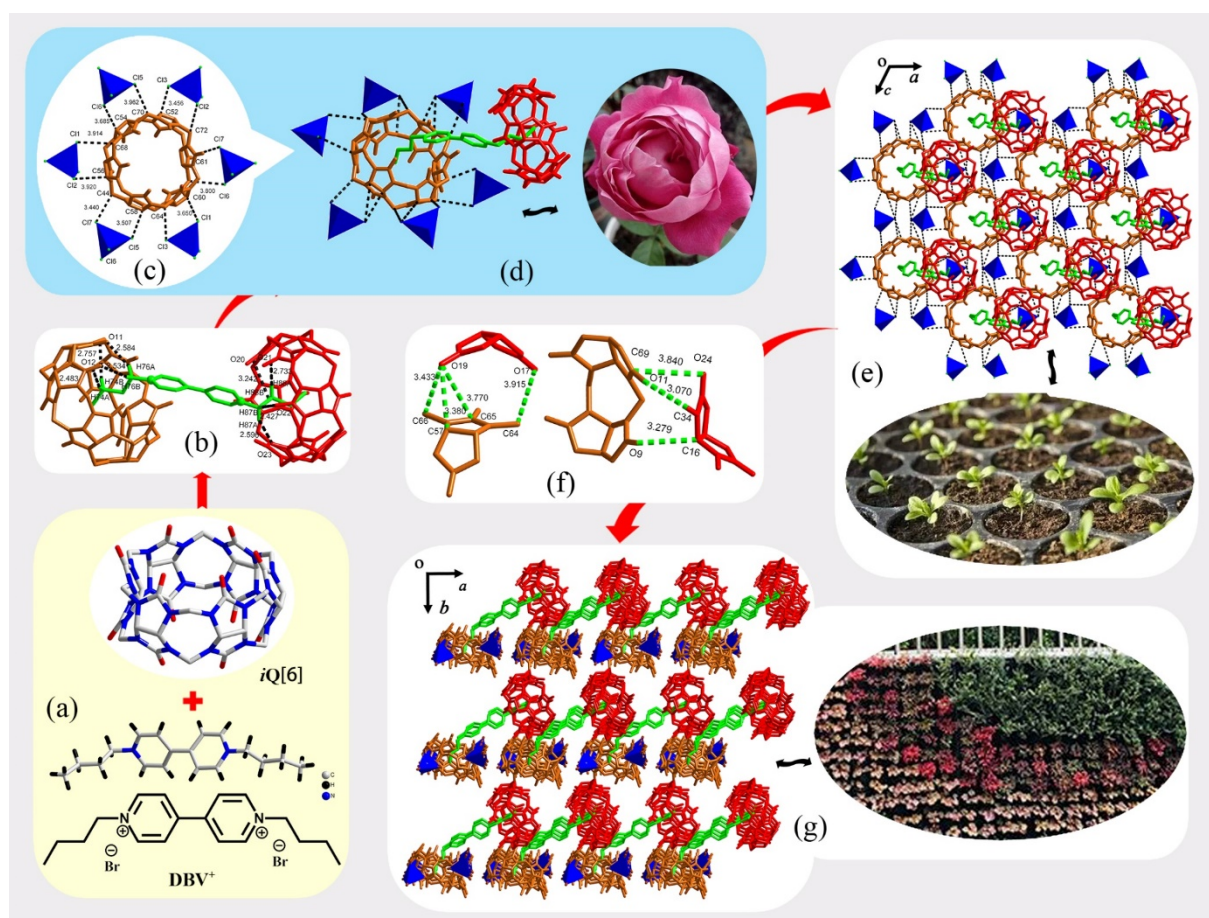


Figure 17. Crystal structures of (a) DBV^{2+} guest; (b) the $\text{DBV}^{2+}@i\text{Q}[6]$ inclusion complex; (c) anion-induced OSIQs formed in the framework; (d) the DBV^{2+} “limb” inserts into the $i\text{Q}[6]$ “soil” via host-guest inclusion (left) and (right) a real single pot flower; (e) the 2D framework constructed by the $\text{DBV}^{2+}@i\text{Q}[6]$ inclusion complexes and $[\text{CdCl}_4]^{2-}$ anions (top) and (down)

the honeycombed flowerpots aligned in neat rows; (f) anion- and self-induced OSIQs formed in the framework; (g) (left) the 3D framework constructed by the $\text{DBV}^+@i\text{Q}[6]$ inclusion complexes and $[\text{CdCl}_4]^{2-}$ anions and (right) the 3D multi-layer flower wall.

Since 2013, Li *et al.* have investigated a series of novel Q[8]-based host-guest supramolecular assemblies and proposed SOFs.^[107,108,125-128] They prepared the long rod-like polyaromatic guest molecules **G1** and **G2** (Figure 18 a and b) and exploited the high affinity of these motifs and their impact on binding stability and selectivity with Q[8]. For comparison, they also prepared three control compounds **G3-G5** (Figure 19 a-c).^[129] X-ray crystal structure analysis revealed that the Q[8] host interacted with guests **G1** or **G2** to form 2:2 host-guest inclusion complexes, and with guests **G3-G5** to form 1:2 host-guest inclusion complexes.

The solid-state structures of all these inclusion complexes have characteristic 2D or 3D frameworks. For example, the interaction of Q[8] with **G1** (Figure 18a) resulted in the formation of a 2:2 **G1**@Q[8] host-guest inclusion complex (Figure 18c). Figure 18f shows the **G1**@Q[8]-based 2D framework, in which adjacent **G1**@Q[8] inclusion complexes interact with each other via self-induced OSIQ (Figure 18e). The 2D framework can further arrange into a **G1**@Q[8]-based 3D framework via self-induced OSIQs. Two different types of single crystals of the products formed between Q[8] and **G2** (Figure 18b), which were obtained from 1:1 solutions containing $\text{Cd}(\text{NO}_3)_2$ and $[\text{CdCl}_4]^{2-}$ anions. Although prepared under different synthetic conditions, the interaction of Q[8] with **G2** resulted in the formation of similar 2:2 **G2**@Q[8] host-guest inclusion complex (Figures 18d), and both can form 2D frameworks (Figures 18i and l). In the $\text{Cd}(\text{NO}_3)_2$ case, the NO_3^- anions can not be observed in the framework (Figure 18i), whereas for $[\text{CdCl}_4]^{2-}$, the $[\text{CdCl}_4]^{2-}$ anions are observed in the framework (Figure 18l). Self-induced OSIQs formed between adjacent Q[8] molecules are the main driving force resulting in the formation of these 2D framework (Figure 18h). Anion-induced OSIQs formed between Q[8] molecules and adjacent $[\text{CdCl}_4]^{2-}$ anions and self-induced OSIQs formed between adjacent Q[8]s are the main driving force resulting in the formation of the other 2D

framework (Figure 18k). Figures 18j and m exhibit two 3D frameworks involving stacking of $\mathbf{G2@Q[8]/NO_3^-}$ -based 2D frameworks via mainly self-induced OSIQ, and $\mathbf{G2@Q[8]/[CdCl_4]^{2-}}$ -based 2D frameworks *via* mainly anion-induced OSIQ, respectively.

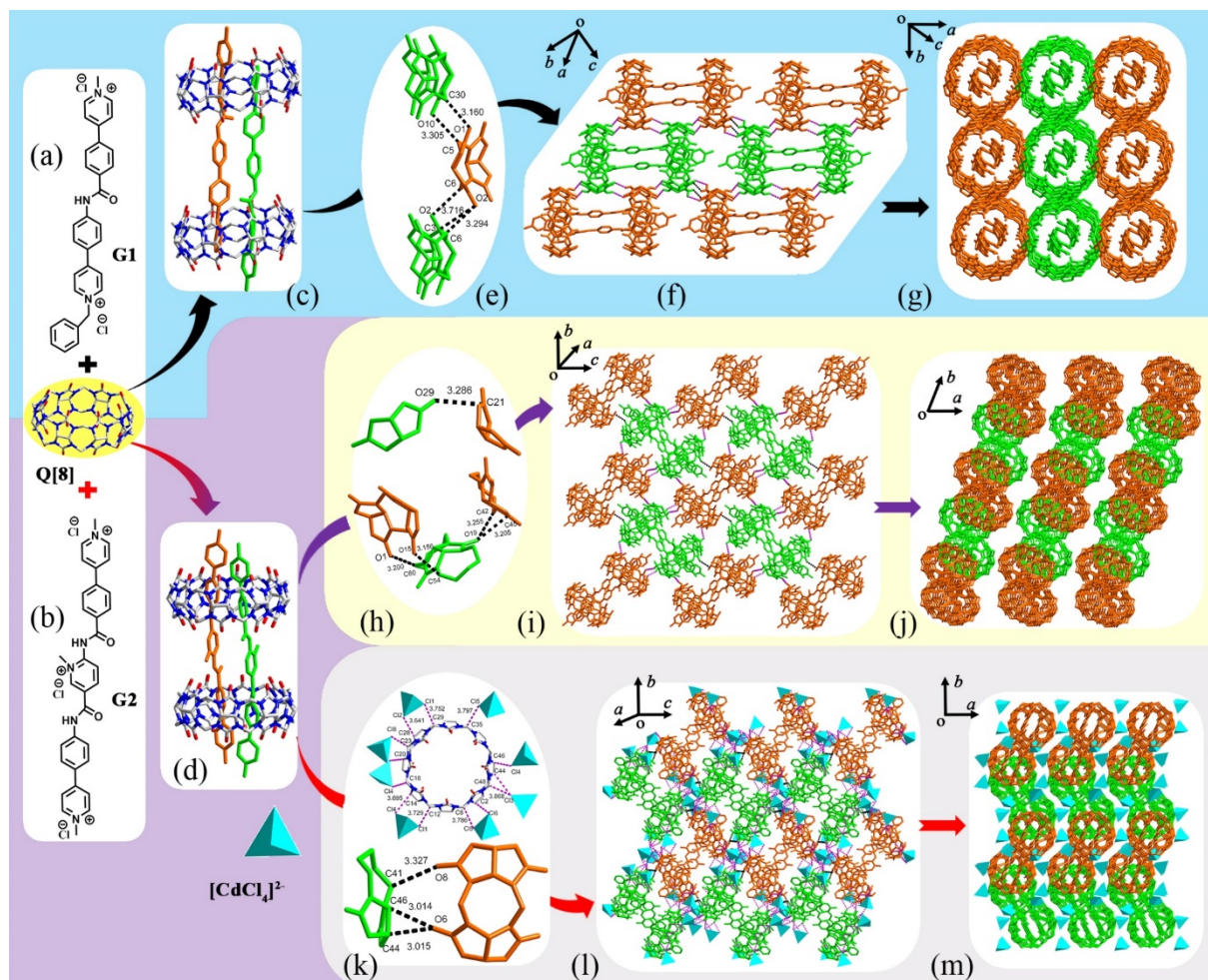


Figure 18. The chemical structure of (a) **G1** guest and (b) **G2** guest; (c) Crystal structure of the 2:2 **G1@Q[8]** host–guest inclusion complex; (d) the 2:2 **G2@Q[8]** host–guest inclusion complex formed in the presence of $\text{Cd}(\text{NO}_3)_2$ or $[\text{CdCl}_4]^{2-}$ anions; (e) self-induced OSIQs; (f) the **G1@Q[8]**-based 2D framework; (g) the 3D framework constructed by the **G1@Q[8]**-based 2D frameworks; (h) self-induced OSIQs; (i) the **G2@Q[8]**-based 2D framework; (j) the 3D framework constructed by the **G2@Q[8]**-based 2D frameworks; (k) anion- and self-induced OSIQs; (l) the **G2@Q[8]/[CdCl₄]²⁻**-based 2D framework; (m) the 3D framework constructed by the **G2@Q[8]/[CdCl₄]²⁻**-based 2D frameworks.

The interaction of Q[8] individually with **G3-G5** (Figure 19a-c) resulted in the formation of 1:2 host-guest inclusion complexes, in which each Q[8] molecule included two guest molecules, with the PhPy⁺ moiety of these guest molecules preferring to stack in an antiparallel manner in

the Q[8] cavity. [Figure 19d](#) shows the 1:2 **G3**@Q[8] inclusion complex, which further arranged into a 2D supramolecular organic framework ([Figure 19f](#)) via self-induced OSIQ ([Figure 19e](#)). The 2D frameworks can further stack into a 3D framework ([Figure 19h](#)) via anion-induced OSIQs formed between the $[\text{CdCl}_4]^{2-}$ anions and Q[8]s ([Figure 19g](#)). For the inclusion complexes of **G4**@Q[8] and **G5**@Q[8], the picolinic acid moieties of the included guests protrude from the portals of the Q[8] host due to the longer guest molecules not being entirely included in the host cavity ([Figures 19i](#) and [n](#)). The **G4**@Q[8] complexes arrange into 2D SOFs via self-induced OSIQs ([Figure 19j](#)). As can be seen from the 3D framework shown in [Figure 19m](#), the protruding picolinic acid moieties do not interact with the Q[8]s via aromatic-induced OSIQs, and so do not contribute to the construction of the 3D framework. The 3D framework is mainly formed via self-induced OSIQs ([Figure 19l](#)). **G5**@Q[8] can also arrange into 2D SOF ([Figure 19p](#)). In addition to the self-induced OSIQs, the driving forces also include interactions formed between the protruding picolinic acid moieties from four adjacent **G5**@Q[8] complexes perpendicular to each other via two orthogonal and one parallel $\pi \cdots \pi$ interaction(s) ([Figure 19o](#)). However, a **G5**@Q[8]-based 3D framework ([Figure 19r](#)) was constructed from the 2D framework mainly via anion-induced OSIQs formed between the $[\text{CdI}_4]^{2-}$ anions and Q[8] molecules ([Figure 19q](#)).

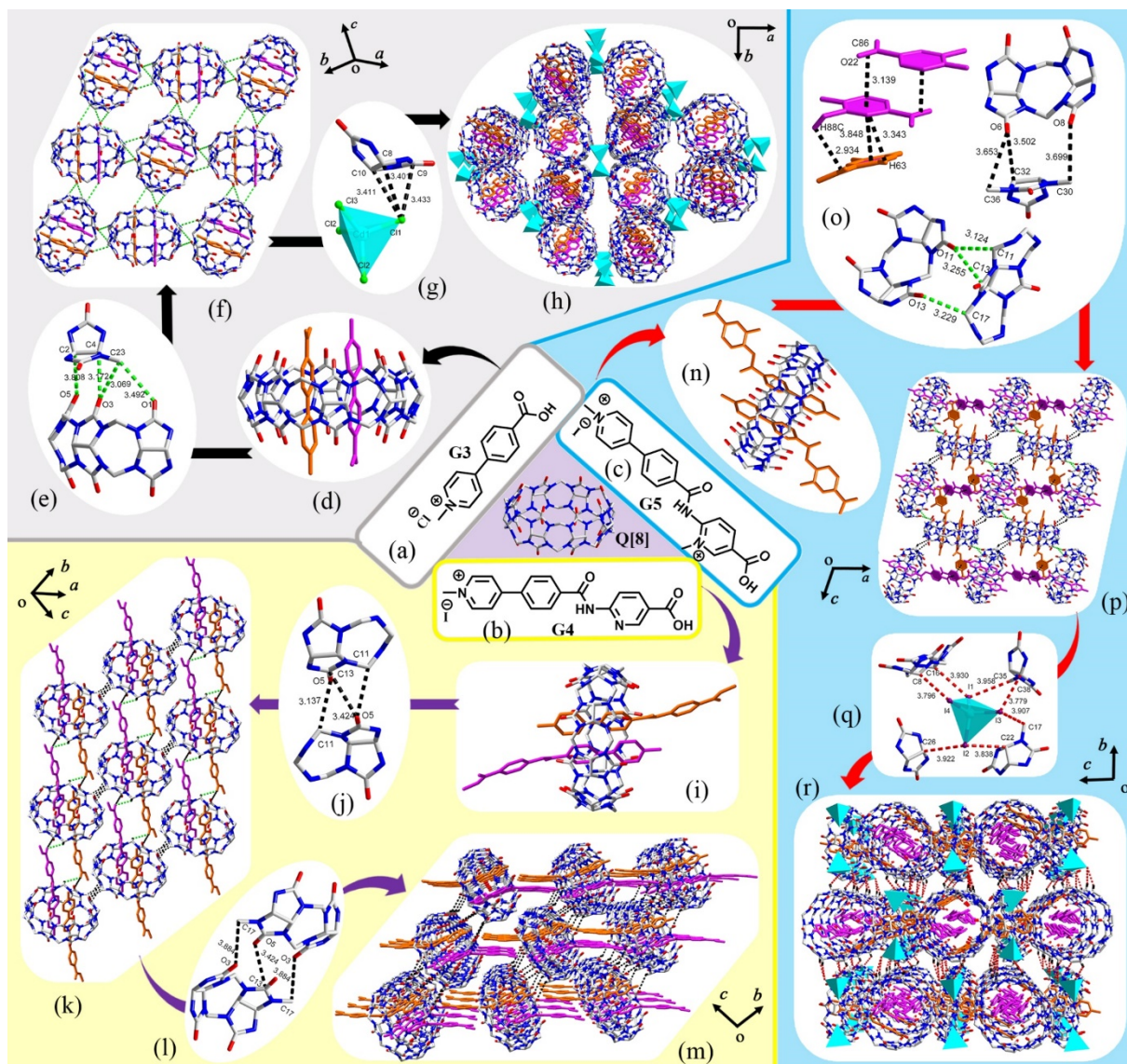


Figure 19. The chemical structure of (a) **G1** guest, (b) **G2** guest and (c) **G3** guest; (d) Crystal structure of the **G3@Q[8]** host-guest inclusion complex; (e) self-induced OSIQs; (f) the **G3@Q[8]/[CdCl₄]²⁻**-based 2D framework; (g) inorganic anion-induced OSIQs; (h) the 3D framework constructed from the **G3@Q[8]/[CdCl₃(H₂O)]⁻**-based 2D frameworks; (i) the **G4@Q[8]** host-guest inclusion complex; (j) self-induced OSIQs; (k) the **G4@Q[8]**-based 2D framework; (l) self-induced OSIQs; (m) the 3D framework constructed from the **G4@Q[8]**-based 2D frameworks; (n) the **G5@Q[8]** host-guest inclusion complex; (o) supramolecular interactions and self-induced OSIQs; (p) the **G5@Q[8]**-based 2D framework; (q) anion-induced OSIQs; (r) the 3D framework constructed from the **G5@Q[8]**-based 2D frameworks.

We have summarized the frameworks constructed using simple Q[*n*]-based host-guest inclusion complexes. In general, for full inclusion host-guest inclusion complexes, the whole or most of the guest molecule(s) are included in the cavity of the host Q[*n*] molecule and their frameworks are usually constructed via self-induced OSIQs formed between the simple host-

guest complexes (Figure 1a) or anion-induced OSIQs between the anions and the outer surface of the Q[n]s (Figure 1b). For simple pseudorotaxane-like host-guest inclusion complexes with protruding aromatic rings, the framework can be constructed by one or more supramolecular interactions, such as $\pi\cdots\pi$ stacking and C–H $\cdots\pi$ interactions between the aromatic rings protruding from the simple host-guest inclusion complexes and the outer surface of the Q[n]s (Figures 1c); $\pi\cdots\pi$ stacking and C–H $\cdots\pi$ interactions formed between the protruding aromatic rings from the simple host-guest inclusion complexes (Figures 1d). From the above summary, we can see that frameworks constructed from simple Q[n]-based host-‘object’ complexes are quite common phenomena. However, extensive research into the construction and potential applications of such frameworks has not attracted much attention.

2.2. Q[n]-based supramolecular organic frameworks constructed by host-guest inclusion supramolecular polymers

In general, Q[n]-based SOFs constructed by host-guest inclusion supramolecular polymers need to utilize guest molecules with multi-action sites and Q[n]s that can encapsulate the two action sites from two different guests. In 2013, Jiang *et al.* selected 5,10,15,20-tetrakis-(*N*-carboxymethyl-4-pyridinium) porphyrin tetrabromide (TCMePyP) with four carboxymethyl ends as the guest (Figure 20a) and TMeQ[6] as the host to prepare a SOF.^[130] It was found that the TCMePyP@TMeQ[6]-based framework not only exists in the solid-state, but also in solution. It is rare that a Q[6] host can include two action sites from two different guest molecules.^[122] However, it can be seen in the TCMePyP@TMeQ[6] case that the X-ray crystal structure shows each TMeQ[6] includes two carboxymethyl moieties from two TCMePyP molecules in the presence of Cu²⁺ cations, which coordinate with the porphyrin core and the carboxyl end interacts with the portal carbonyl oxygen atoms in the TMeQ[6] cavity via hydrogen bonding and π interactions (Figure 20b). Consequently, each TCMePyP interacts with four TMeQ[6]s, thus a combination of these host-guest inclusion complexes results in the formation of a TCMePyP@TMeQ[6]-based 2D framework (Figure 20c). Moreover, each grid

in the 2D framework is interlocked vertically into another grid in an adjacent 2D framework (Figure 20f) and the neighbouring TMeQ[6] molecules in the interlocked grids are connected via self-induced OSIQs (Figure 20d). The result is the formation of a TCMcPyP@TMeQ[6]-based 3D framework (Figures 20e and f). The introduction of metal ions or other guests can depolymerize this framework, and so it has the potential to be used for material delivery.

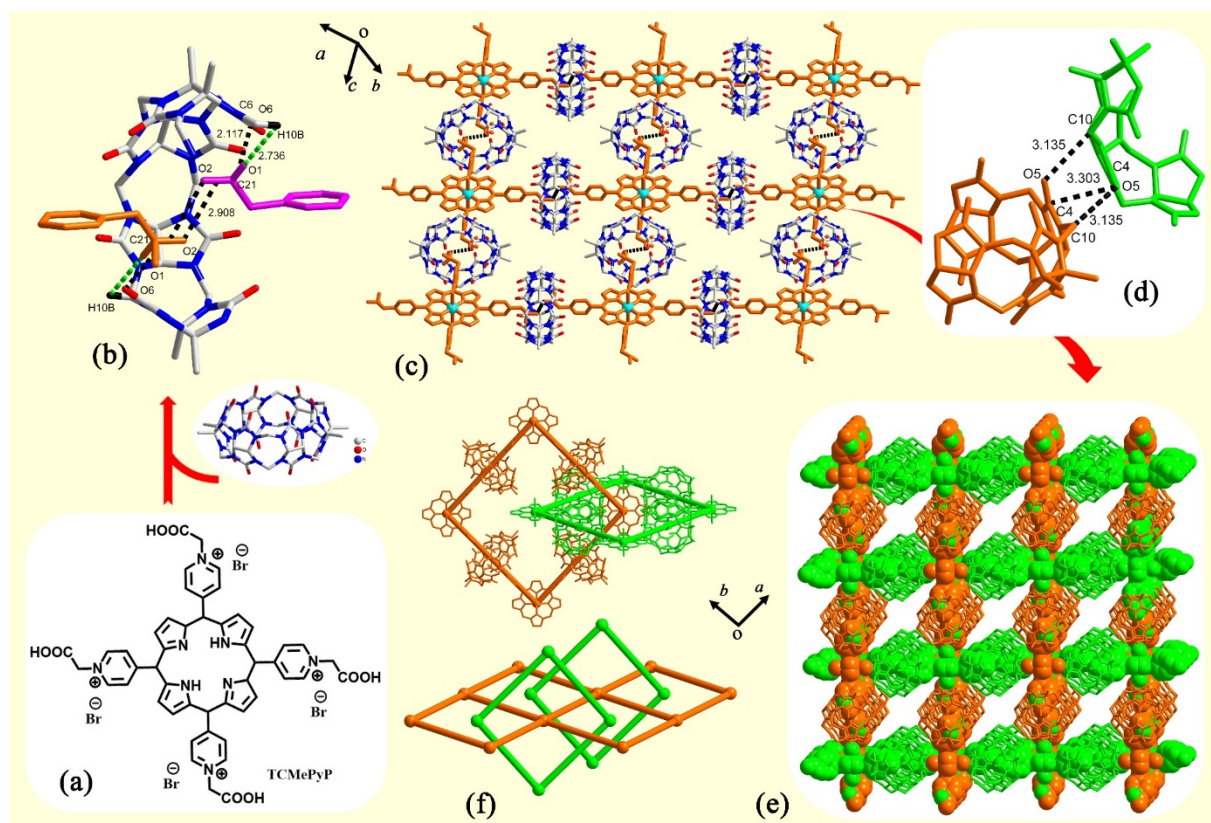


Figure 20. (a) Structure of the TCMcPyP guest molecule; (b) crystal structure of the inclusion complex consisting of the TMeQ[6] host with two carboxyl ends from two TCMcPyP guests; (c) the TCMcPyP@TMeQ[6]-based 2D framework; (d) self-induced OSIQs and (e) the TCMcPyP@TMeQ[6]-based 3D framework; (f) interlocked grids observed in the 2D framework.

Generally, it is difficult to obtain the crystal structure of Q[n]-based SOFs constructed by host-guest inclusion supramolecular polymers. Furthermore, the self-assembly of well-defined supramolecular polymers in solution has been a challenge in supramolecular chemistry. In 2013, Li *et al.* designed a rigid stacking-forbidden 1,3,5-triphenylbenzene compound that bears three 4,4'-bipyridin-1-ium (BP) units on the peripheral benzene rings and three hydrophilic bis(2-

hydroxy-ethyl)carbamoyl groups introduced at the central benzene ring to suppress 1D stacking of the triangular backbone and to ensure solubility in water (Figure 21a). By mixing this triangular preorganized guest with Q[8] in a 2:3 molar ratio in water, they initially obtained a solution-phase single-layer 2D supramolecular organic framework, which was stabilized by strong complexation of Q[8] with two BP units originating from adjacent guests (Figure 21b). The periodic honeycomb 2D framework was characterized by ¹H NMR spectroscopy, dynamic light scattering, X-ray diffraction, scanning probe and electron microscope techniques. The system was compared with the self-assembled structures of the control systems. Unlike the supramolecular organic frameworks constructed using simple Q[n]-based host-guest inclusion complexes, this Q[8]-based supramolecular organic framework was derived from the inclusion interaction of the Q[8] host with the triangular preorganized guest.^[106] On this basis, Li's group designed a guest molecule with similar structural features (Figure 21c), and obtained a structurally similar periodic honeycomb 2D framework upon reacting with the Q[8] host (Figure 21d).¹⁰⁵

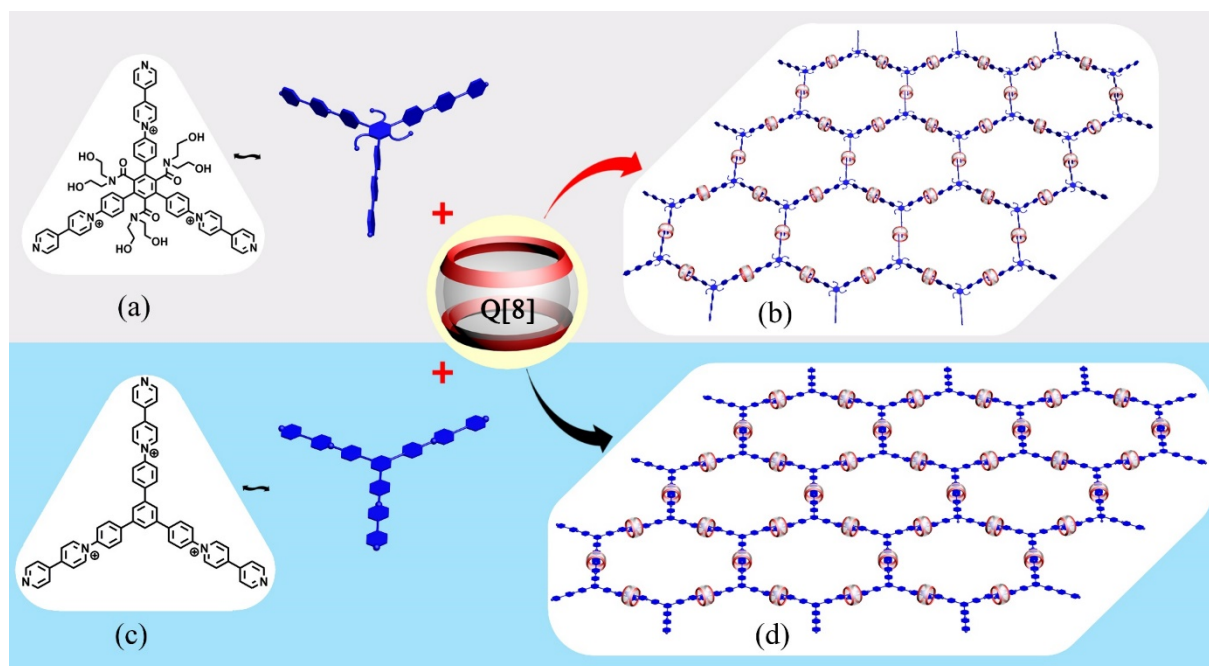


Figure 21. (a) Structure of the triangular preorganized guest molecule; (b) the periodic honeycomb 2D framework formed via the interaction of the triangular preorganized guest and Q[8]; (c) Structure of a similar triangular guest molecule; (d) the periodic honeycomb 2D framework formed through the interaction of the triangular preorganized guest and Q[8].

On the basis of using triangular guest molecules to construct Q[8]-based 2D SOFs, Li *et al.* also developed four action-site guest molecules and constructed highly soluble periodic supramolecular frameworks in a 3D space which possessed high solubility.^[104] For example, they reported an encapsulation motif, which involves the dimerization of two aromatic units within a Q[8], and which can be used to direct the co-assembly of a tetratopic guest with four 4-(4-methoxyphenyl)pyridin-1-ium units (Figure 22a) plus Q[8] into a periodic 3D supramolecular organic framework (Figure 22b), both in the solid state and in water. The periodicity of the supramolecular organic framework was supported by solution-phase small-angle X-ray-scattering and diffraction experiments. Upon evaporating the solvent, the periodicity of the framework was maintained in the porous microcrystals. Acting as a supramolecular ‘ion sponge’, the framework can absorb different kinds of anionic guests, including drugs, in both water and the microcrystals. The drugs absorbed in the microcrystals can be selectively released into water.

In 2017, Li *et al.* prepared a tetrahedral molecule containing four peripheral 4-phenylpyridinium units bearing four aldehyde groups (Figure 22c), which was used to co-assemble with Q[8] to afford a new water soluble 3D diamondoid system SOF-CHO (Figure 22d). An [Ru(BPY)₃]²⁺-attached acylhydrazine was used to afford another 3D diamondoid system SOF-CH=N-[Ru(BPY)₃] (Figure 22e), which was capable of the visible-light-induced recyclable heterogeneous conversion of azides to amines^[101]. In 2015, they also selected a tetraphenylethene (TPE) derivative bearing four 4,4'-bipyridin-1-ium (BP) ends at the periphery of the TPE core (Figure 22f). This was initially used by Zhao *et al.*,^[132] who prepared a 3D SOF with hexagon pores formed upon assembly of Q[8] and the tetraphenylethene guest molecule (Figure 22g).^[99] This ionic framework exhibited an affinity toward photosensitizers in water, and this will be discussed later.

Using the same strategy, Li *et al.* have reported other Q[n]-based SOFs, and in 2016 they established a new self-assembly strategy by designing a ligand bearing two PhPy units (Figure

22h), which can form a rigid octahedral Ru^{2+} complex (Figure 22i).^[102] This resulted in the first homogeneous 3D supramolecular framework (Ru-SOF) in water at room temperature prepared from the hexa-armed $[\text{Ru}(\text{bpy})_3]^{2+}$ -based precursor and a Q[8] host (Figure 22j). They further demonstrated that this 3D framework adsorbs anionic Wells-Dawson-type polyoxometalates (WD-POMs) in a one-cage-one-guest manner to afford a WD-POM@Ru-SOF hybrid assembly (Figure 22k). Upon visible-light (500 nm) irradiation, such hybrids enable fast multi-electron injection from the photo-sensitive $[\text{Ru}(\text{bpy})_3]_2$ units to redox-active WD-POM units, leading to efficient hydrogen production in aqueous and organic media. It is noteworthy that the structure of the above 3D SOFs have been confirmed by small-angle X-ray scattering and diffraction experiments, which was further corroborated by TEM imaging.

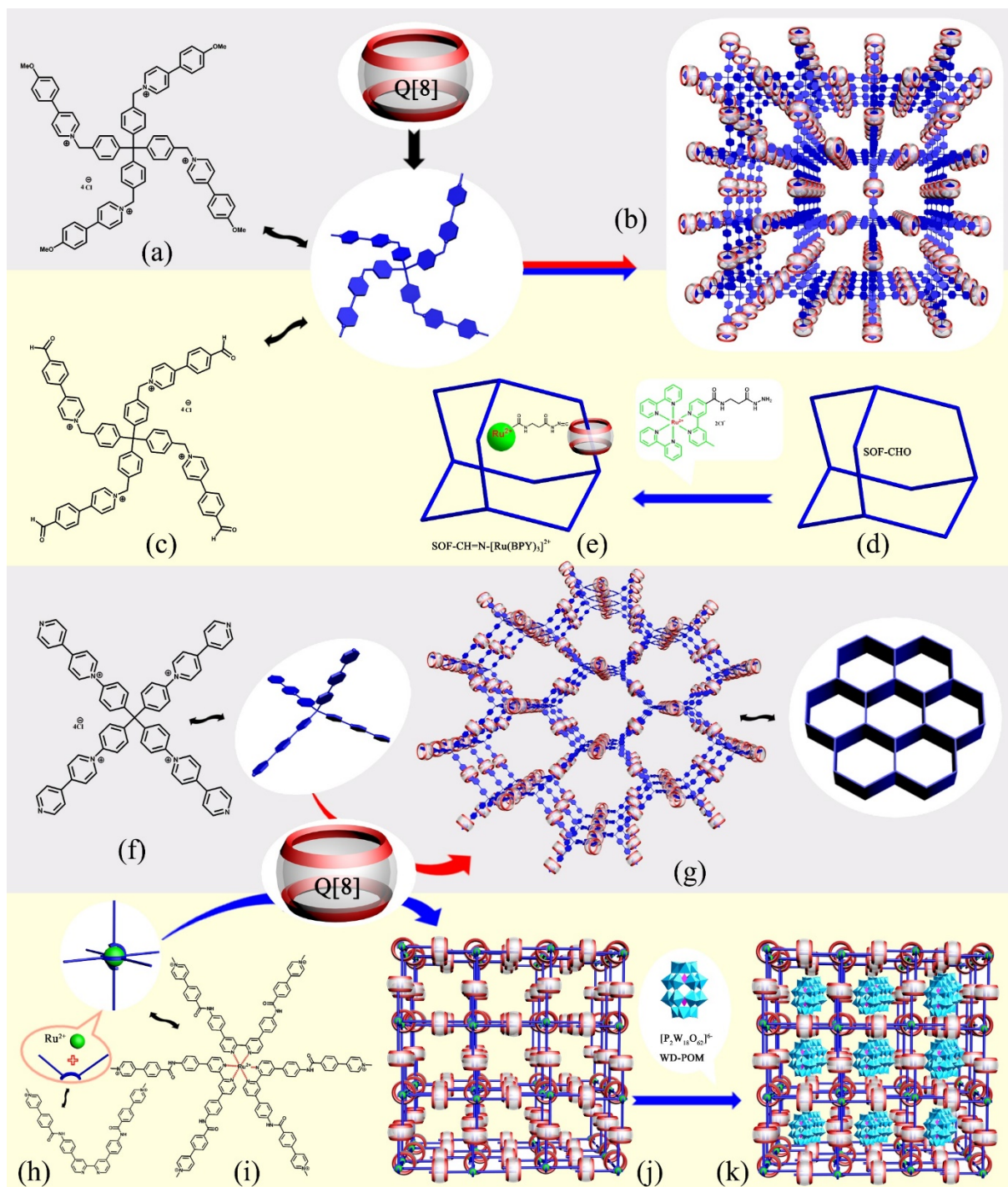


Figure 22. (a) Structure of the tetratopic guest bearing four 4-(4-methoxyphenyl)pyridin-1-ium (PP) units; (b) periodic 3D supramolecular organic framework formed via the interactions between the tetratopic guest and Q[8] molecules; (c) structure of the tetratopic guest bearing four 4-(4-methoxyphenyl)pyridin-1-ium (PP) units; the post-synthetic modification of the 3D diamondoid SOF-CHO with [Ru(BPY)₃]²⁺-attached acylhydrazine (d) used to afford SOF-CHQN-[Ru(BPY)₃]²⁺ (e); (f) structure of the TPE derivative bearing four 4,4'-bipyridin-1-ium (BP) ends; (g) 3D SOF constructed by Q[8] and the TPE derivative; (h) structure of the ligand bearing two PhPy units; (i) the rigid octahedral Ru²⁺ complex formed using the ligand bearing two PhPy units; (j) 3D supramolecular framework (Ru-SOF) formed by the hexa-armed [Ru(bpy)₃]²⁺-based precursor and Q[8] host; (k) WD-POM@Ru-SOF hybrid assembly.

By studying soluble Q[8]-based supramolecular organic frameworks, Li *et al.* initially proposed the concept of Q[*n*]-based SOFs^[106]. This enabled the establishment of construction strategies and characterization methods for Q[*n*]-based SOFs and detailed studies on adsorption and release mechanisms using Q[*n*]-based SOFs. Moreover, this opened up research on Q[8]-based SOFs, and many groups around the world have become active in this area in recent years. For example, the guest mentioned in reference 105, is a 1,3,5-triphenylbenzene derivative bearing three viologen (MV⁺) units on the peripheral benzene rings, and three hydrophilic bis(2-hydroxy-ethyl)carbamoyl groups. On combining this guest with the monomers shown [Figure 23a](#), linear flexible monomers bearing two 2,6-dioxy or 2-hydroxy-6-amino naphthalene subunits can be prepared via encapsulation with Q[8]. The donor–acceptor dimers formed between the electron-rich naphthalene subunits of the linear flexible monomer ([Figure 23b](#)) and the electron-deficient viologen subunits of the 1,3,5-triphenylbenzene compound allowed Li *et al.* to obtain two solution-phase single-layered 2D SOFs ([Figures 23c](#)). These can be tuned reversibly by changing the pH of the medium, and both SOFs exhibit activity against methicillin-resistant *Staphylococcus aureus*.^[105]

In 2015, Feng *et al.* reported the self-assembly of a host–guest enhanced donor–acceptor, consisting of a tris(methoxynaphthyl)-substituted truxene spacer (Np-Trx) ([Figure 23d](#)) and a naphthalene diimide substituted with *N*-methyl viologenyl moieties (MV-NDI) ([Figure 23e](#)) as donor and acceptor monomers, respectively. In combination with Q[8] as the host monomer, the result was the formation of monolayers of an unprecedented 2D SOF ([Figure 23f](#)).^[131] The participating molecules, featuring orthogonal solubility, self-assemble at a liquid–liquid interface, and yield exceptionally large-area, insoluble films. These films were analyzed using transmission electron microscopy, atomic force microscopy and optical microscopy, and were found to be monolayers with a thickness of 1.8 nm. They homogeneously covered areas of up to 0.25 cm² and had the ability to be free-standing over holes of 10 μm². [Characterization with ultraviolet–visible absorption spectroscopy, solid-state NMR spectroscopy, infrared](#)

spectroscopy, and grazing incidence wide-angle X-ray scattering allowed for the confirmation of the successful complexation of all three monomers toward an internal long-range order and gave a strong indication of the expected hexagonal superstructure. This result extends the existing variety of 2D soft nanomaterials prepared using a versatile supramolecular approach. The possibility of varying the functional monomers exists, and has the potential to increase their adaptability for different applications such as use in membranes, sensors, molecular sieves, and optoelectronics.

In 2016, Zhao *et al.* also designed a new building block by incorporating three 4-(*p*-methoxy-phenyl)-1-pyridinium (MPP) units at the periphery of a triphenylamine skeleton (Figure 23g).^[132] A 2D SOF was constructed via the co-assembly of the triphenylamine-based building block and Q[8] as the host. Fluorescence turn-off of the non-emissive building block was observed upon the formation of the 2D SOF (Figure 23h), which could be used for the highly selective and sensitive recognition of picric acid over a variety of other related nitroaromatic compounds by observing the fluorescence emission changes (Figures 23i).

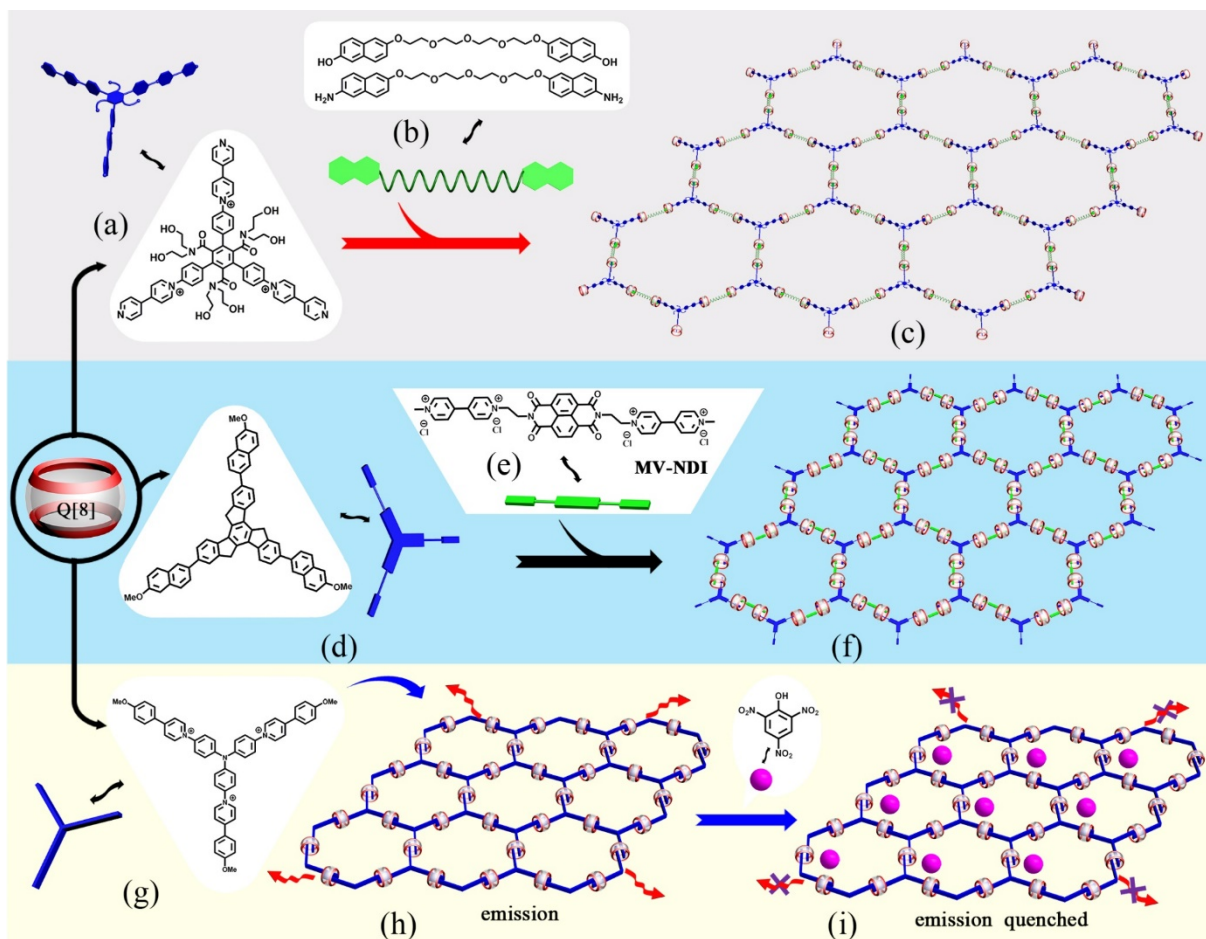


Figure 23. (a) Structures of the 1,3,5-triphenylbenzene derivative bearing electron-deficient viologen subunits and a linear flexible monomer bearing electron-rich naphthalene subunits; (b) the electron-rich naphthalene subunits of the linear flexible monomer; (c) 2D supramolecular framework; (d) structure of the tris(methoxynaphthyl)-substituted truxene spacer (Np-Trx) and (e) naphthalene diimide substituted with *N*-methyl viologenyl moieties (MV-NDI); (f) periodic 3D SOF formed via the interactions between Np-Trx, MV-NDI and the Q[8] host; (g) structure of the TPE derivative bearing four 4,4'-bipyridin-1-ium (BP) ends and (h) the single-layer 2D SOF; (i) the changes observed in the fluorescence intensity of the second 2D SOF upon the addition of different nitroaromatic compounds.

Zhao *et al.* have designed a tetraphenylethene (TPE) derivative with four 4,4'-bipyridin-1-ium (BP) ends at the periphery of the TPE core (Figure 24a).^[132] They demonstrated the formation of a novel single-layered 2D SOF with parallelogram pores assembled from the Q[8] host and the designed guest molecule. Moreover, the supramolecular assembly of this 2D SOF turned on the fluorescence emission of a non-emissive building block (Figure 24b), and the emission could be further enhanced by aggregation of the as-prepared 2D monolayers following

the addition of THF. This is because the aggregation of the single-layer SOFs resulted in further inhibition of the rotation of TPE units in the stacked layers (Figure 24c).

Liu *et al.* synthesized a tetraphenylethene (TPE) derivative with four 1,1-dimethyl-4,4'-bipyridinium dicationic (DMV²⁺) units (Figure 24d, shown in pink) and an azobenzene derivative (*trans*-2) (Figure 24e, shown in green), and reported a novel cross-linked 2D SOF (Figure 24g) constructed by a ternary host-guest molecular recognition motif formed between Q[8] and the above mentioned guest molecules in water.^[134] In addition, the presence of an azobenzene moiety acts as a photoswitch for this 2D SOF possessing UV-responsive properties, making it possible to achieve reversible polymer-oligomer transitions (Figure 24h). More interestingly, the introduction of tetraphenylethene endowed the crosslinked 2D SOF with interesting AIE properties.

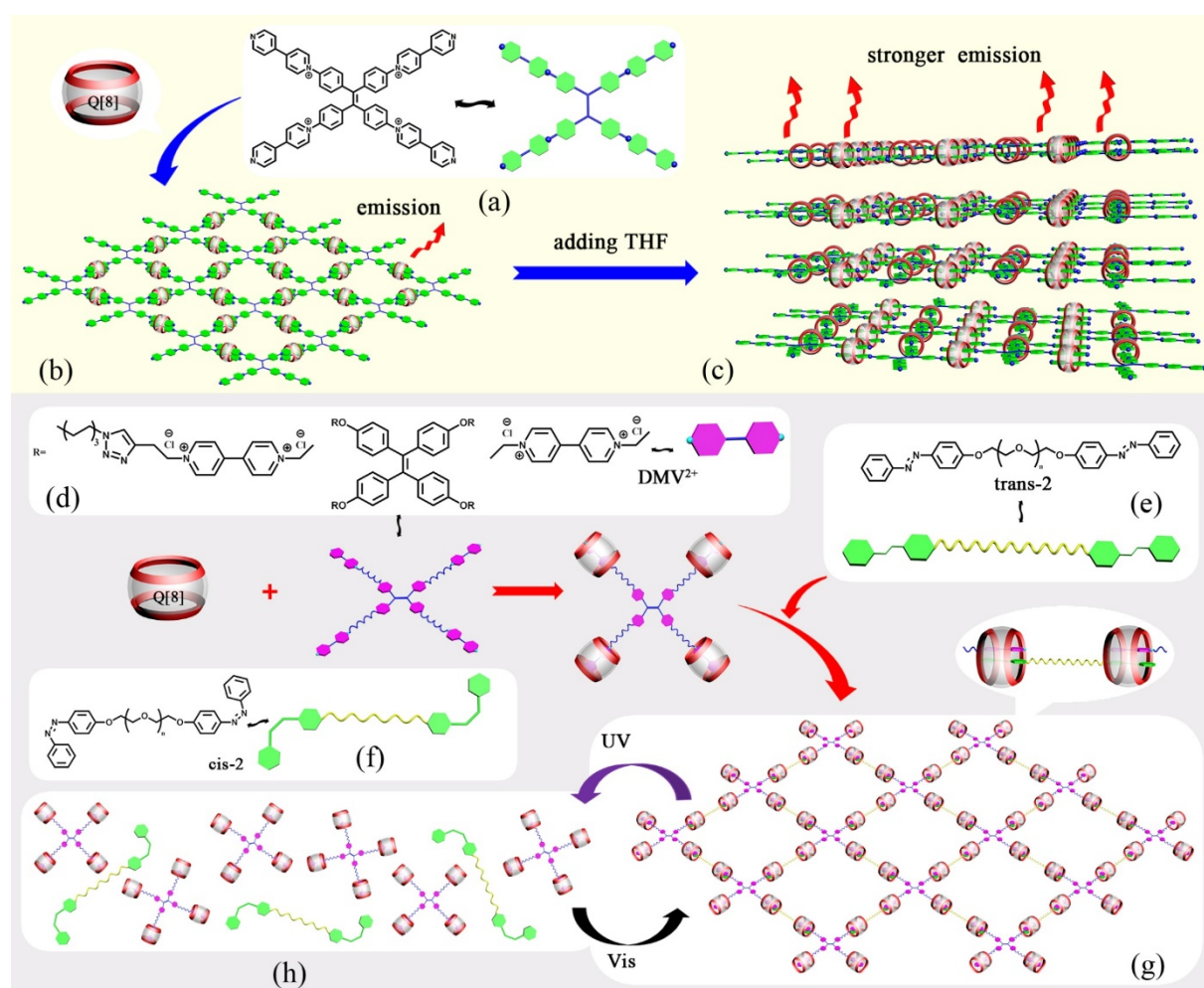


Figure 24. (a) Structure of the TPE derivative bearing four 4,4'-bipyridin-1-ium (BP) ends and (b) the single-layer 2D SOF; (c) the aggregation of the as-prepared 2D monolayers after the

addition of THF; (d) structure of the TPE derivative bearing four 1,1-dimethyl-4,4-bipyridinium dication (DMV^{2+}) units; the azobenzene guest molecule (e) *trans*-2 and (c) *cis*-2; (f) the cross-linked 2D SOF constructed using Q[8] and the above-mentioned guest molecules; (g) the UV-responsive 2D SOF.

We have utilized a twisted cucurbit[14]uril (*t*Q[14], Figure 25b) as a host, which bears two side cavities, in combination with a four-arm 5,10,15,20-tetrakis(*N*-butyl-4-pyridinium)porphyrin tetrabromide (TBPYP, Figure 25a) guest, and obtained a TBPYP@Q[14]-based SOF via host–guest interactions (Figure 25c).^[135] This represented the first example of a *t*Q[14]-involved host-guest SOF. The presence of a metal cation, such as K^+ , can disaggregate the original TBPYP@Q[14]-based SOF resulting in the formation of the coordination complex between Q[14] and K^+ .

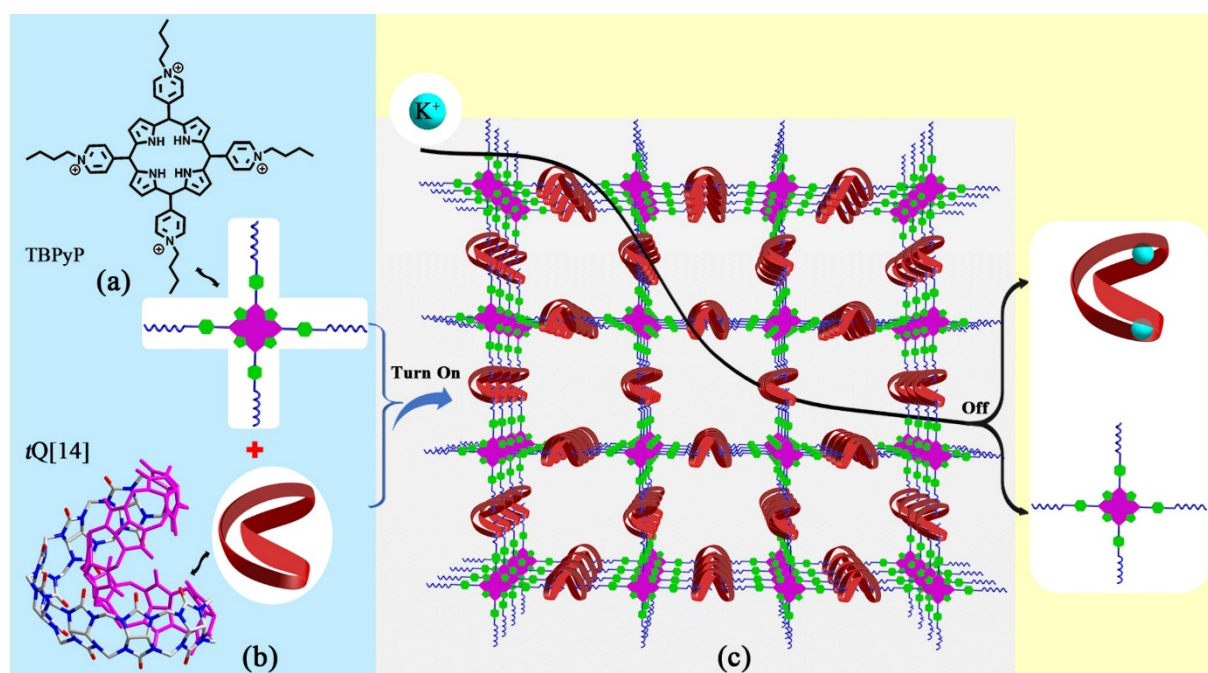


Figure 25. Structure of (a) *t*Q[14] host and (b) TBPYP guest; (c) single-layered 2D SOF constructed from *t*Q[14] and TBPYP.

In the above, we have summarized frameworks constructed from Q[*n*]-based host-guest inclusion complexes, in which the Q[*n*] molecule includes two moieties from two different guest molecules and the guest bears at least two binding sites. In general, the Q[*n*] host and guest molecules are organic compounds, and the inclusion interactions are supramolecular

interactions. Therefore, the resulting frameworks are generally SOFs.

2.3. Q[n]-based supramolecular organic frameworks constructed by host–guest exclusion complexes

In the process of summarizing Q[n]-based host-guest SOFs reported to date, we have mainly observed SOFs constructed from inclusion complexes, namely host-guest inclusion complexes formed by guest molecules entering the cavity of the Q[n] host. However, during the formation of the interactions between Q[n]s and guest molecules, there is another kind of product formed upon interaction between the guest and portal carbonyl oxygen atoms, namely Q[n]-based host–guest exclusion complexes. The driving forces are derived from hydrogen bonds and ion-dipole interactions formed between the guest and the portals of the Q[n] host. For example, in 2013, Jiang *et al.* prepared a host-guest exclusion complex, which was formed between cationic tetrakis(4-pyridyl)porphyrin species (H₆TPyP)⁴⁺·4Cl⁻ (Figure 26a) and TMeQ[6], which utilized hydrogen bonding and ion-dipole interactions (Figure 26b).^[136] Single crystal X-ray diffraction analysis revealed supramolecular features for this TMeQ[6]-(H₆TPyP)⁴⁺·4Cl⁻ host-guest compound. This represented the first example of a structurally characterized cucurbit[n]uril-porphyrin host-guest exclusion complex. Close inspection revealed that the exclusion interactions formed between TMeQ[6] and (H₆TPyP)⁴⁺·4Cl⁻ resulted in the formation of a 2D SOF (Figure 26c) and the extra interactions between (H₆TPyP)⁴⁺·4Cl⁻ and two adjacent TMeQ[6] molecules from the adjacent 2D SOFs via self- and aromatic-induced OSIQs (Figure 26d) led to the formation of a 3D porous framework (Figure 26e). Further investigation revealed that this cucurbit[n]uril-porphyrin supramolecular structure exhibited iodine adsorption behaviour.

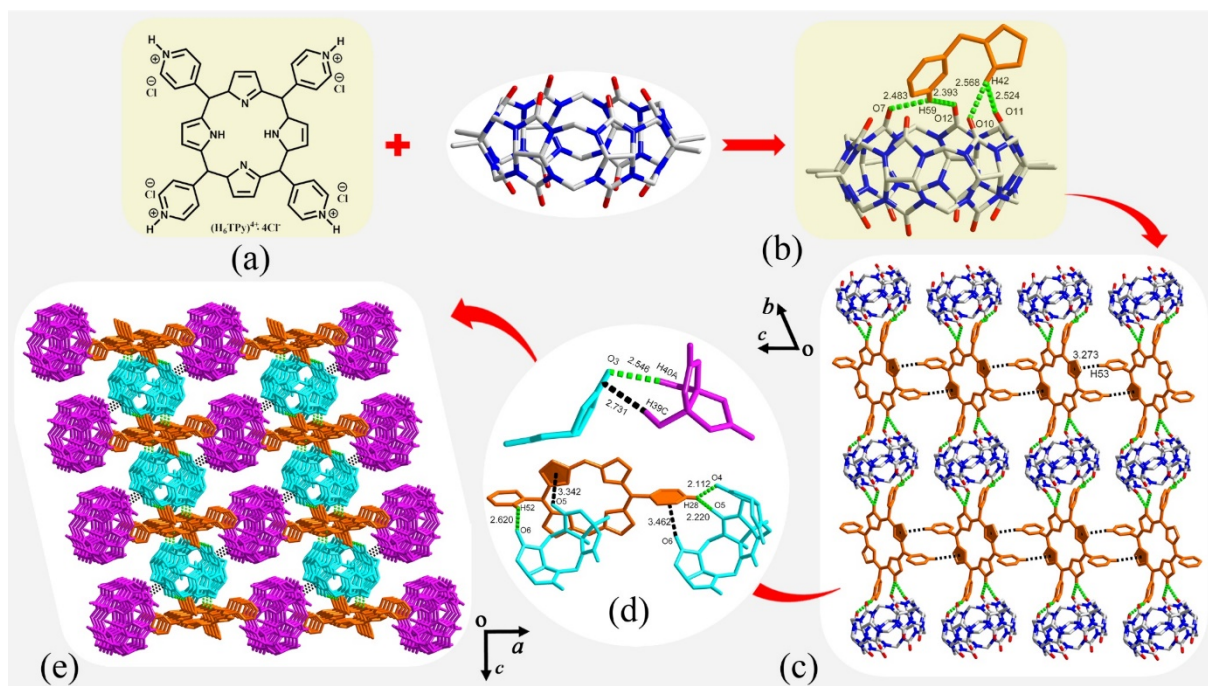


Figure 26. (a) Structure of the $(\text{H}_6\text{TPyP})^{4+}$ guest and crystal structure of the TMeQ[6] host; (b) exclusion interactions formed between $(\text{H}_6\text{TPyP})^{4+}$ and TMeQ[6]; (c) 2D SOF constructed by $(\text{H}_6\text{TPyP})^{4+}$ and TMeQ[6]; (d) detailed self- and aromatic-induced OSIQs formed between $(\text{H}_6\text{TPyP})^{4+}$ and TMeQ[6] from the adjacent 2D SOFs; (e) 3D SOF constructed from $(\text{H}_6\text{TPyP})^{4+}$ and TMeQ[6] (the H atoms, free water molecules and Cl^- anions are omitted for clarity).

In 2015, Wang *et al.* reported a new host $\text{Me}_{10}\text{TD}[5]$, which was prepared for the first time from propanediurea formaldehyde and was soluble in both water and common organic solvents.^[137] The exclusion interaction between 1,4-xylylene diamine dihydrochloride (Figure 27a) and $\text{Me}_{10}\text{TD}[5]$ (Figure 27b) via hydrogen bonding and ion-dipole interactions (Figure 27c) resulted in the formation of a linear supramolecular polymer. This can further arrange into a 2D SOF (Figure 27e) via the $\text{C}-\text{H}\cdots\pi$ interaction formed between the aromatic ring of the 1,4-xylylene diamine dihydrochloride guest and outer surface of the $\text{Me}_{10}\text{TD}[5]$ molecules of the adjacent linear polymers (Figure 27d). The $\text{Me}_{10}\text{TD}[5]$ /1,4-xylylene-based 2D SOFs can further stack into a 3D framework via anion-induced OSIQs formed between Cl^- anions and $\text{Me}_{10}\text{TD}[5]$ in the 2D SOFs (Figure 27f).

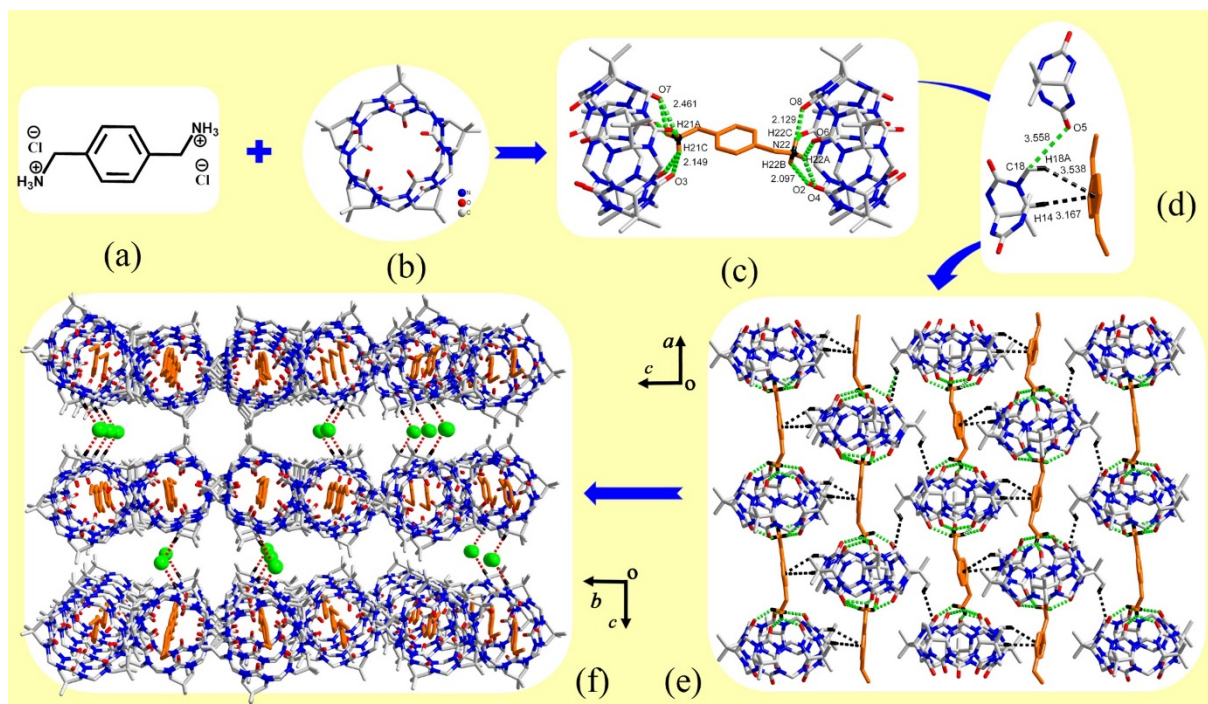


Figure 27. (a) Structure of the 1,4-xylylene diamine dihydrochloride guest and crystal structure of the Me₁₀TD[5] host; (c) Crystal structure of the exclusion complex formed using Me₁₀TD[5] and 1,4-xylylene diamine; (d) the C–H··· π interactions; (e) 2D SOF constructed by Me₁₀TD[5] and 1,4-xylylene diamine via C–H··· π interactions; (f) 3D SOF formed by the stacked Me₁₀TD[5]/1,4-xylylene-based 2D SOFs.

In 2016, Danylyuk *et al.* demonstrated the co-crystallization of the trypanocide drug diminazene (Figure 28a) with an acid-free Q[6], where the diminazene guest molecules are complexed *exo* to the host cavity, namely, as-formed host–guest exclusion complexes utilize hydrogen bonding and ion-dipole interactions.^[138] It is interesting to note that there are three different exclusion complexes: i) A 1:4 type of exclusion complex, in which each portal of the Q[6] molecule interacts with two diminazene molecules (Figure 28b); ii) a 1:5 type exclusion complex, in which one portal of the Q[6] molecule interacts with two diminazene molecules and another portal of the Q[6] molecule interacts with three diminazene molecules (Figure 28c); iii) a 1:6 type exclusion complex, in which each portal of the Q[6] molecule interacts with three diminazene molecules (Figure 28d). Thus, the Q[6] host and the diminazene guest can assemble into a novel 3D SOF (Figure 28f), in which the layers of the Q[6] molecules interact via self-induced OSIQs (Figure 28e) and the diminazene molecules are stacked alternatively.

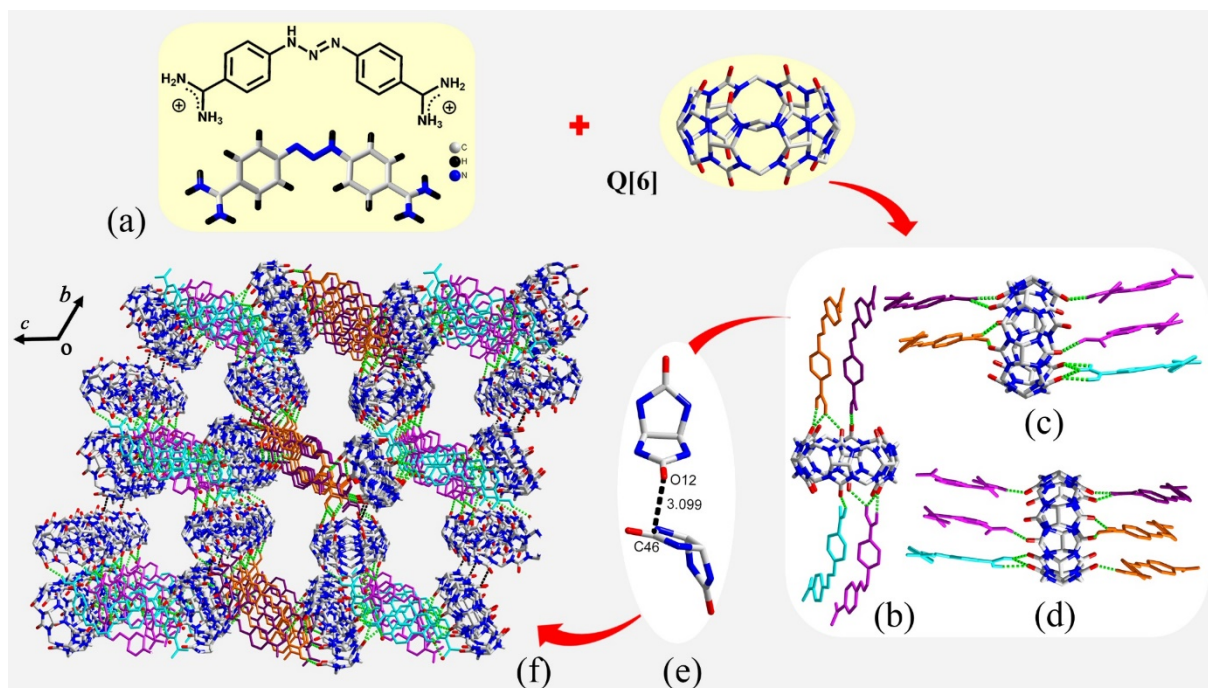


Figure 28. (a) Crystal structure of the trypanocide drug: diminazene; (b-d) the three types of exclusion complexes formed by Q[6] and diminazene; (e) self-induced OSIQs; (f) 3D SOF formed by the stacked Q[6] and diminazene layers.

More recently, Wang *et al.* have carried out much work on the synthesis of new Q[5] derivatives and have obtained several different exclusion SOFs using high-resolution TEM and DLS techniques. For example, they prepared a planar 120° triammonium salt, 1,3,5-tri(4-aminophenyl)benzene hydrochloride (TAPB, Figure 29a), and its hydrogen-bond-directed interactions with Me₁₀TD[5] (Figure 29b) resulted in the formation of a 2D hexagonal framework in water (Figure 29c).^[139] A new Q[5] derivative, CyP₅TD[5] (Figure 29d), and a TPE derivative (Figure 29e) were used to construct an exclusion SOF (Figure 29f) via portal interactions, namely, hydrogen bonding and ion-dipole interactions formed between protonated amine groups of the guest and portal carbonyl oxygen atoms. In addition, the supramolecular polymers exhibited a strong fluorescence in aqueous solution because of their aggregation-induced emission.^[140]

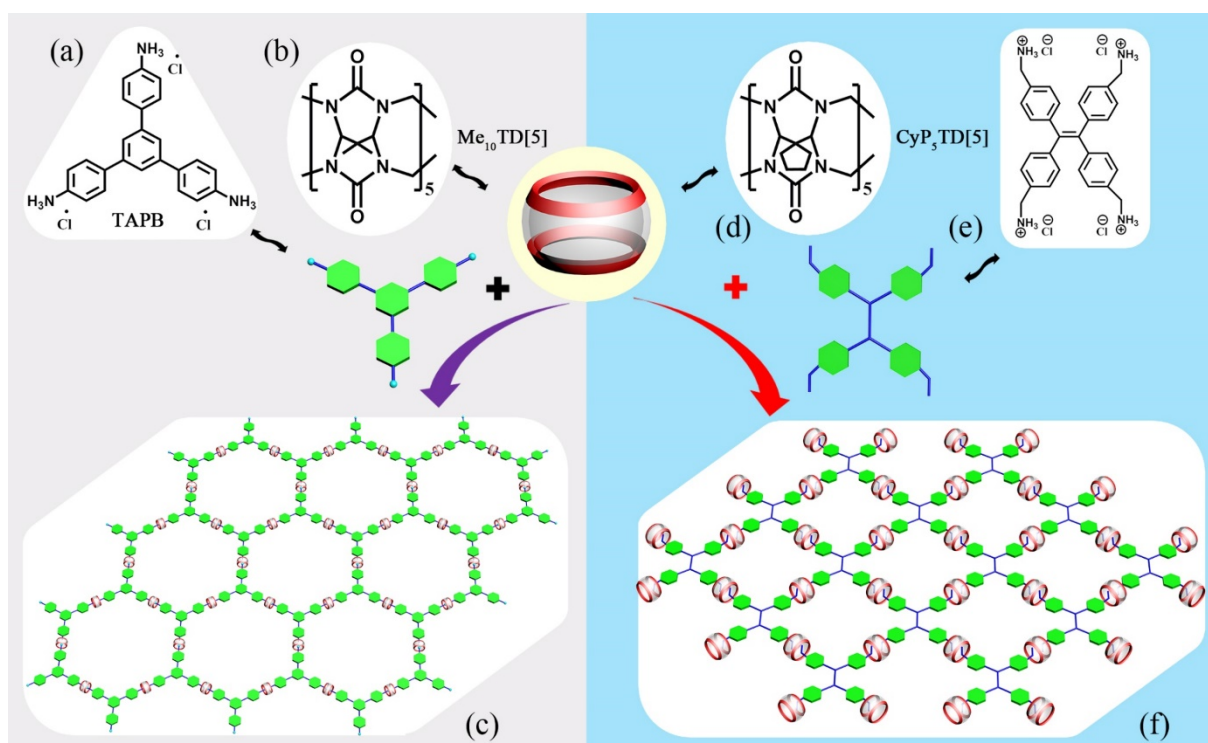


Figure 29. Structure of (a) the TAPB guest and (b) Me₁₀TD[5]; (c) 2D exclusion SOF constructed by Me₁₀TD[5] and the TAPB guest; structure of (d) new CyP₅TD[5] host and (e) the TPE derivative; (f) the 2D exclusion SOF constructed by CyP₅TD[5] and the TPE derivative.

As mentioned above, we have used the inclusion complex formed by *i*Q[6] and the dibutyl viologen guest (DBV²⁺, Figure 17a) to construct an *i*Q[6]-based SOF (Figure 17b). In this work, we also obtained an *i*Q[6]-based exclusion SOF constructed from *i*Q[6] and the ethyl viologen guest (DEV²⁺, Figure 30a) in the presence of [CdCl₂Br₂]²⁻ anions.^[124] Single crystal X-ray diffraction analysis revealed that a 3D honeycomb-like framework along the *c*-axis (Figure 30d) was constructed by the DEV²⁺@*i*Q[6] exclusion complexes and [CdCl₂Br₂]²⁻ anions (Figure 30c). This 3D framework can also be regarded as the stacking of numerous chains. Figure 30b shows a representative chain, which is constructed by the DEV²⁺@*i*Q[6] exclusion complexes and [CdCl₂Br₂]²⁻ anions formed via ion-dipole interactions between the portal carbonyl oxygen atoms and DEV²⁺ cations as well as static interactions between DEV²⁺ cations and [CdCl₂Br₂]²⁻ anions. Every six chains piled into a hexagon channel and there are numerous [CdCl₂Br₂]²⁻ anions located in the channel, in which the driving force is anion-induced OSIQ (Figure 30c).

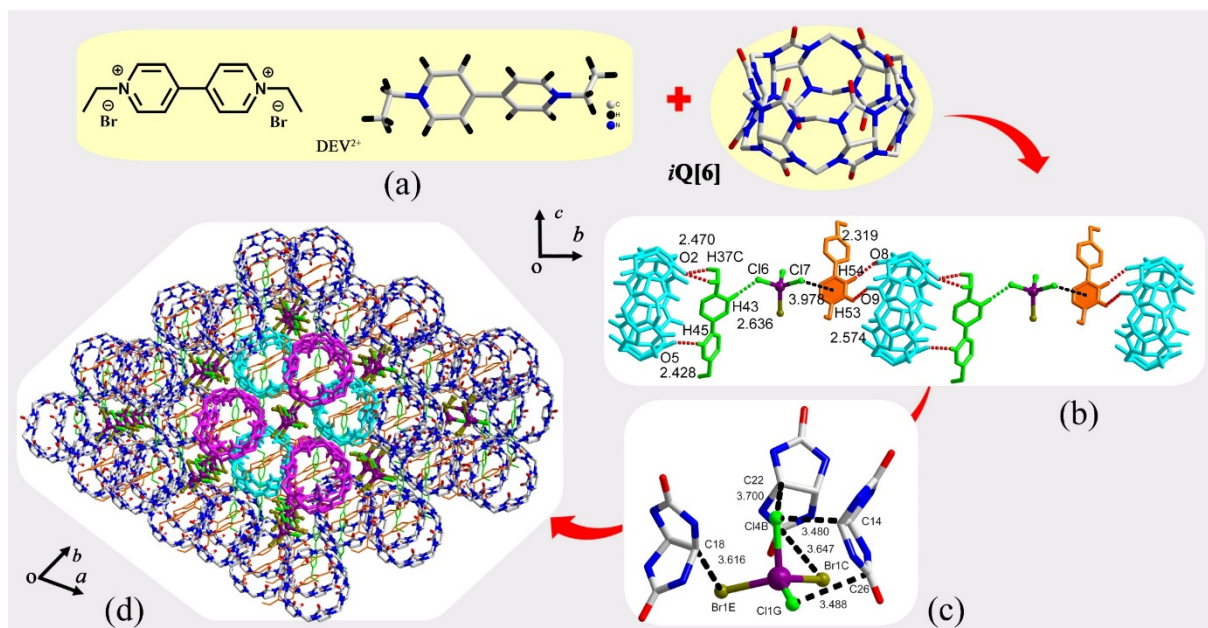


Figure 30 (a) Crystal structure of the DEV^{2+} guest; (b) 1D $\text{DEV}^{2+}@i\text{Q}[6]/[\text{CdCl}_2\text{Br}_2]^{2-}$ chain through the non-covalent interactions; (c) anion-induced OSIQs formed in the channel; (d) 3D framework constructed by the $\text{DEV}^{2+}@i\text{Q}[6]$ exclusion complexes and $[\text{CdCl}_2\text{Br}_2]^{2-}$ anions.

2.4. $\text{Q}[n]$ -based frameworks constructed by coordination of host–guest inclusion complexes with metal ions

We have discussed supramolecular frameworks based on $\text{Q}[n]$ -based host-guest complexes through supramolecular interactions, including host-guest interaction, the three kinds of OSIQs, $\pi\cdots\pi$ stacking and $\text{C}-\text{H}\cdots\pi$ interactions formed between the guest molecules, hydrogen bonding and ion-dipole interactions and other weak intermolecular interactions. Herein, we will introduce another kind of $\text{Q}[n]$ -based framework, which involves the coordination of $\text{Q}[n]$ -based host-guest complexes with metal ions ($\text{guest}@i\text{Q}[n]/\text{M}^{n+}$). According to the characteristics of the coordination products formed by $\text{Q}[n]$ -based host-guest complexes and metal ions, we will introduce the $\text{Q}[n]$ -based frameworks in the order of the 1D, 2D and 3D coordination polymers constructed.

2.4.1. Q[n]-based frameworks constructed by 1D guest@Q[n]/Mⁿ⁺ polyrotaxanes

Generally, the formation of Q[n]-based frameworks constructed by 1D guest@Q[n]/Mⁿ⁺ coordination polymers also needs to make use of extra supramolecular interactions, the most common one is OSIQ. For example, in 1997, Kim *et al.* were the first to construct guest@Q[n]/Mⁿ⁺-based frameworks.^[141] They demonstrated the first guest@Q[n]/Mⁿ⁺-based framework (Figure 31f), which was constructed from numerous 1D Q[6]-based coordination polymers (Figure 31c). The linear coordination polymer was constructed by threading Q[6] with *N,N*-bis(4-pyridylmethyl)-1,4-diaminobutane dihydronitrate (C4N4, Figure 31a), followed by coordination of the resulting inclusion complex (Figure 31b) with the Ag⁺ cation from Ag(CH₃C₆H₆SO₃). This 3D framework (Figure 31f) can also be considered as a stacking product of C4N4@Q[6]/Ag⁺-based 2D frameworks (Figure 31e). The driving forces that link the C4N4@Q[6]/Ag⁺-based 1D coordination polymers (Figure 31c) in the 2D framework include self-induced OSIQs formed with the Q[6] molecules of adjacent linear polymers (Figure 31d top); aromatic-induced OSIQs formed between protruding pyridyl rings and Q[6] molecules of adjacent linear polymers; the $\pi\cdots\pi$ stacking interactions formed between protruding pyridyl rings in adjacent linear polymers (Figure 31d bottom).

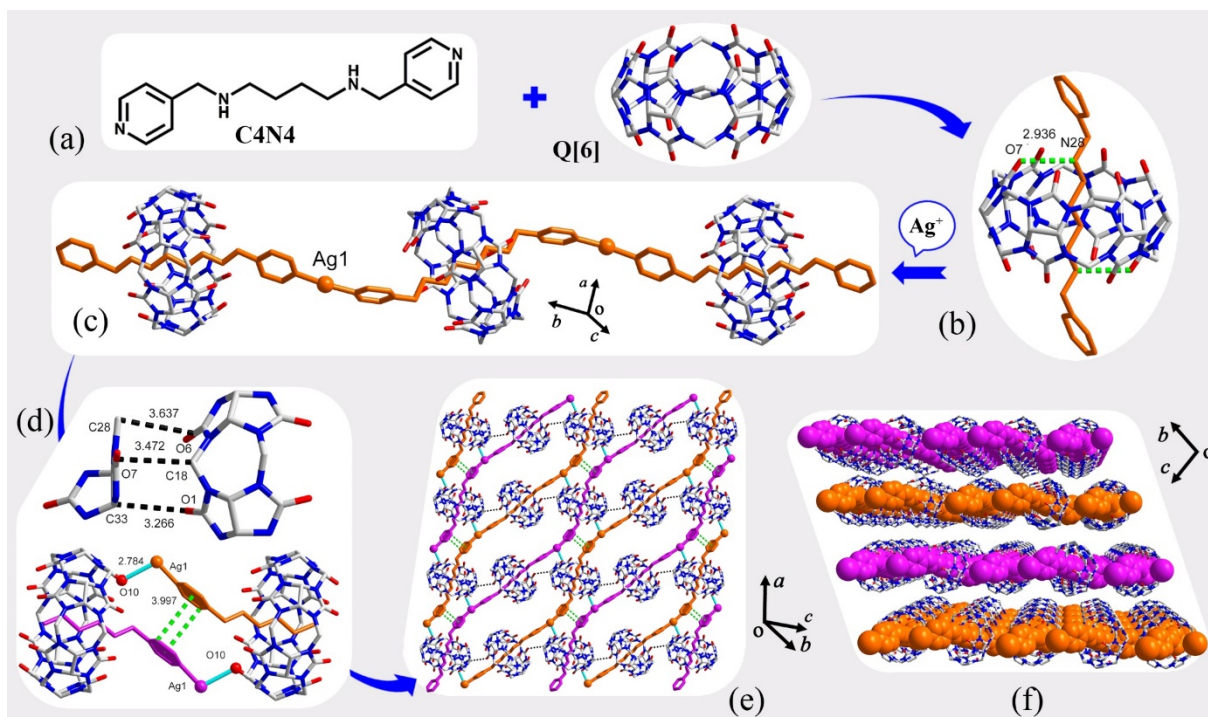


Figure 31. (a) The chemical structure of C4N4 guest; (b) the C4N4@Q[6] inclusion complex; (c) the C4N4@Q[6]-based 1D coordination polymer; (d) supramolecular interactions; (e) 2D framework constructed by the C4N4@Q[6]-based 1D coordination polymers; (f) the 3D framework constructed by the C4N4@Q[6]-based 1D coordination polymers.

In 2010, our group also utilized C4N4 (Figure 31a), and synthesized *N,N'*-bis(3-pyridylmethyl)-1,4-butanediamine (C4N3, Figure 32k) as guests in a system with TMeQ[6] as a host, and prepared three 3D frameworks, namely C4N4@TMeQ[6]/Cu²⁺-, C4N4@TMeQ[6]/Ag⁺- and C4N3@TMeQ[6]/Ag⁺-based 3D frameworks, constructed using C4N3@TMeQ[6]/Ag⁺, C4N4@TMeQ[6]/Cu²⁺ and the C4N4@TMeQ[6]/Ag⁺-based 1D polyrotaxanes, respectively.^[142] X-ray diffraction analyses revealed that all three polyrotaxanes basically have 1D linear chain structures possessing different shapes. For example, the adjacent protruding pyridyl nitrogens of the C4N4@TMeQ[6] inclusion complexes coordinate with the Cu²⁺ cations to form a 1D linear chain (Figures 32a) in C4N4@TMeQ[6]-Cu²⁺ based 3D frameworks; whereas each Ag⁺ cation links a protruding pyridyl nitrogen in the C4N4@TMeQ[6] inclusion complex and the portal carbonyl oxygen atoms of an adjacent TMeQ[6] molecule to form a 1D chain and $\pi\cdots\pi$ stacking interactions exist between adjacent

protruding pyridyl nitrogens in C₄N₄@TMeQ[6]-Cu²⁺ based 3D frameworks (Figures 32f). In the C₄N₃@TMeQ[6] system, the adjacent protruding pyridyl nitrogens of the C₄N₃@TMeQ[6] inclusion complexes coordinate with the Ag⁺ cations to form a bow-like 1D chain (Figure 32l) in the C₄N₃@TMeQ[6]-Ag⁺ based 3D frameworks. Moreover, the supramolecular interactions formed between the 1D linear chains in the above 3D frameworks are different. In the C₄N₄@TMeQ[6]-Cu²⁺ based 3D frameworks, the supramolecular interactions formed between adjacent 1D linear chains include C-H... π interactions (Figure 32b) formed between protruding pyridyl rings and TMeQ[6] molecules in adjacent 1D chains (Figure 32a), as well as self-induced OSIQs formed between TMeQ[6] molecules in adjacent 1D chains. This results in the formation of a 2D C₄N₄@TMeQ[6]/Cu²⁺-based framework (Figure 32c), and the self-induced OSIQ (Figure 32d) formed among the TMeQ[6] molecules in adjacent 2D frameworks result in the formation of a 3D C₄N₄@TMeQ[6]/Cu²⁺-based framework (Figure 32e). In the C₄N₄@TMeQ[6]-Ag⁺ based 3D frameworks, the supramolecular interactions formed between adjacent 1D linear chains include C-H... π interactions formed between protruding pyridyl rings and the substituted methyl groups of the TMeQ[6] molecules in adjacent 1D chains, as well as self-induced OSIQ (Figure 32g) formed between TMeQ[6] molecules in adjacent 1D chains (Figure 32f). In addition, hydrogen bonding interactions formed between coordinated water molecules in adjacent 1D chains result in the formation of a 2D C₄N₄@TMeQ[6]/Ag⁺-based framework (Figure 32h). However, the stacking of the 3D C₄N₄@TMeQ[6]/Ag⁺-based frameworks (Figure 32j) is derived from anion-induced OSIQs of the numerous nitrate anions (Figure 32i) formed between adjacent 2D C₄N₄@TMeQ[6]/Ag⁺-based frameworks. In the C₄N₃@TMeQ[6]-Ag⁺ based 3D frameworks, the supramolecular interactions formed between adjacent 1D linear chains include π ... π stacking of the protruding pyridyl rings (Figure 32m), as well as self-induced OSIQs formed between adjacent TMeQ[6] molecules in adjacent 1D chains. These supramolecular interactions result in the formation of a 2D C₄N₃@TMeQ[6]/Ag⁺-based framework (Figure 32n), which can further stack into a 3D

C4N3@TMeQ[6]/Ag⁺-based framework (Figure 32p) with the aid of self-induced OSIQ (Figure 32o).

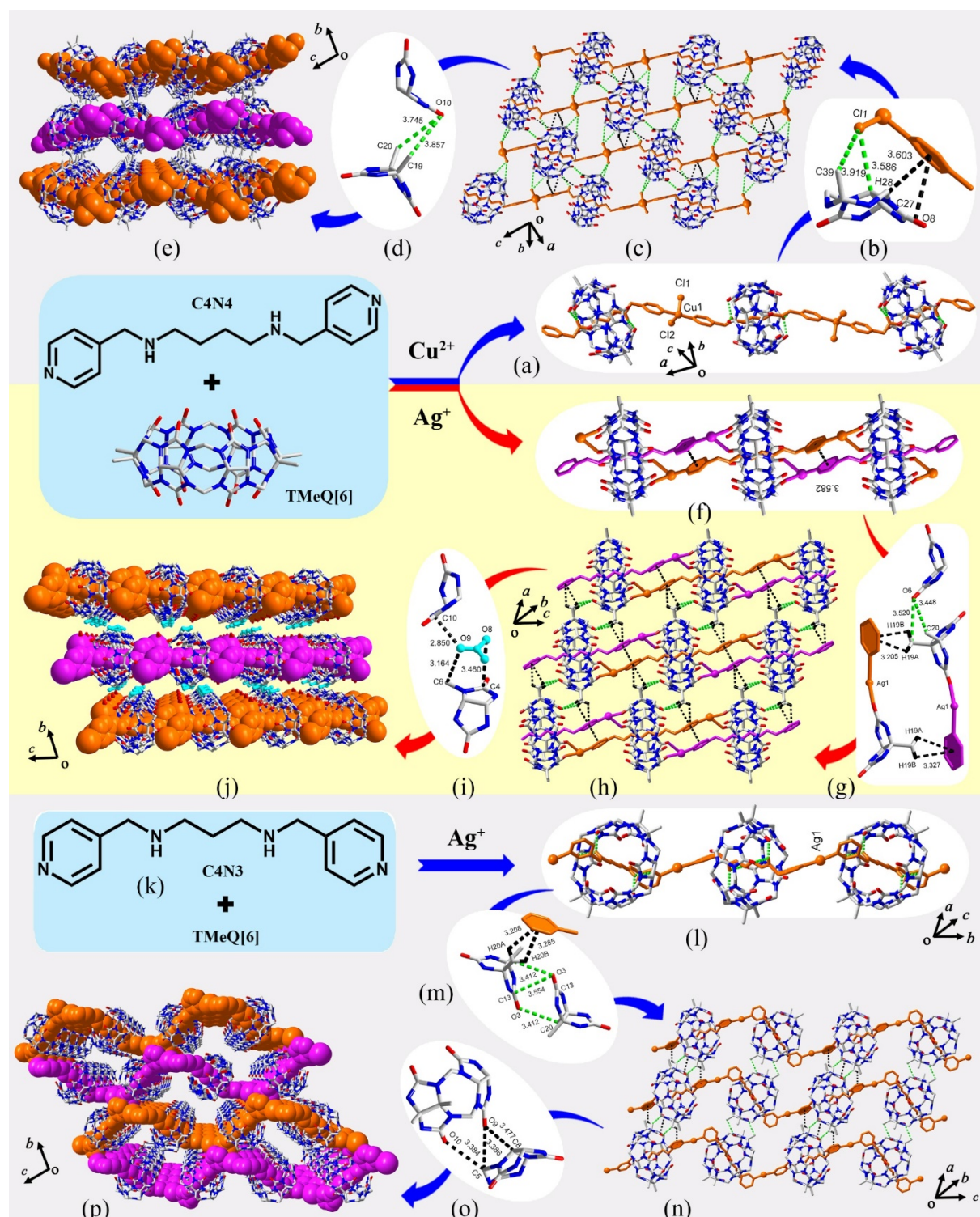


Figure 32. (a) The 1D C4N4@TMeQ[6]/Cu²⁺-based chain; (b) aromatic-induced OSIQs; (c) the 2D framework constructed by the 1D C4N4@TMeQ[6]/Cu²⁺-based chains; (d) self-induced OSIQs; (e) the 3D framework constructed by the 1D C4N4@TMeQ[6]/Cu²⁺-based chains; (f) the 1D C4N4@TMeQ[6]/Ag⁺-based chain; (g) self- and aromatic-induced OSIQs; (h) the 2D framework constructed by the 1D C4N4@TMeQ[6]/Ag⁺-based chains; (i) anion-induced OSIQs; (j) the 3D framework constructed by the 1D C4N4@TMeQ[6]/Ag⁺-based chains; (k) C4N3@TMeQ[6]/Ag⁺-based framework; (l) the 1D C4N3@TMeQ[6]/Ag⁺-based chain; (m) self-induced OSIQs; (n) the 2D framework constructed by the 1D C4N3@TMeQ[6]/Ag⁺-based chains; (o) self-induced OSIQs; (p) the 3D framework constructed by the 1D C4N3@TMeQ[6]/Ag⁺-based chains.

the chemical structure of C₄N₃ guest; (l) the 1D C₄N₃@TMeQ[6]/Ag⁺-based chain; (m) self- and aromatic-induced OSIQs; (n) the 2D framework constructed by the 1D C₄N₃@TMeQ[6]/Ag⁺-based chains; (o) self-induced OSIQs; (p) the 3D framework constructed by the 1D C₄N₃@TMeQ[6]/Ag⁺-based chains.

We have also used TMeQ[6] as a host in combination with the achiral ligand, C₆N₂ as a source of conformational chirality (Figure 33a) to prepare a TMeQ[6]-based helical polyrotaxane using AgNO₃.^[143] The product was characterized using X-ray crystallography and ¹H NMR spectroscopy. The chirality of the polyrotaxane was generated from the twisting of the hexylidene of the C₆N₂ “string” when bound within the hydrophobic cavity of TMeQ[6]. Two opposite chiral helical polyrotaxanes (Figures 33c and d) crystallized as a racemic 3D C₆N₂@TMeQ[6]/Ag⁺-based framework (Figure 33b). This can also be thought of as the product formed from alternatively stacked 2D frameworks made up of the same chiral helical polyrotaxanes (Figure 33g) and the 2D frameworks made up of the same opposite chiral helical polyrotaxanes (Figure 33h). Close inspection revealed that the driving forces include self-induced OSIQs formed between the TMeQ[6] molecules in adjacent chiral helical polyrotaxanes as well as anion-induced OSIQs formed between coordinated nitrate anions with TMeQ[6] molecules in adjacent chiral helical polyrotaxanes (Figures 33e and f).

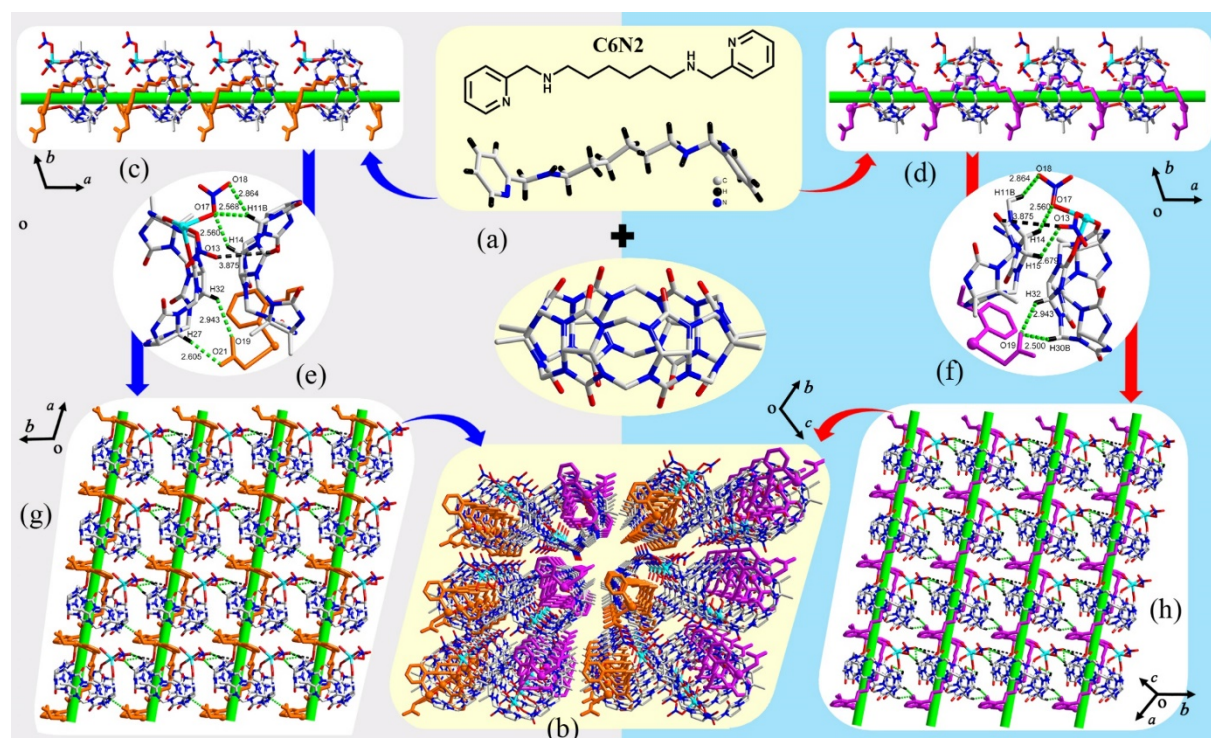


Figure 33. (a) Crystal structure of the C₆N₂ guest; (b) the 3D framework constructed using the same amount of chiral helical polyrotaxanes; (c, d) two C₆N₂@TMeQ[6]/Ag⁺-based opposite chiral helical polyrotaxanes; (e, f) the detailed OSIQs existing in the framework; (g, h) the 2D framework constructed by the same and opposite chiral helical polyrotaxanes.

In 2014, we used TMeQ[6] as the host, and C₄N₂ and C₆N₂ as guests (Figure 34a and b) to prepare another two frameworks, {Cd₂Cl₆(C₄N₂)@TMeQ[6]}·6H₂O and {Cd(H₂O)Cl₃(C₆N₂)@TMeQ[6]}·Cl₁₆H₂O, in the presence of CdCl₂. This resulted in not only polychloride anions, such as [Cd₂Cl₆]²⁻ and [Cd(H₂O)Cl₃]⁻, but also in coordination to the pyridyl moieties of the included guest molecules, resulting in the formation of C₄N₂@TMeQ[6]/[Cd₂Cl₆]Cd₂Cl₆²⁻ and C₆N₂@TMeQ[6]/[Cd(H₂O)Cl₃]⁻-based polyrotaxanes (Figure 34g and h).^[144] The adjacent polyrotaxanes were linked through C–H···π interactions formed between protruding pyridyl rings and TMeQ[6] molecules, as well as self-induced OSIQs (Figure 34d and i) formed among the TMeQ[6] molecules in adjacent polyrotaxanes, thereby forming 2D frameworks (Figure 34e and j). The 2D frameworks can further stack into 3D frameworks, in which the driving forces are mainly anion-induced OSIQs and self-induced OSIQs formed between adjacent polyrotaxanes (Figure 34f and k).

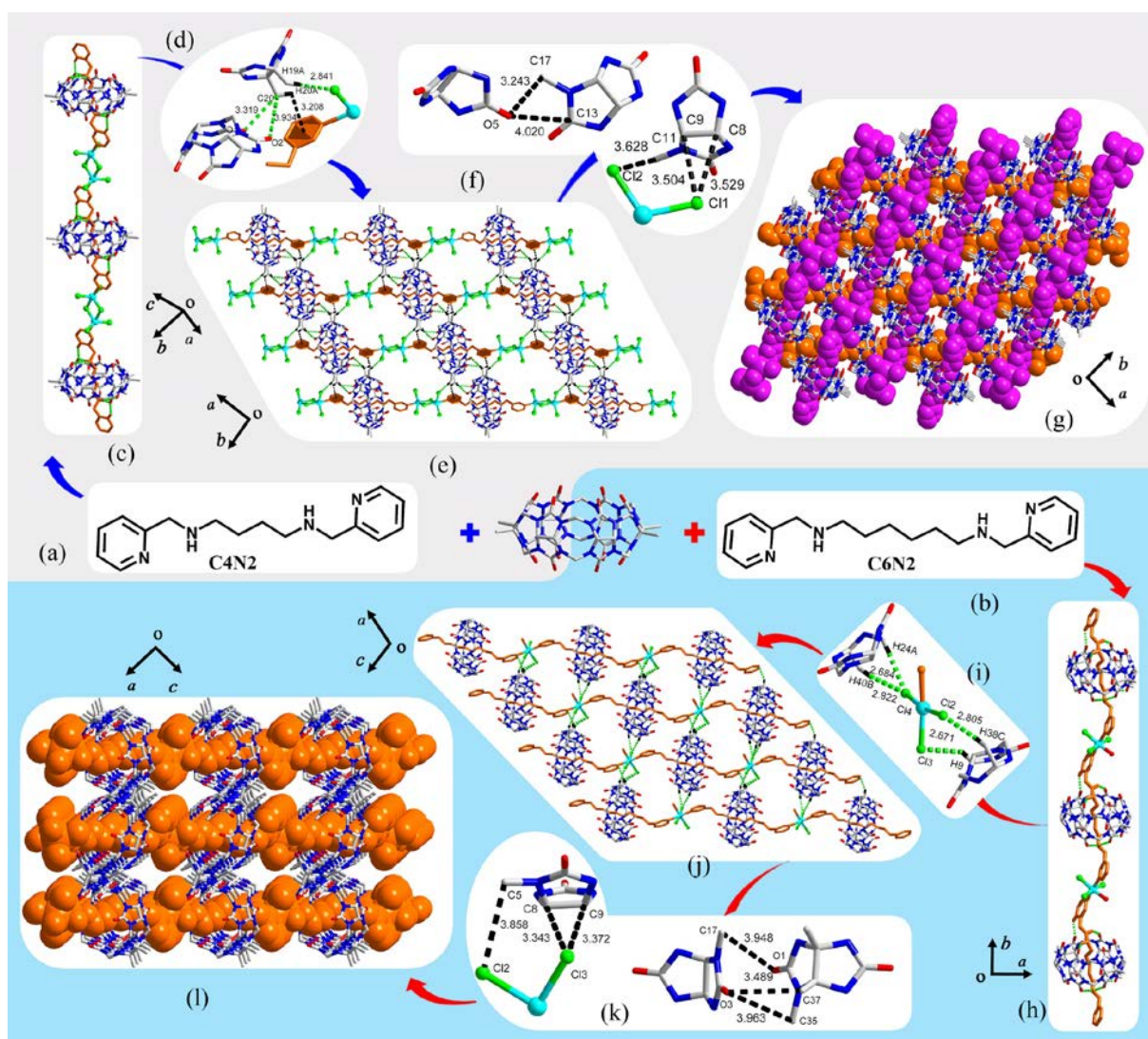


Figure 34. Chemical structure of (a) **C4N2** and (b) C6N2 guests; (c) the 1D **C4N2**@TMeQ[6]/[Cd₂Cl₆]²⁻-based polyrotaxanes; (d) C–H···π interactions and self-induced OSIQs; (e) the 2D framework constructed by the 1D **C4N2**@TMeQ[6]/[Cd₂Cl₆]²⁻-based polyrotaxanes; (f) Cl–H···π interactions and self-induced OSIQs; (g) the 3D framework constructed by the 1D **C4N2**@TMeQ[6]/[Cd₂Cl₆]²⁻-based polyrotaxanes; (h) the 1D C6N2@TMeQ[6]/[Cd(H₂O)Cl₃]⁻-based polyrotaxanes; (i) Cl–H···π interactions; (j) the 2D framework constructed by 1D C6N2@TMeQ[6]/[Cd(H₂O)Cl₃]⁻-based polyrotaxanes; (k) Cl–H···π interactions and self-induced OSIQs; (l) the 3D framework constructed by the 1D C6N2@TMeQ[6]/[Cd(H₂O)Cl₃]⁻-based polyrotaxanes.

In 2014, Shi *et al.* initiated studies on the coordination of Q[n]-based host-guest inclusion complexes with metal ions, especially actinides, and they constructed a series of Q[n]-based frameworks.^[145] For example, a pseudorotaxane precursor consisting of *N,N'*-bis(3-cyanobenzyl)-1,4-diammoniumbutane dinitrate (C4CN3, Figure 35a) and Q[6] was prepared. The pseudorotaxane was then reacted with uranyl-nitrate hexahydrate under hydrothermal

conditions to produce yellow platelet crystals, in which the C4CN3 was hydrolyzed *in situ* to form *N,N'*-bis(3-carboxylbenzyl)-1,4-diammoniobutane (C4CA3, Figure 35b) and the uranyl cations coordinated to the protruding carboxyl groups to form one dragon-like C4CA3@Q6/UrO₂²⁺-based polyrotaxane (Figure 35c). The adjacent polyrotaxanes were linked through C-H... π interactions formed between protruding pyridyl rings and Q[6] molecules in adjacent polyrotaxanes, namely aromatic-induced OSIQs, as well as the self-induced OSIQs (Figures 35d) formed among the Q[6] molecules in adjacent polyrotaxanes. This resulted in the formation of a 2D framework (Figures 35e), and these further stack into 3D frameworks (Figures 35g) mainly via self-induced OSIQs (Figures 35f) formed between the Q[6] molecules in adjacent 2D frameworks.

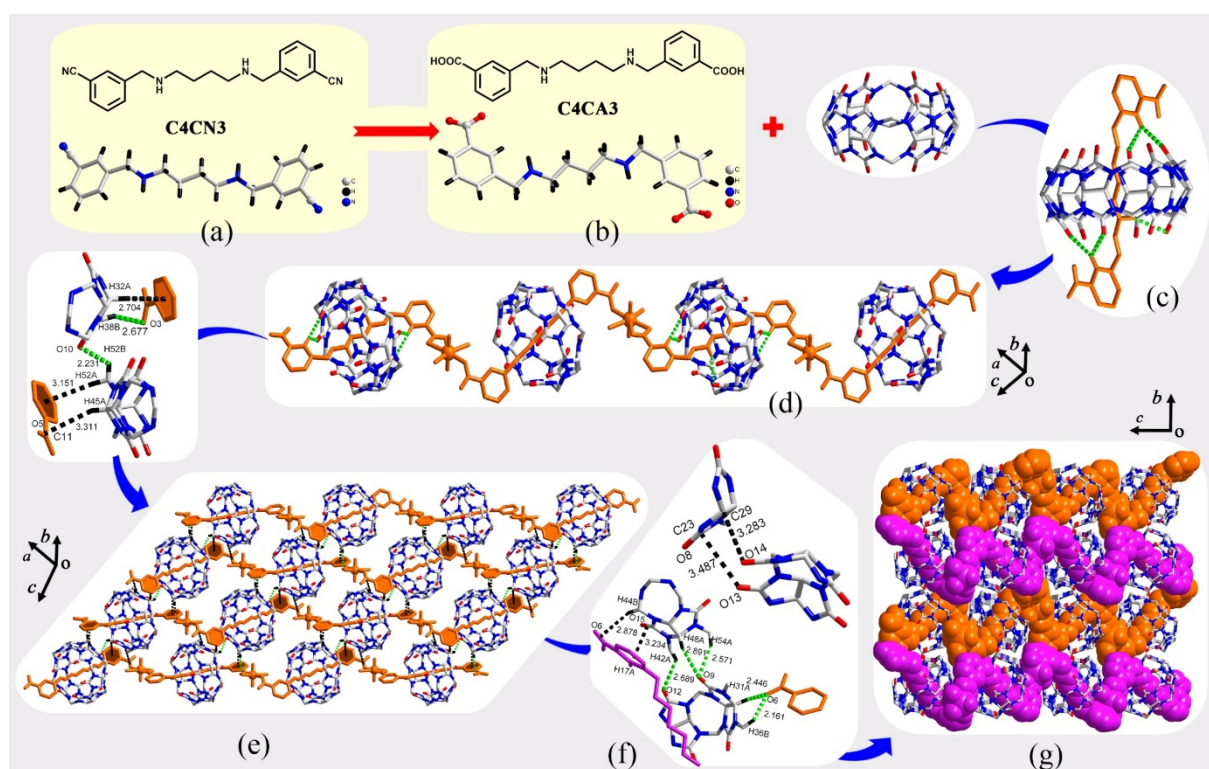


Figure 35. Crystal structure of (a) the precursor C4CN3 guest and (b) the transformed C4CA3 guest; (c) the 1D C4CA3@Q[6]/UrO₂²⁺-based polyrotaxane; (d) the OSIQs formed between the adjacent 1D polyrotaxanes; (e) the 2D framework constructed by the 1D C4CA3@Q[6]/UrO₂²⁺-based polyrotaxanes; (f) the OSIQs formed between the adjacent 2D frameworks; (g) the 3D framework constructed by the 1D C4CA3@Q[6]/UrO₂²⁺-based polyrotaxanes.

A year later, the same group used this strategy to prepare two pseudorotaxane precursors

comprised of *N,N'*-bis(3-cyanobenzyl)-1,4-diammoniopentane (C5CN3) or *N,N'*-bis(3-cyanobenzyl)-1,4-diammoniohexane (C6CN3) and Q[6], respectively.^[146] These pseudorotaxanes were then reacted with uranyl-sulfate hydrate under hydrothermal conditions to afford pseudorotaxanes (C5CA3, Figure 36a; C6CA3, Figure 36b). The uranyl ions formed tetramers and coordinated with the protruding carboxyl groups of the guests resulting in the formation of C5CA3@Q6/(UO₂)₄-based and C6CA3@Q6/(UO₂)₄-based polyrotaxane chains, respectively (Figures 36c and h). As for the above mentioned guest@Q[*n*]/Mⁿ⁺-based polyrotaxane chains, these uranyl systems can stack into similar guest@Q[*n*]/Mⁿ⁺-based 2D frameworks (Figures 36e and j) by utilizing similar supramolecular interactions. For example, in the C5CA3@Q6/(UO₂)₄- and C6CA3@Q6/(UO₂)₄-based 2D frameworks, besides the typical aromatic-induced OSIQs formed between protruding benzyl units and Q[6]s in adjacent chains, a type of special OSIQ (Figures 36d and i) was formed. In particular, multiple C–H⋯O hydrogen bonds exist between tetrameric uranyl units and C–H_{methine or methylene} units of Q[6] molecules. In addition, the C5CA3@Q6/(UO₂)₄- and C6CA3@Q6/(UO₂)₄-based 2D frameworks can stack into 3D frameworks via self-induced OSIQs (Figures 36f and k).

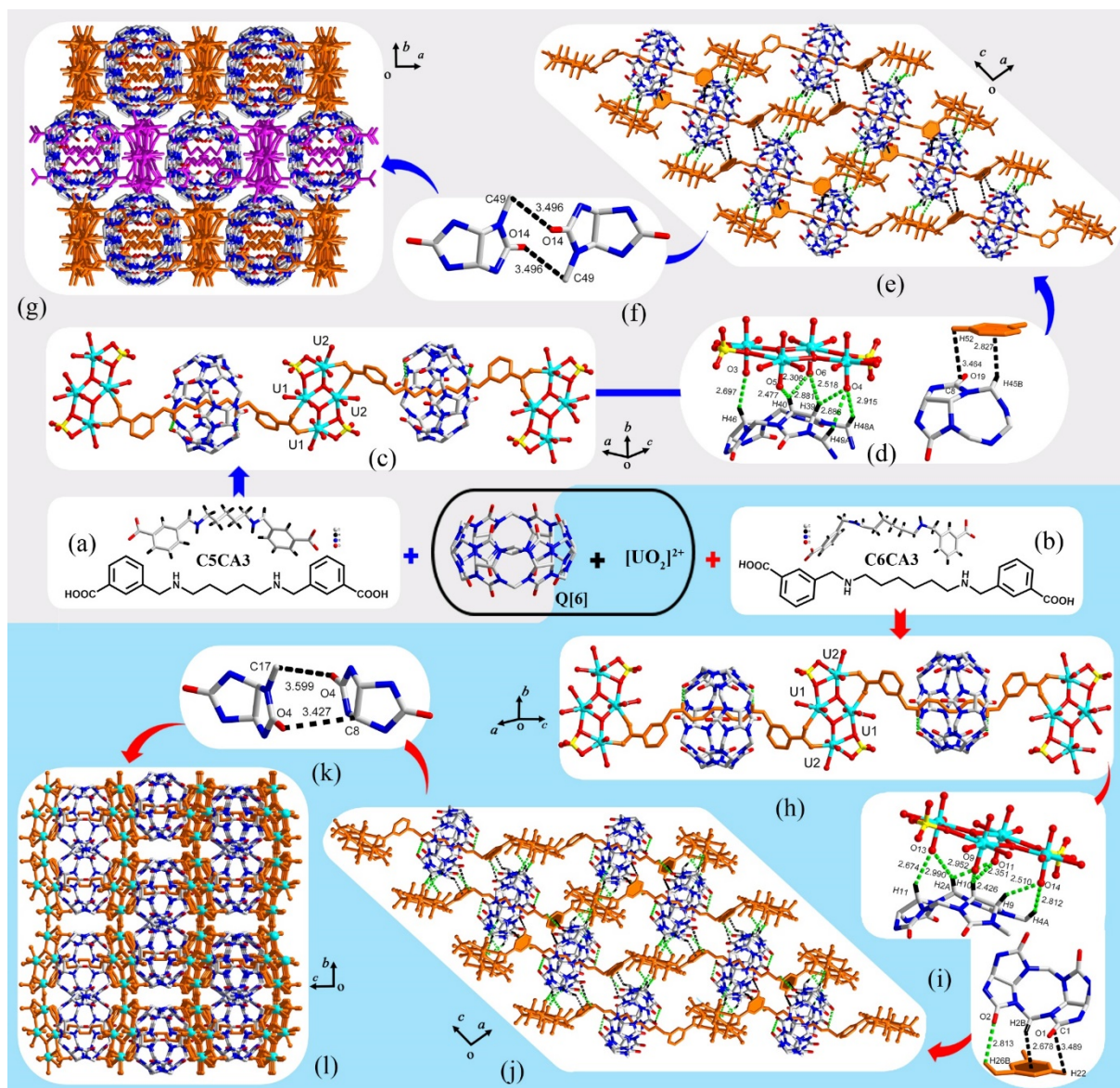


Figure 36. Crystal structures of (a) C5CA3 and (b) C6CA3 guests; (c) the 1D C5CA3@Q[6]/(UO₂)₄-based polyrotaxane; (d) aromatic-induced OSIQs and H-bonding interactions; (e) 2D framework constructed by the 1D C5CA3@Q[6]/(UO₂)₄-based polyrotaxanes; (f) self-induced OSIQs; (g) the 3D framework constructed by the 1D C5CA3@Q[6]/(UO₂)₄-based polyrotaxanes; (h) the 1D C6CA3@Q[6]/(UO₂)₄-based polyrotaxanes; (i) aromatic-induced OSIQs and H-bonding interactions; (j) the 2D framework constructed by the 1D C6CA3@Q[6]/(UO₂)₄-based polyrotaxanes; (k) self-induced OSIQs; (l) the 3D framework constructed by the 1D C6CA3@Q[6]/(UO₂)₄-based polyrotaxanes.

Shi *et al.* have utilized the known 1,1'-(hexane-1,6-diyl)bis(4-(ethoxycarbonyl)pyridin-1-ium) bromide salt as a guest ([C6BPCA]Br₂, Figure 37a),^[147, 148] and the larger cucurbit[*n*]uril, Q[7] as the host to obtain a C6BPCA@Q[7]/UO₂-based polyrotaxane chain (Figure 37b) upon reacting [C6BPCA]Br₂ and Q[7] with uranyl cation under hydrothermal conditions. These

C6BPCA@Q[7]/UO₂-based polyrotaxane chains can stack into 2D frameworks (Figures 37d) via self-induced OSIQs (Figures 37c) and the 2D frameworks can also stack into a C6BPCA@Q[7]/UO₂-based 3D framework (Figure 37f). Close inspection showed the main supramolecular interactions in the 3D frameworks included self-induced OSIQs formed between adjacent Q[7] molecules, as well as C–H···O hydrogen bonding interactions formed between the uranyl cations and C–H_{methine or methylene} units in the Q[7]s (Figure 37e).^[147]

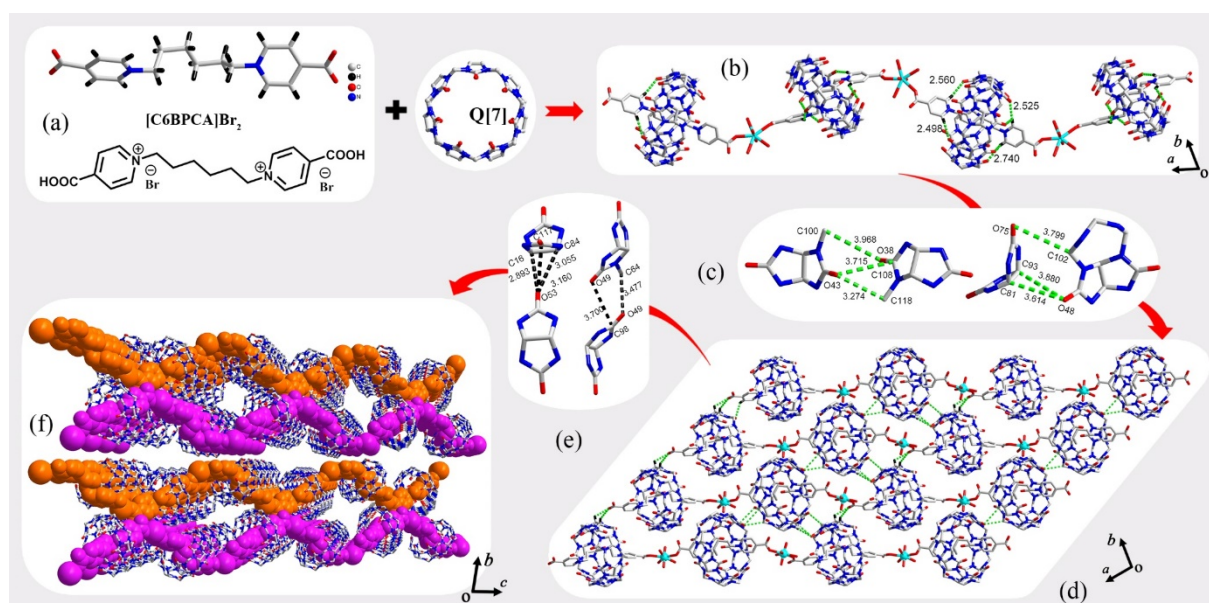


Figure 37. (a) Crystal structure of the [C6BPCA] guest; (b) the [C6BPCA]@Q[7]/UO₂²⁺-based 1D polyrotaxane chain; (c) self-induced OSIQs; (d) the [C6BPCA]@Q[7]/UO₂²⁺-based 2D framework; (e) self-induced OSIQs; (f) [C6BPCA]@Q[7]/UO₂²⁺-based 3D framework.

In 2017, Shi *et al.* further developed their strategy by introducing different anions at different pH, such as the use of oxalate with the [C6BPCA]@Q[6]/UO₂ systems which led to two different [C6BPCA]@Q[6]/UO₂²⁺-based 3D frameworks (Figures 38e and j).^[148] For example, at low pH (1.47-1.89), each oxalate anion coordinated to two uranyl cations, which linked two [C6BPCA]@Q[6] inclusion complexes, resulting in the formation of a 1D chain via the coordination of protruding carboxyl groups with uranyl cations (Figure 38a). The Q[6]-based host-guest inclusion-coordination chains can be stacked into 2D frameworks (Figure 38c) via anion-induced OSIQs formed between the nitrate anions and oxalate anions and Q[6]s from adjacent chains (Figure 38b). This is also present self-induced OSIQs formed between Q[6]s in

adjacent chains (Figure 38b). The final 3D frameworks (Figure 38e) can be built by H-bonding between the Q[6]s and the ligand in adjacent 2D layers (Figure 38d). However, at higher pH (4.31-7.21), the two adjacent [C6BPCA]@Q[6] inclusion complexes are linked by a uranyl cation and are coordinated with an extra oxalate anion, resulting in the formation of a zig-zag [C6BPCA]@Q[6]/UO₂-based 1D chain (Figure 38f). The [C6BPCA]@Q[6]/UO₂-based 1D chains can stack into 2D frameworks (Figure 38h), while the [C6BPCA]@Q[6]/UO₂-based 2D frameworks further stack into 3D frameworks (Figure 36j) via extensive OSIQs. These include anion-induced OSIQs (Figure 38g) formed between oxalate anions and Q[6]s in adjacent chains, self-induced OSIQs (Figure 38i) formed among Q[6]s in adjacent chains and aromatic-induced OSIQs formed between protruding pyridyl groups and adjacent Q[6]s in the frameworks.

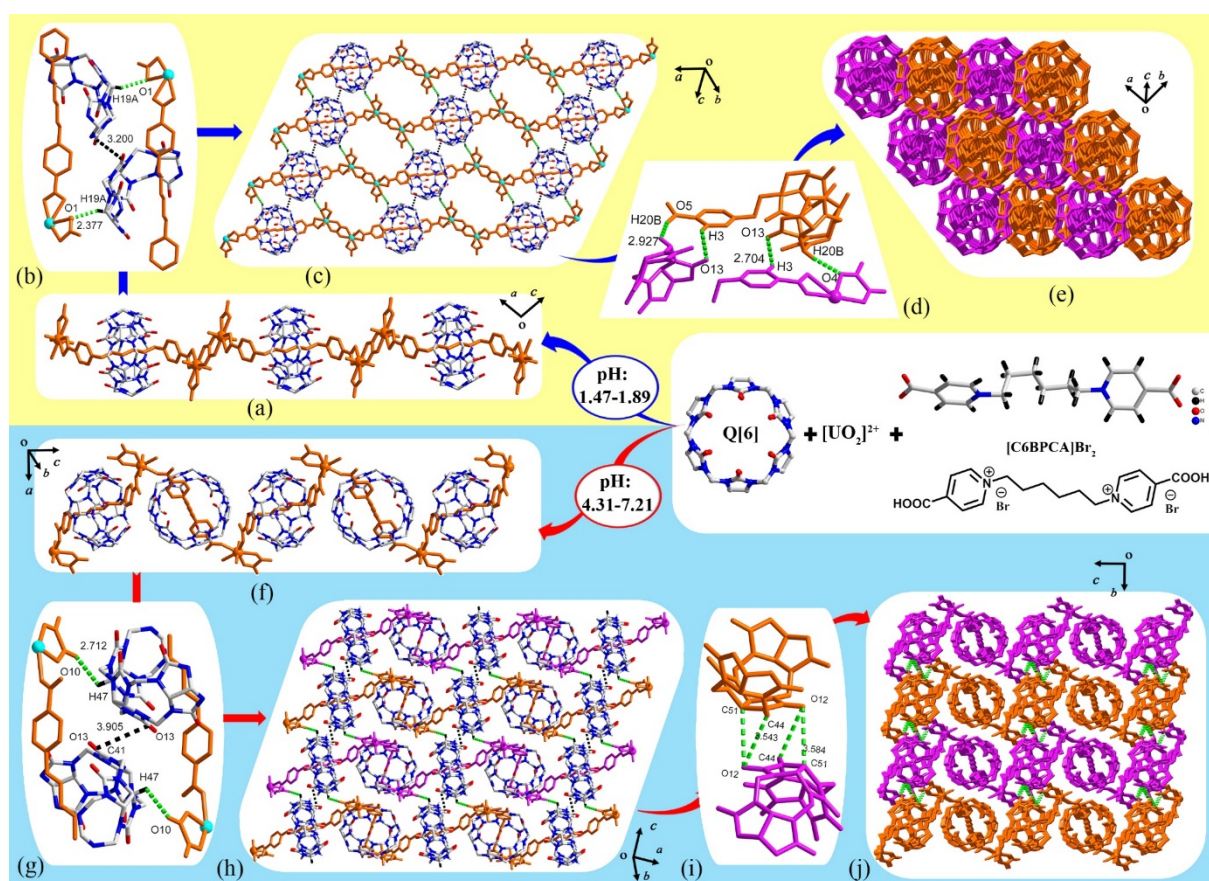


Figure 38 (a) Crystal structure of [C6BPCA]@Q[6]/UO₂²⁺/C₂O₄²⁻-based 1D polyrotaxane chain; (b) self-induced OSIQs and H-bonding interactions; (c) the [C6BPCA]@Q[6]/UO₂²⁺/C₂O₄²⁻-based 2D framework; (d) H-bonding interactions; (e) the [C6BPCA]@Q[6]/UO₂²⁺/C₂O₄²⁻-based 3D framework; (f) the [C6BPCA]@Q[6]/UO₂²⁺-based 1D polyrotaxane chain; (g) self-induced OSIQs and H-bonding interactions; (h) the [C6BPCA]@Q[6]/UO₂²⁺-based 2D framework; (i) self-induced OSIQs; (j) the [C6BPCA]@Q[6]/UO₂²⁺-based 3D framework.

By changing the ratio of the Q[6]-based pseudorataxane and uranyl cation used, Shi *et al.* obtained a C6CA3@Q[6]/UO₂²⁺-based 3D framework (Figure 39a), in which there were two different chains.^[149] One chain was constructed by the C6CA3@Q[6] inclusion complexes and UO₂²⁺ cations via coordination of protruding carboxyl groups with UO₂²⁺ cations (Figure 39b) and the other was constructed by the C6CA3@Q[6] inclusion complexes via hydrogen bonding interactions formed between protruding carboxyl groups and portal carbonyl oxygen atoms in the Q[6]s (Figure 39e). Both C6CA3@Q[6]/UO₂²⁺-based and C6CA3@Q[6]-based chains can stack into 2D frameworks (Figures 39d and g), respectively via aromatic-induced OSIQs formed between the protruding aromatic rings and Q[6]s, as well as self-induced OSIQs formed among the Q[6]s in adjacent chains (Figures 39c and f). The 3D framework was constructed by alternatively stacking the two different 2D frameworks (Figures 39d and g).

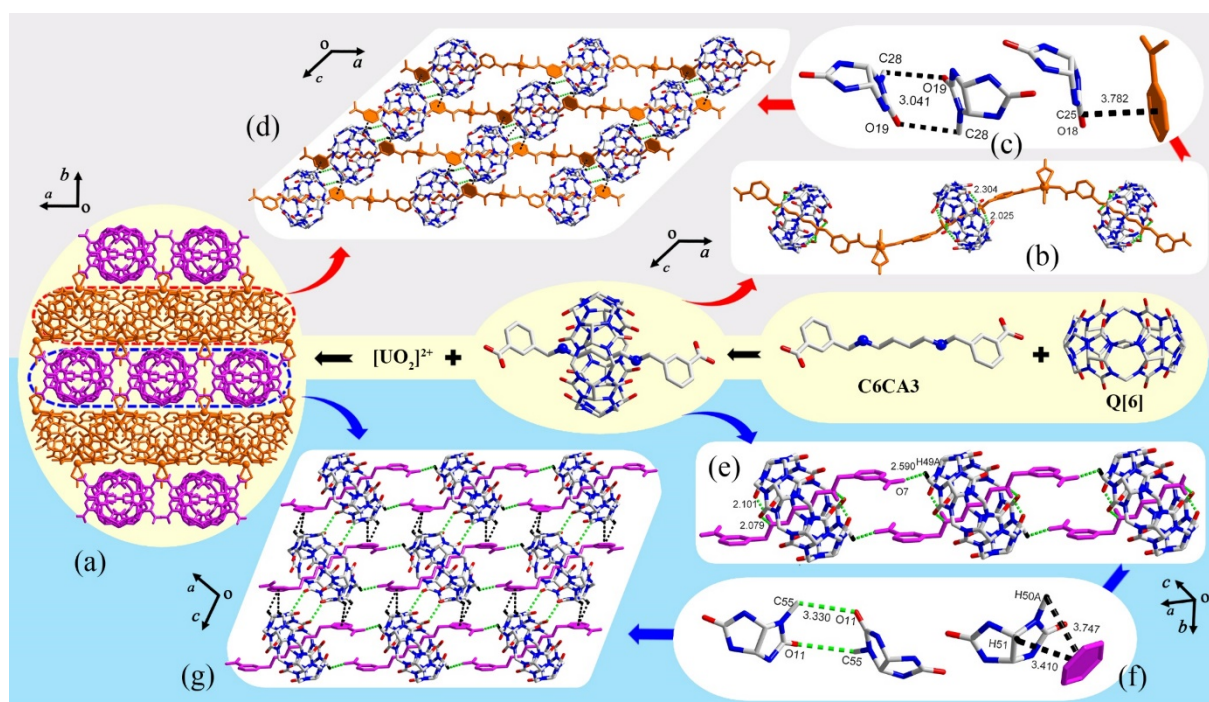


Figure 39. (a) Crystal structure of [C6CA3]@Q[6]/UO₂²⁺-based 3D framework; (b) the [C6CA3]@Q[6]/UO₂²⁺-based 1D polyrotaxane chain; (c) the OSIQs in the 2D and 3D frameworks; (d) the [C6CA3]@Q[6]/UO₂²⁺-based 2D framework; (e) the [C6CA3]@Q[6]-based 1D supramolecular chain; (f) the OSIQs in the 2D and 3D frameworks; (g) the [C6CA3]@Q[6]-based 2D framework.

Shi *et al.* made an important discovery in the construction of [C_nBPCA]@Q[6]/UO₂-based

frameworks, namely that the uranyl cation can coordinate with not only protruding carboxyl groups in adjacent [C6BPCA]@Q[6]-based pseudorotaxanes with varying spacers ($C_n = C_5, C_7, \text{ and } C_8$) to form polyrotaxanes, but also with portal carbonyl oxygens of Q[6] molecules in adjacent [C n BPCA]@Q[6]-based pseudorotaxanes to form unusual linear coordinated polyrotaxane chains or frameworks.^[150] For example, on using H₂SO₄ and HBr to adjust the pH (2.5-3.0) of the [C7BPCA]@Q[6]/UO₂ system, two different [C7BPCA]@Q[6]/UO₂-based frameworks were obtained (Figure 40f and j). In the first case, namely H₂SO₄, every second uranyl cation coordinates with two sulfate anions to form a UO₂-SO₄ cluster, which is linked with two protruding carboxyl groups in two adjacent [C7BPCA]@Q[6]-based pseudorotaxanes to form a [C7BPCA]@Q[6]/UO₂-based coordination polyrotaxane chain. Moreover, it can coordinate to a portal carbonyl oxygen atom of a Q[6] in an adjacent [C7BPCA]@Q[6]/UO₂-based coordination polyrotaxane chain, resulting in the formation of double [C7BPCA]@Q[6]/UO₂-based 1D coordination polyrotaxane chains (Figure 40b), which can stack into a 2D framework (Figure 40d). The 2D frameworks can further stack into a 3D framework (Figure 40f). To understand the formation of the [C7BPCA]@Q[6]/UO₂-based 2D or 3D frameworks, an understanding of the supramolecular interactions formed between the adjacent double [C7BPCA]@Q[6]/UO₂-based polyrotaxane chains is needed. These interactions include anion-induced OSIQs of the sulfate anions (Figure 40c), which coordinate to the uranyl cations and Q[6] molecules in adjacent chains, and aromatic-induced OSIQs formed between Q[6] molecules and C7BPCA guest in adjacent chains (Figure 40e). In the second case (HBr), a uranyl cation coordinates with only one protruding carboxyl group of a [C7BPCA]@Q[6]-based pseudorotaxane. Meanwhile, it coordinates to the portal carbonyl oxygen in the Q[6] of an adjacent [C7BPCA]@Q[6]-based pseudorotaxane, which results in the formation of a zig-zag like polyrotaxane chain (Figure 40g). The [C7BPCA]@Q[6]/UO₂-based polyrotaxane chains can stack into a 2D framework (Figure 40h), which can further stack into a 3D framework (Figure 40j). Unlike the first case in which the supramolecular interactions

in the 2D and 3D frameworks are similar, in the second case, the supramolecular interactions in the 2D framework include self-induced OSIQs formed between Q[6]s in adjacent chains and the $\pi\cdots\pi$ interaction formed between protruding pyridyl rings in adjacent [C7BPCA]@Q[6]/UO₂-based coordination polyrotaxane chains. The supramolecular interactions formed in the 3D framework include mainly self-induced OSIQs (Figure 40i left) and anion-induced OSIQs formed between Br⁻ clusters and adjacent Q[6]s (Figure 40i right).

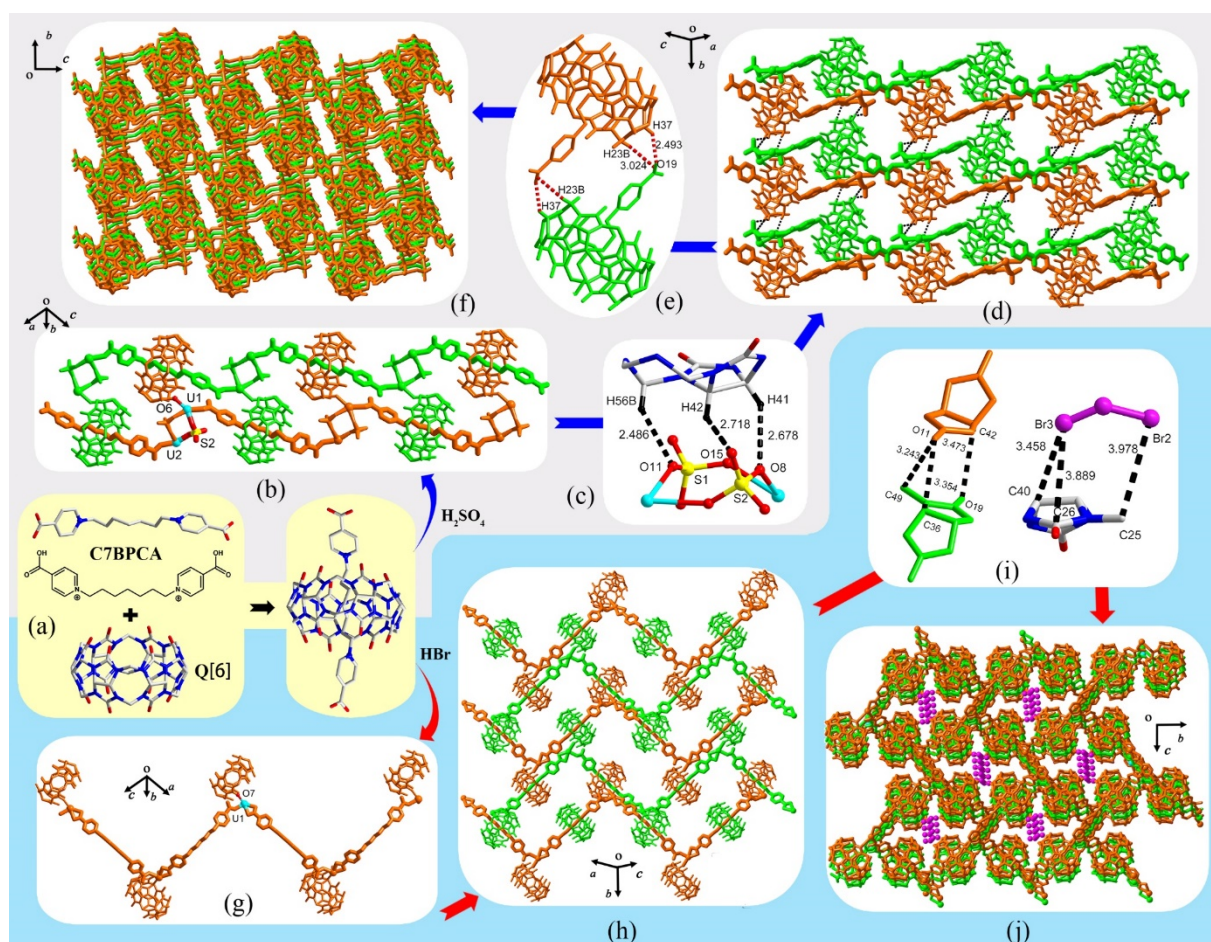


Figure 40. (a) Chemical and crystal structure of the [C7BPCA] guest; (b) crystal structure of the double [C7BPCA]@Q[6]/UO₂-based 1D coordination polyrotaxane chain; (c) the anion-induced OSIQs; (d) 2D framework constructed by the double 1D coordination polyrotaxane chains; (e) aromatic-induced OSIQs; (f) the [C7BPCA]@Q[6]/UO₂-based 3D framework; (g) the zig-zag-like [C7BPCA]@Q[6]/UO₂-based 1D coordination polyrotaxane chain; (h) the 2D framework constructed by the zig-zag-like [C7BPCA]@Q[6]/UO₂-based 1D coordination polyrotaxane chains; (i) the anion- and self-induced OSIQs; (j) the 3D framework constructed by the [C7BPCA]@Q[6]/UO₂-based 2D frameworks.

2.4.2. Q[n]-based frameworks constructed by 2D guest@Q[n]/Mⁿ⁺ polyrotaxanes

It can be said that Kim pioneered research into the construction of Q[n]-based frameworks. Efficient syntheses of 1D, 2D and 3D polyrotaxanes with high structural regularity and molecular necklaces was achieved by using a combination of self-assembly and coordination chemistry.^[151] In early work, Kim *et al.* reported not only a Q[6]-based framework (Figure 31f) constructed from stacked C4N4@Q[6]/Ag⁺(CH₃C₆H₆SO₃)-based polyrotaxane chains (Figure 31b),^[141] but also mechanically interlocked molecules incorporating Q[6] as a molecular ‘bead’ and a C4N4@Q[6]/Ag⁺(NO₃)-based polyrotaxane 2D framework (Figure 31e).^[140] The difference to the structure shown in Figure 41a is that each Ag⁺ cation coordinates to three protruding pyridyl nitrogen atoms from three adjacent C4N4@Q[6] pseudorotaxanes, which results in the formation of a corrugated honeycomb-like 2D framework (Figure 41b). This can further stack into a 3D framework via self-induced OSIQs (Figures 41c), formed between Q[6] molecules in adjacent 2D frameworks (Figures 41d).

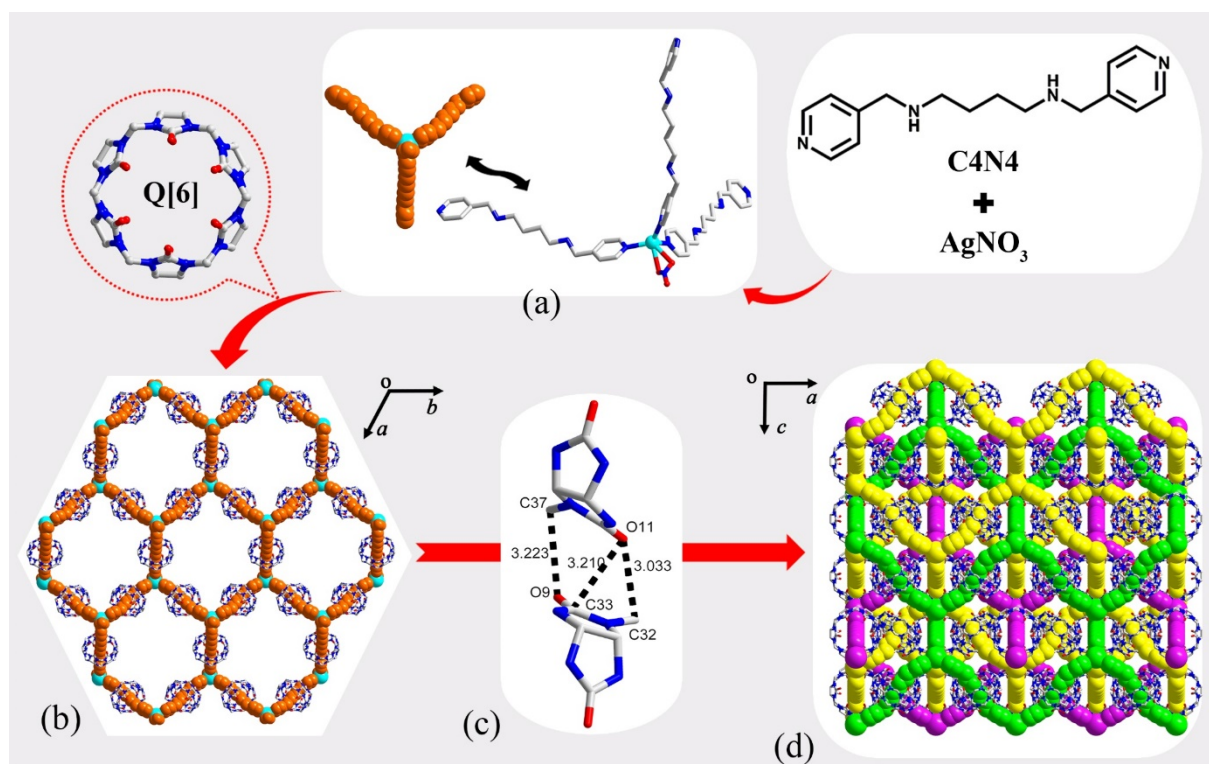


Figure 41. (a) The C4N4/Ag⁺/NO₃⁻ cluster; (b) crystal structure of C4N4@Q[n]/Ag⁺(NO₃)-based polyrotaxane 2D framework; (c) the self-induced OSIQs; (d) 3D framework constructed by the C4N4@Q[n]/Ag⁺(NO₃)-based polyrotaxane 2D frameworks.

Replacing C4N4 with *N,N'*-bis(3-cyanobenzyl)-1,4-diammoniumbutane dinitrate (C4CN3 as a precursor, which can hydrolyze to C4CA4, Figures 42a) and AgNO₃ with Tb(NO₃)₃, a C4CA4@Q[6]/Tb³⁺-based corrugated honeycomb-like 2D framework was obtained (Figure 42c).^[152] This is similar to the system shown in Figure 41b, in which each Tb³⁺ cation coordinates to three protruding carboxyl groups from three adjacent C4CA4@Q[6] pseudorotaxanes (Figure 42e). The corrugated C4CA4@Q[6]/Tb³⁺-based 2D frameworks can also further stack into a 3D framework (Figures 42g and h). This is unlike the C4N4@Q[*n*]/Ag⁺(NO₃)-based 3D framework (Figure 41d) in which the C4N4@Q[*n*]/Ag⁺(NO₃)-based 2D frameworks were simply stacked (Figure 41b), *i.e.* the C4CA4@Q[6]/Tb³⁺-based 2D frameworks are stacked in an interlocked manner (Figures 42e and f).

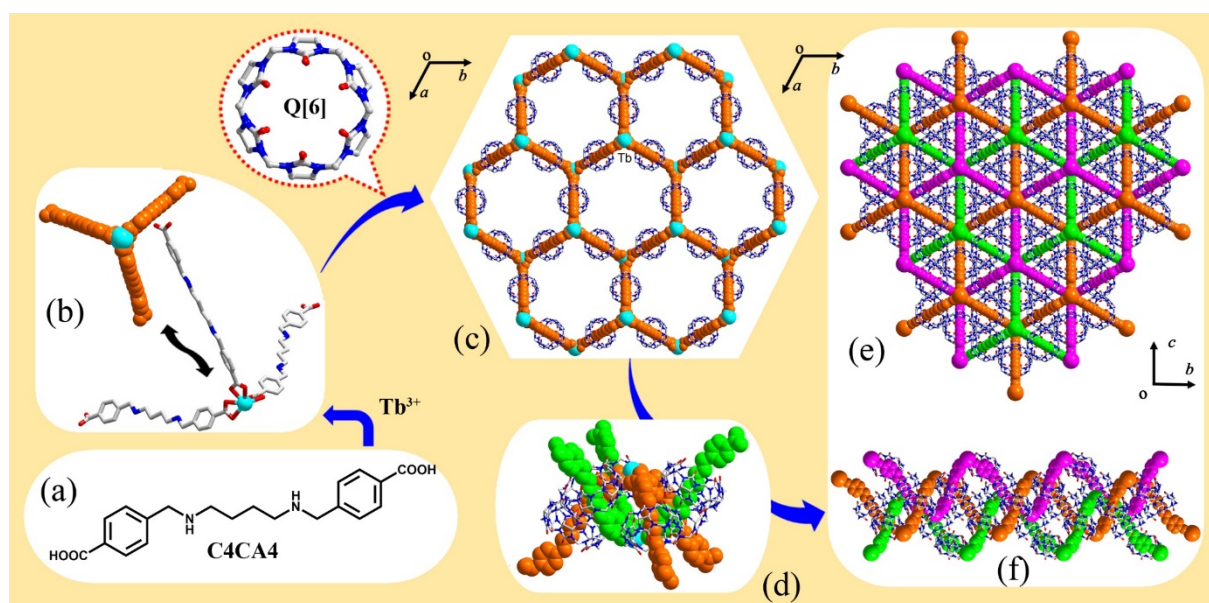


Figure 42. (a) Chemical structure of the C4CA4 guest; (b) the C4CA4/Tb³⁺ cluster; (c) crystal structure of C4CA4@Q[6]/Tb³⁺-based 2D framework; (d) the interlocked unit; (e, f) 3D framework stacked by the C4CA4@Q[6]/Tb³⁺-based 2D frameworks.

Upon introducing oxalate (Na₂C₂O₄) into the C5N3@Q[6]/Cu²⁺ system, Kim *et al.* obtained another polyrotaxane-based 2D framework (Figure 43c),^[153] in which each Cu²⁺ cation was

coordinated to two protruding pyridyl nitrogen atoms from two adjacent C5N3@Q[6] pseudorotaxanes. The oxalate anion was coordinated to two such Cu^{2+} cations to form a C5N3@Q[6] pseudorotaxane tetramer (Figure 43b), and the C5N3@Q[6]/ Cu^{2+} -based 2D framework (Figure 43c) was constructed from the tetramer. The 2D frameworks can further stack into a C5N3@Q[6]/ Cu^{2+} -based 3D framework (Figure 43e and f) via self-induced OSIQs formed between Q[6] molecules in adjacent 2D frameworks and aromatic-induced OSIQs between Q[6]s and adjacent protruding pyridyl rings (Figure 43d) from adjacent 2D frameworks.

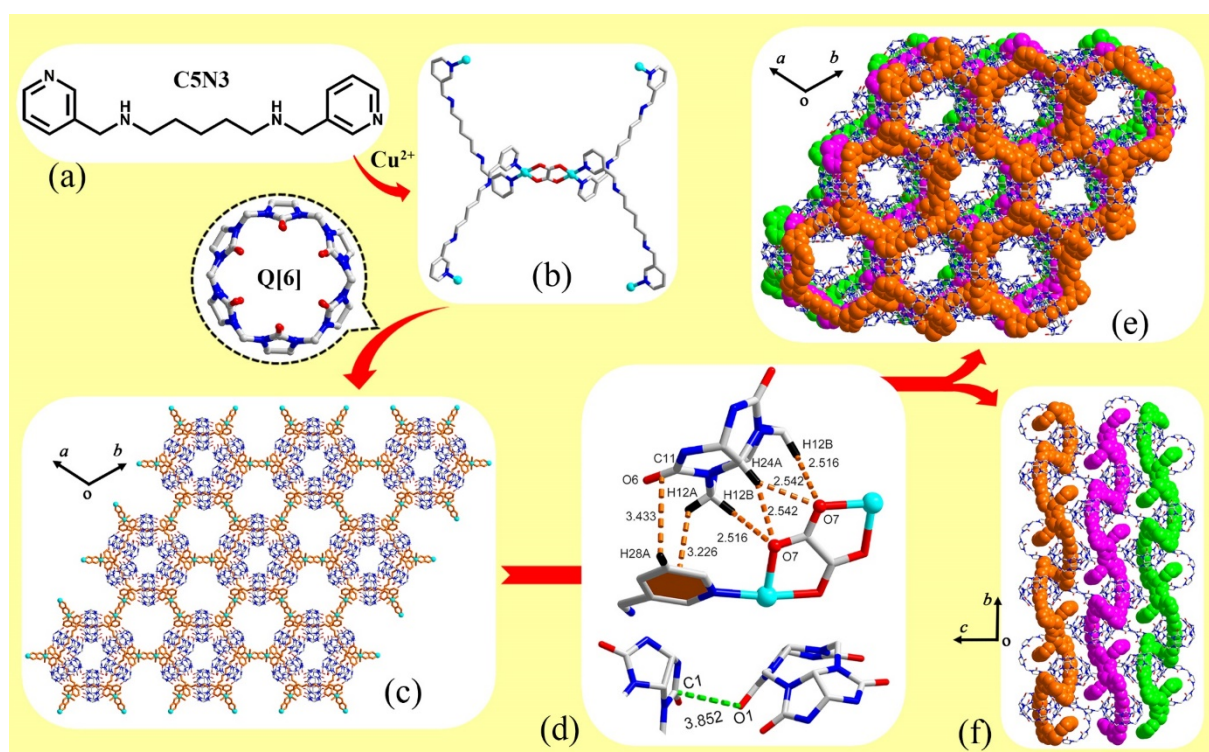


Figure 43. (a) Chemical structure of the C5N3 guest; (b) the C5N3/ Cu^{2+} / $\text{C}_2\text{O}_4^{2-}$ cluster; (c) crystal structure of C5N3@Q[6]/ Cu^{2+} / $\text{C}_2\text{O}_4^{2-}$ -based 2D framework; (d) the self- and aromatic-induced OSIQs; (e, f) the C5N3@Q[6]/ Cu^{2+} / $\text{C}_2\text{O}_4^{2-}$ -based 3D framework viewed along the c - and a -axis, respectively.

Following the work of Kim *et al.*, Shi *et al.* further developed the coordination chemistry of guest@Q[n] inclusion complexes with metal ions to construct Q[n]-based frameworks. They focused on the framework systems constructed upon the coordination of actinide metal cations with guest@Q[6]-based pseudorotaxanes. They not only developed various Q[6]-based frameworks from 1D coordination polyrotaxanes,^[145,146,147-150] but also created a variety of

Q[6]-based frameworks constructed from 2D polyrotaxanes. For example, they selected C6BPCA as a guest and prepared C6BPCA@Q[6]-based pseudorotaxanes bearing different counter anions [(SO₄)²⁻ and Br⁻], which resulted in the formation of different polyrotaxane frameworks when coordinated with uranyl cations.^[147] In the (SO₄)²⁻ case, every two uranyl cations form a cluster in which each uranyl cation is coordinated to a sulfate anion. One protruding carboxyl group from an isolated [C6BPCA]@Q[6]-based pseudorotaxane and two protruding carboxyl groups in two adjacent [C6BPCA]@Q[6]-based pseudorotaxanes share another uranyl cation in the cluster (Figure 44a). Thus, a [C6BPCA]@Q[6]/UO₂-based 2D framework can be formed from the cluster (Figure 44b). Moreover, these 2D frameworks can stack into a [C6BPCA]@Q[6]/UO₂-based 3D framework (Figure 44c). Self-induced OSIQs are the key driving forces that link the adjacent [C6BPCA]@Q[6]/UO₂-based 2D frameworks. In the Br⁻ case, each uranyl cation is coordinated to four protruding carboxyl groups from four adjacent [C6BPCA]@Q[6]-based pseudorotaxanes (Figure 44d), and this coordination affords a [C6BPCA]@Q[6]/UO₂-based 2D framework (Figure 44e), which can stack to form a 3D framework (Figures 44f and g). Again, the self-induced OSIQs are the key driving forces leading to the formation of the 3D framework.

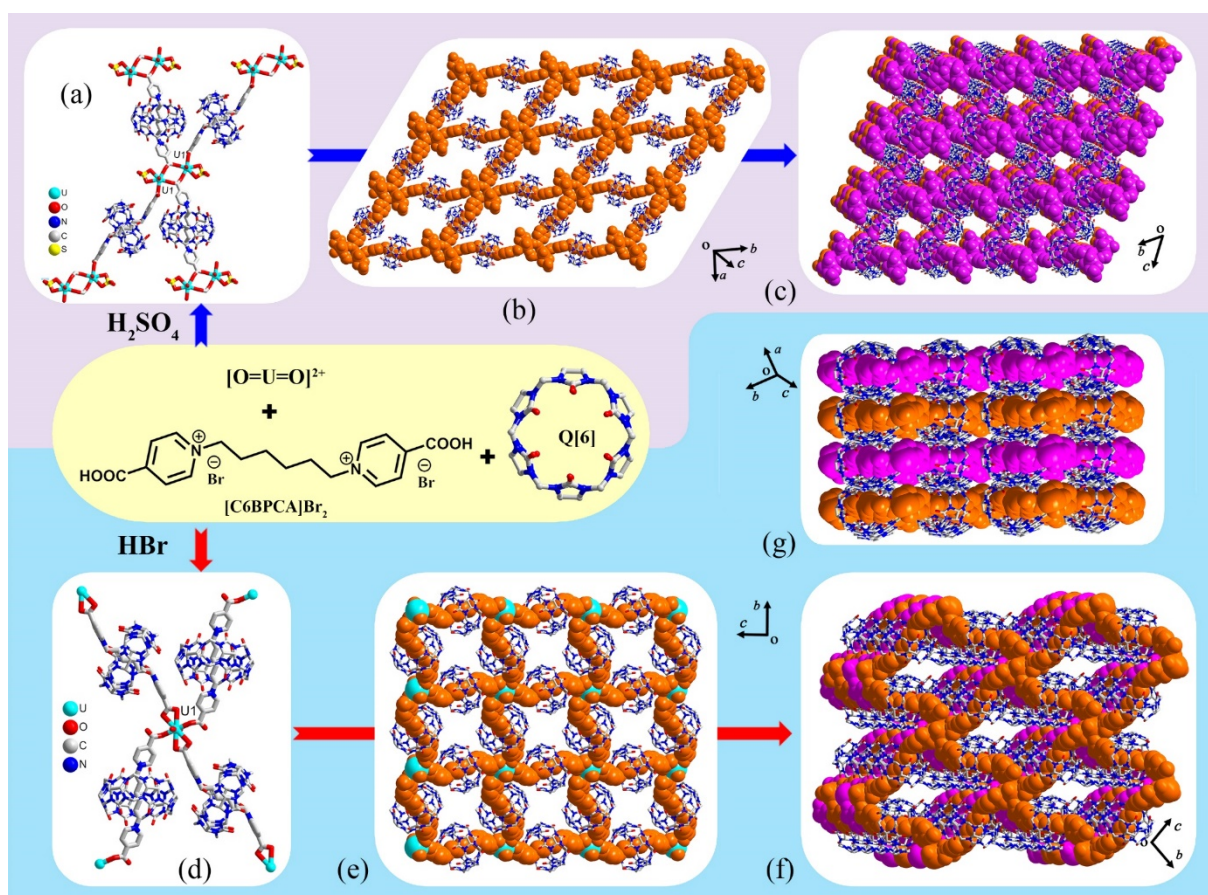


Figure 44. (a) Crystal structure of [C6BPCA]@Q[6]/UO₂(SO₄²⁻)-based cluster; (b) the [C6BPCA]@Q[6]/UO₂(SO₄²⁻)-based coordination polyrotaxane 2D framework; (c) the [C6BPCA]@Q[6]/UO₂(SO₄²⁻)-based 3D framework viewed along *bc* plane; (d) The coordination complex formed from [C6BPCA]@Q[6] and UO₂(Br⁻) cations; (e) the [C6BPCA]@Q[6]/UO₂(Br⁻)-based coordination polyrotaxane 2D framework; (f and g) the 3D framework formed by stacking of the [C6BPCA]@Q[6]/UO₂(Br⁻)-based coordination polyrotaxane 2D frameworks viewed from different directions.

A slight adjustment in the [C6BPCA]@Q[6]/UO₂(SO₄²⁻) system, such as adjusting the pH to 1.30 with HNO₃, led to a [C6BPCA]@Q[6]/UO₂(SO₄²⁻)-based 2D polyrotaxane framework (Figure 45a). Each protruding carboxyl group in each [C6BPCA]@Q[6] pseudorotaxane coordinates one uranyl cation, whilst the adjacent uranyl cations of both sides of the [C6BPCA]@Q[6] pseudorotaxane are linked by the sulfate anions via coordination. The anion-induced OSIQ of the coordinated sulfate anions (Figure 45b) can play an important role in the formation of a [C6BPCA]@Q[6]/UO₂(SO₄²⁻)-based 3D framework (Figure 45c). Introducing an oxalate anion into the [C6BPCA]@Q[6]/UO₂(SO₄²⁻) system at different pH can also yield different [C6BPCA]@Q[6]/UO₂-based 2D polyrotaxane frameworks (Figures 45d and g). For

example, on adding $\text{Na}_2\text{C}_2\text{O}_4$ to the $[\text{C6BPCA}]@\text{Q}[6]/\text{UO}_2$ system and adjusting the pH to 1.98 with HNO_3 , Shi *et al.* obtained a different $[\text{C6BPCA}]@\text{Q}[6]/\text{UO}_2$ -based 2D polyrotaxane framework (Figure 45d).^[148] In this 2D framework, each protruding carboxyl group in each $[\text{C6BPCA}]@\text{Q}[6]$ pseudorotaxane is also coordinated to one uranyl cation and adjacent uranyl cations on both sides of the $[\text{C6BPCA}]@\text{Q}[6]$ pseudorotaxane are connected via coordination with the oxalate anions instead of sulfate anions. Anion-induced OSIQs (Figure 45e) are the main driving force that result in the formation of the $[\text{C6BPCA}]@\text{Q}[6]/\text{UO}_2$ -based 3D framework (Figure 45f). Upon adjusting pH to 6.1-6.8 using NaOH , the $[\text{C6BPCA}]@\text{Q}[6]/\text{UO}_2/\text{C}_2\text{O}_4$ system can yield similar $[\text{C6BPCA}]@\text{Q}[6]/\text{UO}_2$ -based 2D polyrotaxane frameworks (Figure 45g). In this case, every four uranyl cations form a uranyl tetramer cluster, which coordinates to two protruding carboxyl groups in two adjacent $[\text{C6BPCA}]@\text{Q}[6]$ pseudorotaxanes. The adjacent tetramers are connected by the oxalate anions. The self- and aromatic-induced OSIQs (Figure 45h) now appear to be the main driving forces that result in the $[\text{C6BPCA}]@\text{Q}[6]/\text{UO}_2$ -based 3D framework formed upon stacking of the $[\text{C6BPCA}]@\text{Q}[6]/\text{UO}_2$ -based 2D polyrotaxane frameworks (Figure 45i).

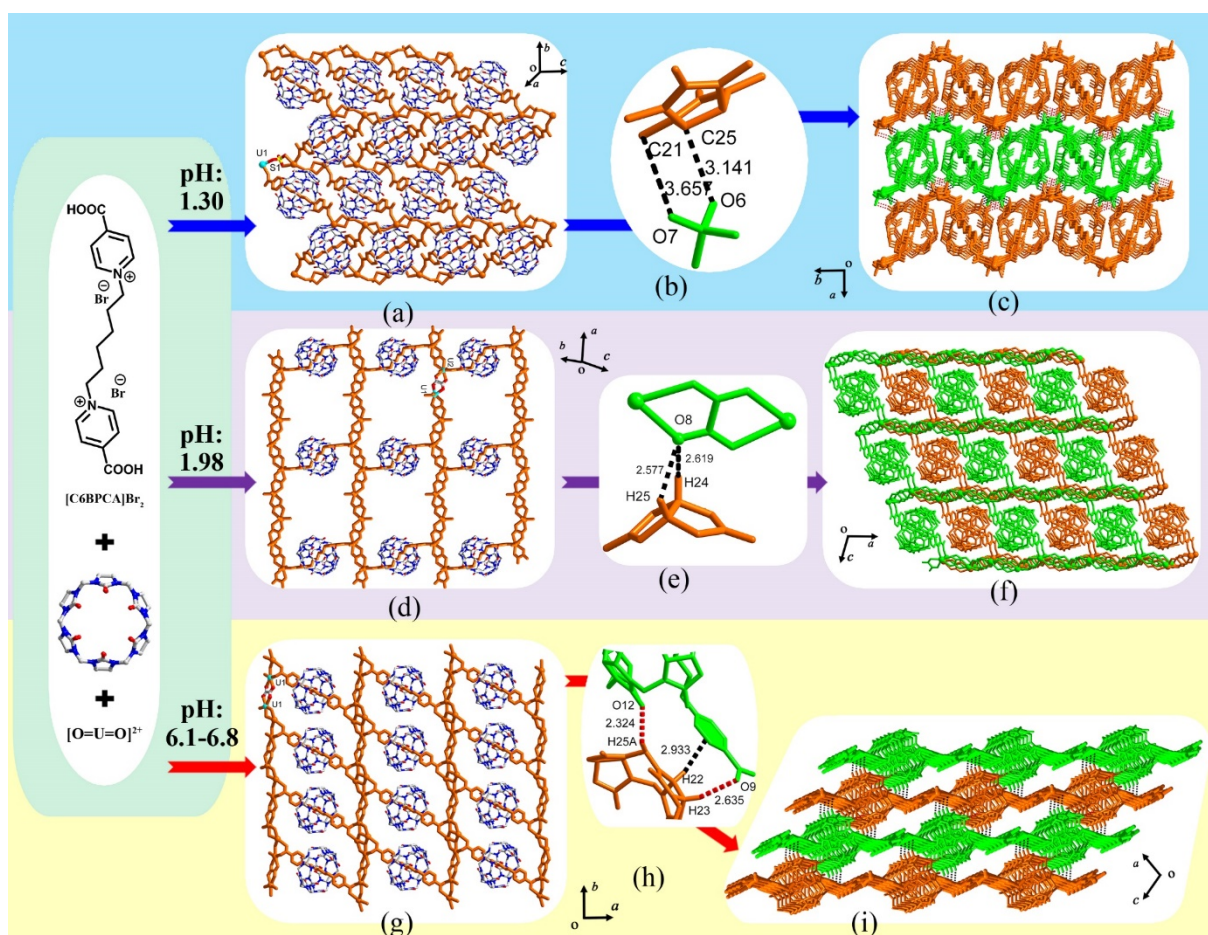


Figure 45. (a) Crystal structure of [C6BPCA]@Q[6]/ $\text{UO}_2^{2+}/\text{SO}_4^{2-}$ -based 2D polyrotaxane framework; (b) the anion-induced OSIQ; (c) [C6BPCA]@Q[6]/ $\text{UO}_2^{2+}/\text{SO}_4^{2-}$ -based 3D framework; (d) [C6BPCA]@Q[6]/ $\text{UO}_2^{2+}/\text{C}_2\text{O}_2^{2-}$ -based 2D framework; (e) the anion-induced OSIQ; (f) [C6BPCA]@Q[6]/ $\text{UO}_2^{2+}/\text{C}_2\text{O}_2^{2-}$ -based 3D framework; (g) [C6BPCA]@Q[6]/ $[\text{UO}_2^{2+}]_4/\text{C}_2\text{O}_2^{2-}$ -based 2D framework; (h) the self- and aromatic-induced OSIQs; (i) [C6BPCA]@Q[6]/ $[\text{UO}_2^{2+}]_4/\text{C}_2\text{O}_2^{2-}$ -based 3D framework.

On reacting C6CA4@Q[6] with uranyl cations, Shi *et al.* obtained a hetero-framework containing C6CA4@Q[6]/ UO_2^{2+} -based 1D polyrotaxane chains and 2D polyrotaxane frameworks.^[151] In the 1D polyrotaxane chain, two adjacent C6CA4@Q[6] pseudorotaxanes are connected by dimeric uranyl cations via coordination of the protruding carboxyl groups in the C6CA4@Q[6] pseudorotaxanes and the dimeric uranyl cations (Figure 46a). By contrast, in the 2D polyrotaxane framework, six adjacent C6CA4@Q[6] pseudorotaxanes are connected by a hexameric uranyl cation via coordination of protruding carboxyl groups of the C6CA4@Q[6] pseudorotaxanes and hexameric uranyl cations (Figure 46b). Moreover, every

three C6CA4@Q[6] pseudorotaxanes and a hexameric uranyl cation create a trapezoidal hole in the 2D polyrotaxane framework. Each trapezoidal hole is obliquely inserted with a C6CA4@Q[6] pseudorotaxane in a 1D polyrotaxane chain formed via self-induced OSIQs between the Q[6] molecules in adjacent 1D polyrotaxane chains and 2D polyrotaxane frameworks, as well as aromatic-induced OSIQs formed between protruding aromatic rings in the chains and Q[6]s in adjacent 2D polyrotaxane frameworks (Figure 46c). Thus, the 1D dimeric uranyl polyrotaxane chains link all the 2D hexameric uranyl polyrotaxane frameworks via a threading pattern to construct a unique two-fold nested polyrotaxane framework (Figure 46d).

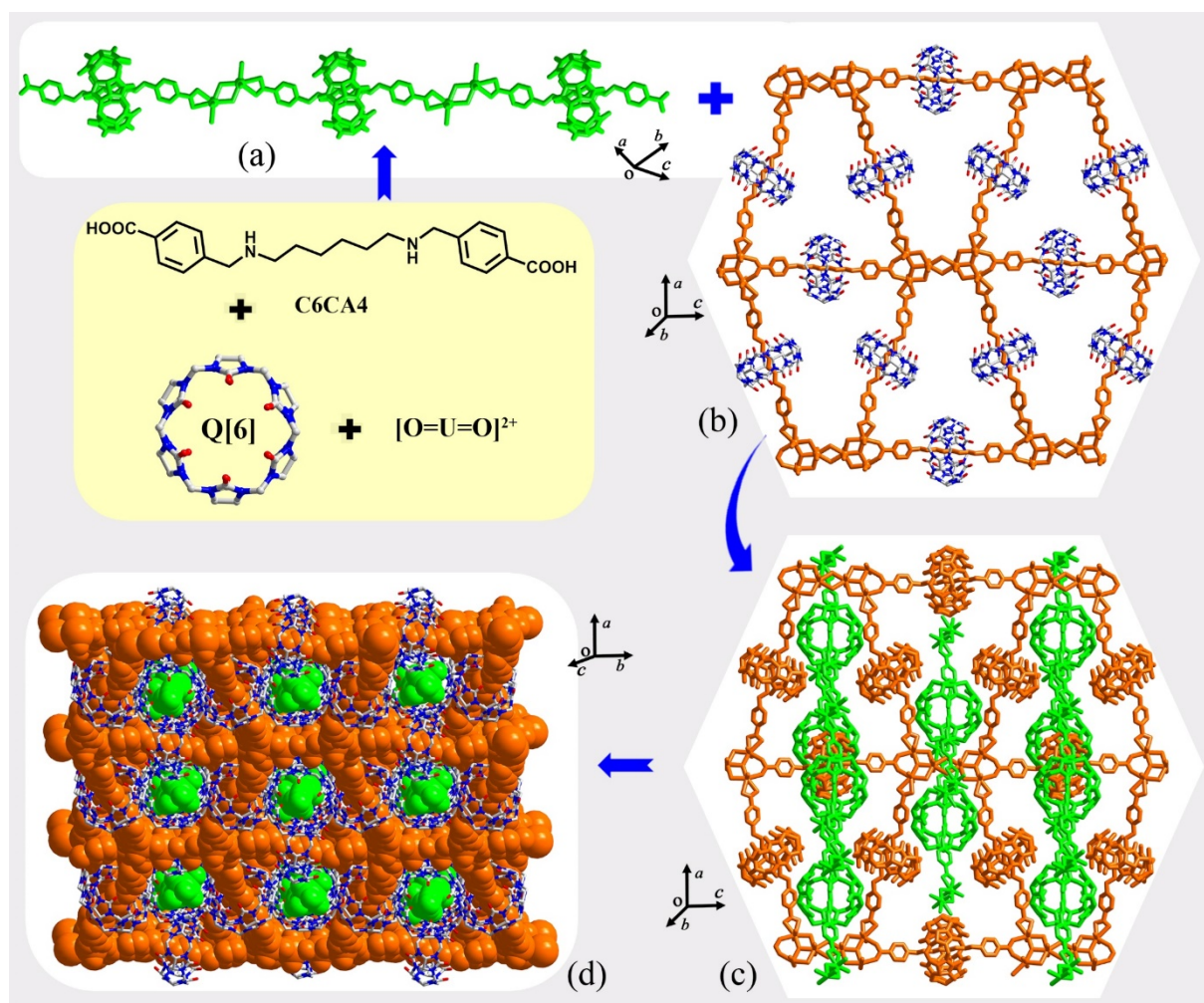


Figure 46. (a) Crystal structure of the C6CA4@Q[6]/UO₂²⁺-based 1D polyrotaxane chain; (b) the C6CA4@Q[6]/UO₂²⁺-based 2D polyrotaxane framework; (c) the interactions observed between the Q[6] molecules in the adjacent 1D polyrotaxane chains and 2D polyrotaxane frameworks; (d) the two-fold nested polyrotaxane framework constructed by the 1D dimeric uranyl polyrotaxane chains and 2D hexameric uranyl polyrotaxane frameworks viewed from

different directions.

By reacting [C6BPCA]@Q[6] with Np^{5+} or UO_2^{2+} , Shi *et al.* obtained two different [C6BPCA]@Q[6]-based frameworks.^[154] In the Np^{5+} case, each Np^{5+} cation coordinates with two protruding carboxyl groups in two adjacent [C6BPCA]@Q[6] pseudorotaxanes, as well as coordinating to the portal carbonyl oxygen of a Q[6] from an adjacent [C6BPCA]@Q[6] pseudorotaxane. This results in the formation of a [C6BPCA]@Q[6]/ Np^{5+} -based triangular node, which can form a 2D [C6BPCA]@Q[6]/ Np^{5+} -based polyrotaxane framework (Figure 47a). Only the coordination of the Np^{5+} cation with the portal carbonyl oxygen of the Q[6] molecule results in the interlocking of the adjacent 2D [C6BPCA]@Q[6]/ Np^{5+} -based polyrotaxane framework (Figure 47a). In addition, self-induced OSIQs (Figure 47b) formed among the Q[6] molecules exist in the adjacent 2D frameworks and lead to the formation of a 3D framework (Figure 47c). For the UO_2^{2+} case, each UO_2^{2+} cation coordinates with four protruding carboxyl groups in four adjacent [C6BPCA]@Q[6] pseudorotaxanes, and can then form a 2D [C6BPCA]@Q[6]/ UO_2^{2+} -based polyrotaxane framework (Figure 47d). This can stack into a 3D [C6BPCA]@Q[6]/ UO_2^{2+} -based polyrotaxane framework (Figure 47f) via self-induced OSIQs (Figure 47e) formed between Q[6] molecules in adjacent 2D frameworks.

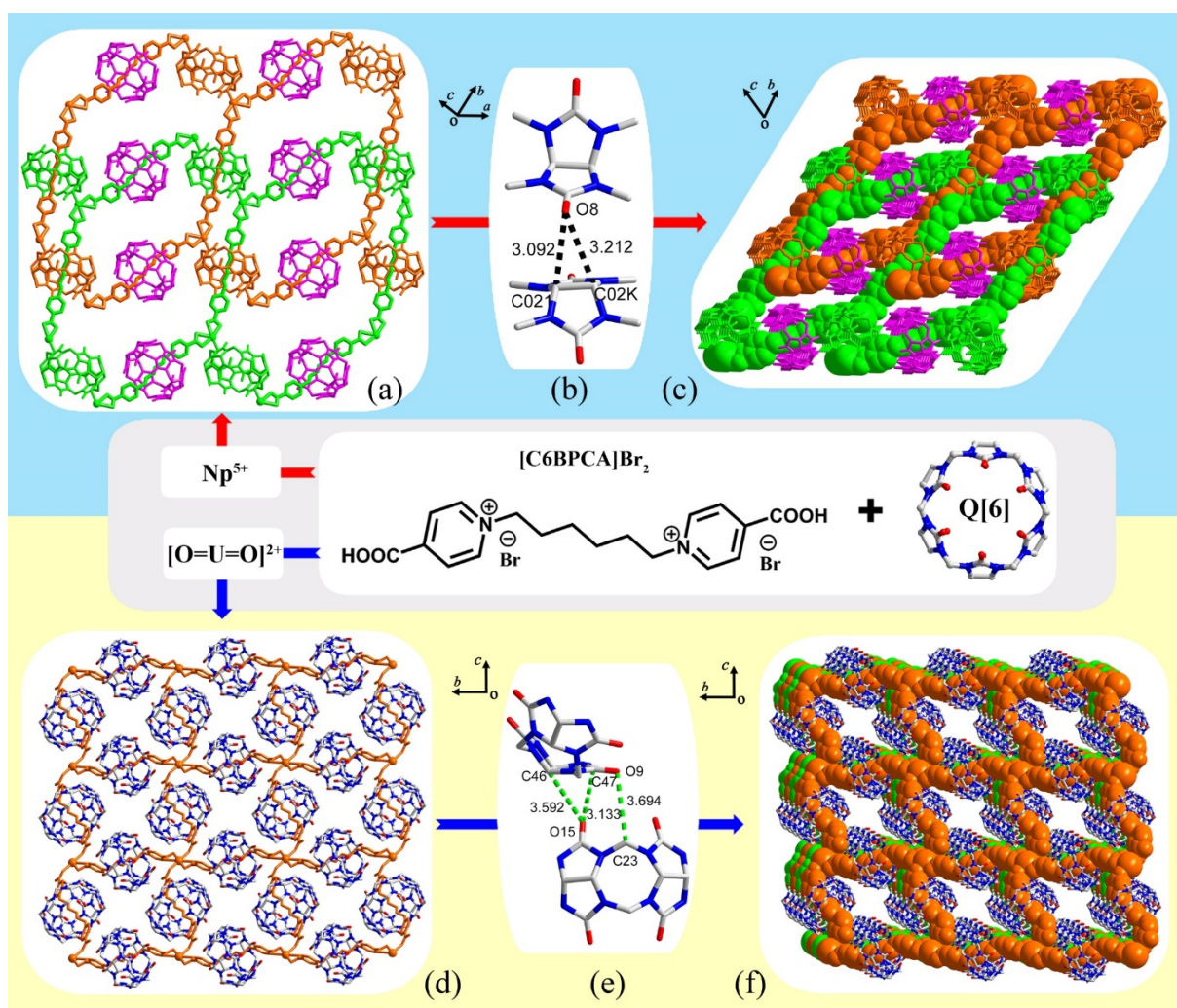


Figure 47. (a) Crystal structure of the 2D [C6BPCA]@Q[6]/Np⁵⁺-based polyrotaxane framework; (b) self-induced OSIQs; (c) the 3D framework constructed by the 2D [C6BPCA]@Q[6]/Np⁵⁺-based polyrotaxane frameworks; (d) the 2D [C6BPCA]@Q[6]/UO₂²⁺-based polyrotaxane framework; (e) self-induced OSIQs; (f) the 3D framework constructed by the 2D [C6BPCA]@Q[6]/UO₂²⁺-based polyrotaxane frameworks.

Shi *et al.* found that using the [C_nBPCA]@Q[6] pseudorotaxane to construct frameworks can lead to metal cations, such as UO₂²⁺ and Np⁵⁺ coordinating not only with the protruding carboxyl groups in adjacent [C_nBPCA]@Q[6] pseudorotaxanes, but also portal carbonyl oxygens of Q[6] molecules in adjacent [C_nBPCA]@Q[6] pseudorotaxanes. This results in the formation of some unusual linear coordinated polyrotaxane chains or frameworks.^[150, 154] They demonstrated two such frameworks: the first one involved coordination of the [C5BPCA]@Q[6] pseudorotaxane using [C5BPCA]Br₂ guest (Figure 48a) with UO₂ cations, in which each

cation coordinated with two protruding carboxyl groups in two adjacent [C5BPCA]@Q[6] pseudorotaxanes. Meanwhile, they were coordinated to the portal carbonyl oxygen atom of a Q[6] of a third [C5BPCA]@Q[6]-based pseudorotaxane. This formed a [C5BPCA]@Q[6]/Np⁵⁺-based triangle node, which can create a [C5BPCA]@Q[6]/UO₂-based polyrotaxane 2D framework (Figure 48b) and stack into a 3D framework (Figure 48d) via self-induced OSIQs (Figure 48c) formed between the Q[6] molecules in adjacent 2D frameworks. In the [C8BPCA]@Q[6]/UO₂ system, every two sulfate anions (counter anions) coordinate to two uranyl cations to form a dimeric uranyl cluster, which coordinates with two protruding carboxyl groups of two adjacent [C8BPCA]@Q[6] pseudorotaxanes. Meanwhile, it coordinates to two portal carbonyl oxygen atoms in two Q[6] molecules from another two [C8BPCA]@Q[6]-based pseudorotaxanes, thus, coordinating the [C8BPCA]@Q[6] pseudorotaxanes and dimeric uranyl clusters to create a [C8BPCA]@Q[6]/UO₂-based polyrotaxane 2D framework (Figure 48f). This can further stack into a 3D framework (Figure 48h) via self-induced OSIQs (Figure 48g) formed between Q[6] molecules in adjacent 2D frameworks.

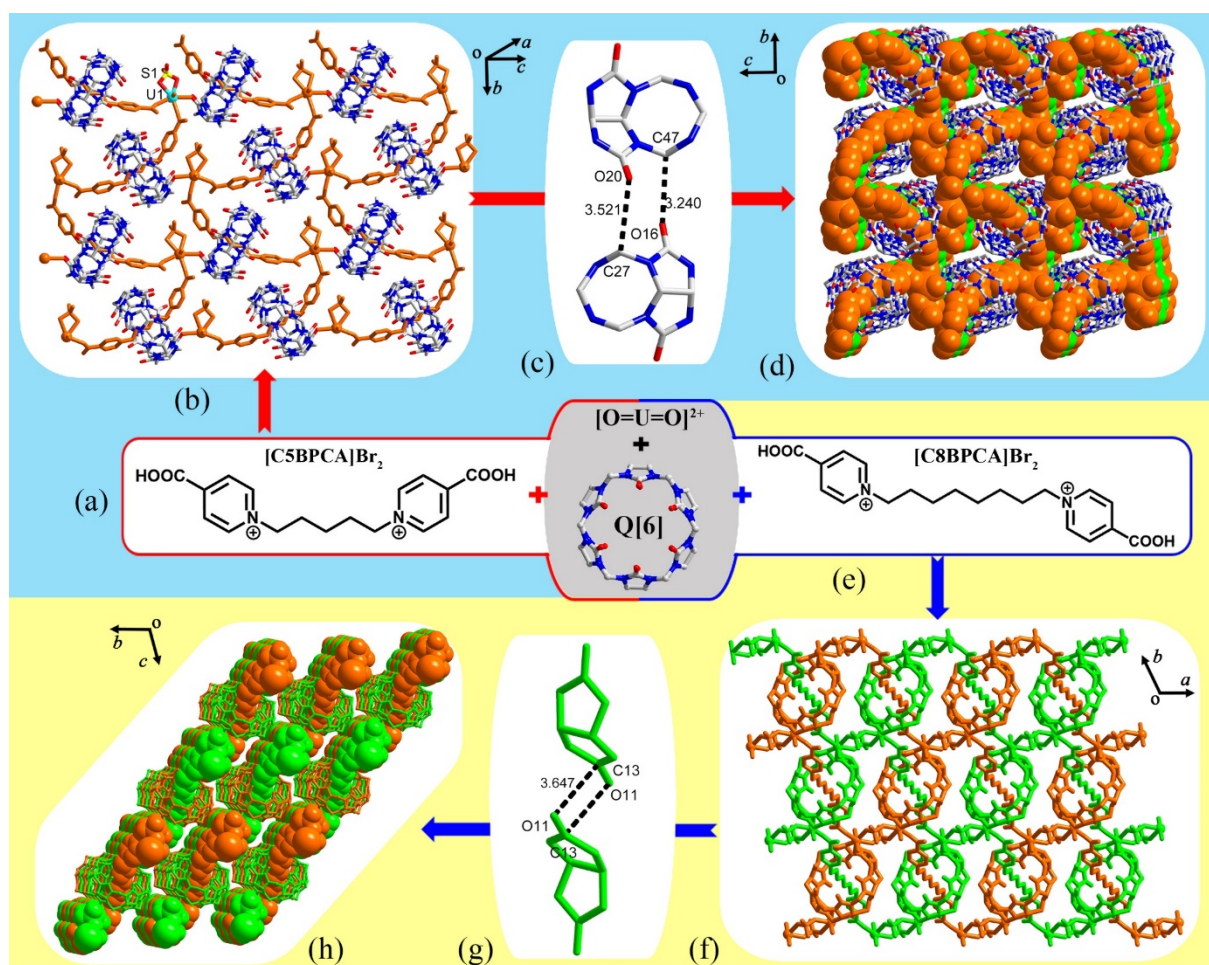


Figure 48. (a) Chemical structure of the [C5BPCA]Br₂ guest; (b) self-induced OSIQs; (c) crystal structure of the 2D [C5BPCA]@Q[6]/UO₂²⁺-based polyrotaxane framework; (d) the 3D framework constructed by the 2D [C5BPCA]@Q[6]/UO₂²⁺-based polyrotaxane frameworks; (e) chemical structure of the [C8BPCA]Br₂ guest; (f) the 2D [C8BPCA]@Q[6]/UO₂²⁺-based polyrotaxane framework; (g) self-induced OSIQs; (h) the 3D framework constructed by the 2D [C8BPCA]@Q[6]/UO₂²⁺-based polyrotaxane frameworks.

Wu and Cao reported a number of supramolecular organic frameworks constructed from simple Q[6]-based pseudorotaxanes using guests bearing 4,4'-bipyridin-1-ium units.^[119] More recently, Wang and Su developed a strategy to construct C₆N₃ or C₆N₄@Q[6]/Cd or Zn²⁺-based frameworks by introducing different rigid carboxylate ligands of varied geometry.^[155] For example, by introducing 4,4'-biphenyldicarboxylic acid (H₂BPDC) into the C₆N₄@Q[6]/Cd²⁺ system, a 2D C₆N₄@Q[6]/Cd²⁺-based polyrotaxane framework resulted. Here, each Cd²⁺ cation coordinates to a protruding pyridyl nitrogen atom in the C₆N₄@Q[6] pseudorotaxane and two H₂BPDC molecules. In turn, each H₂BPDC molecule coordinates two

of the aforementioned Cd^{2+} cations which results in the fusing of the C6N4@Q[6] pseudorotaxane into a 2D C6N4@Q[6]/Cd^{2+} -based polyrotaxane framework (Figure 49a). This is aided by self-induced OSIQs between Q[6] molecules in adjacent 2D frameworks and aromatic-induced OSIQs between H_2BPDC molecules and adjacent Q[6] molecules. The 2D frameworks simply stack into a 3D C6N4@Q[6]/Cd^{2+} -based polyrotaxane framework (Figures 49b and c). Introducing 1,3-benzenedicarboxylic acid ($m\text{-H}_2\text{BDC}$) into the C6N4@Q[6]/Zn^{2+} system also results in the formation of a 2D C6N4@Q[6]/Zn^{2+} -based polyrotaxane framework. A similar coordination can be observed, namely, each Zn^{2+} cation coordinates to a protruding pyridyl nitrogen atom in the C6N4@Q[6] pseudorotaxane and two $m\text{-H}_2\text{BPDC}$ molecules. In turn, each $m\text{-H}_2\text{BPDC}$ molecule coordinates two such Zn^{2+} cations resulting in the formation of a 2D C6N4@Q[6]/Zn^{2+} -based polyrotaxane framework (Figure 49d). This stacks into a 3D C6N4@Q[6]/Zn^{2+} -based polyrotaxane framework with the aid of self-induced OSIQs formed between Q[6] molecules in adjacent 2D frameworks and aromatic-induced OSIQs between $m\text{-H}_2\text{BPDC}$ molecules and adjacent Q[6] molecules (Figures 49e and f).

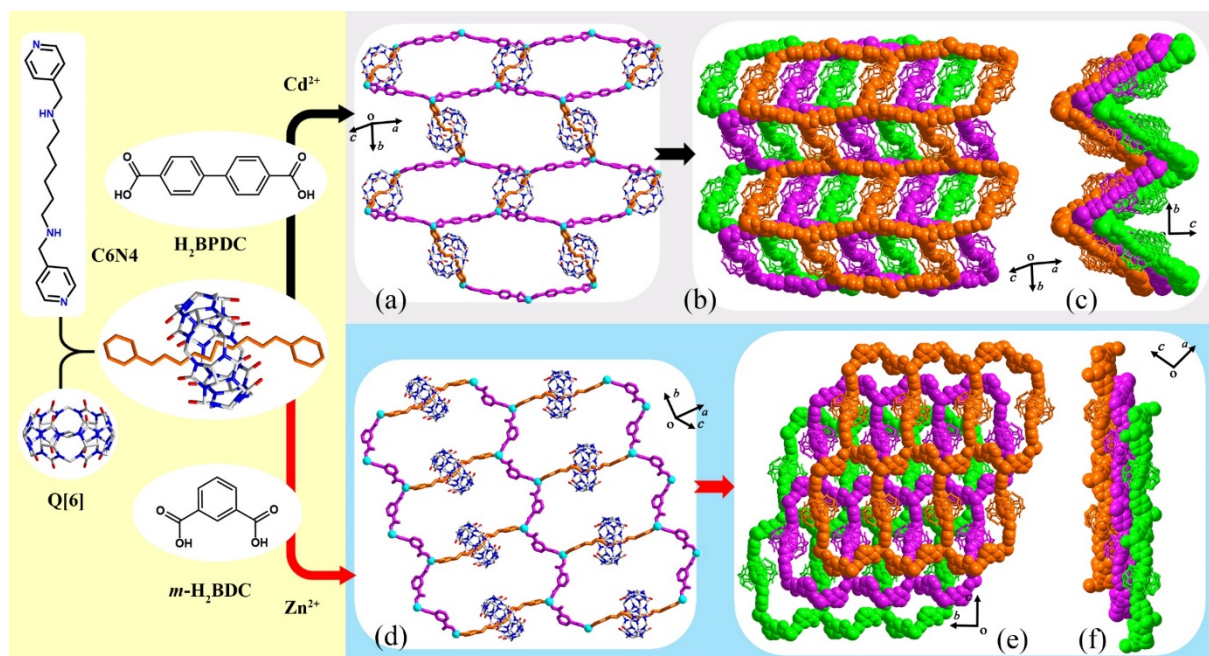


Figure 49. (a) Crystal structure of the 2D $[\text{C6N4}]\text{@Q[6]}/\text{Cd}^{2+}$ -based polyrotaxane framework; (b, c) the 3D framework constructed by the 2D $[\text{C6N4}]\text{@Q[6]}/\text{Cd}^{2+}$ -based polyrotaxane frameworks viewed from different directions; (d) the $[\text{C6N4}]\text{@Q[6]}/\text{Zn}^{2+}$ -based polyrotaxane framework; (e, f) the 3D framework constructed by the 2D $[\text{C6N4}]\text{@Q[6]}/\text{Zn}^{2+}$ -based polyrotaxane frameworks viewed from different directions.

2.4.3. Q[n]-based frameworks constructed by 3D guest@Q[n]/Mⁿ⁺ polyrotaxanes

Thus far, we have introduced and discussed Q[n]-based frameworks constructed by 1D and 2D guest@Q[n]/Mⁿ⁺ polyrotaxanes via various supramolecular interactions, especially OSIQs. However, Q[n]-based frameworks constructed by 3D guest@Q[n]/Mⁿ⁺ polyrotaxanes is a relatively simple process because the basic building blocks can directly interact with each other to form the 3D guest@Q[n]/Mⁿ⁺ frameworks. Kim *et al.*, using C4CN3, which can be hydrolyzed into C4CA3 as the guest, and Q[6] as the host, added Tb(NO₃)₃ in order to prepare a 3D C4CA3@Q[6]/Tb³⁺-based polyrotaxane framework.^[153] Every two Tb³⁺ cations formed a dimeric Tb³⁺ cluster, which coordinates to six protruding carboxyl groups from six adjacent C4CA3@Q[6] pseudorotaxanes (Figure 50a). Fusing this hexameric C4CA3@Q[6]/Tb³⁺ polyrotaxane resulted in the formation of a 3D C4CA3@Q[6]/Tb³⁺ polyrotaxane framework (Figures 50b and c). Figure 50d shows a schematic representation of the 3D C4CA3@Q[6]/Tb³⁺-based polyrotaxane framework.

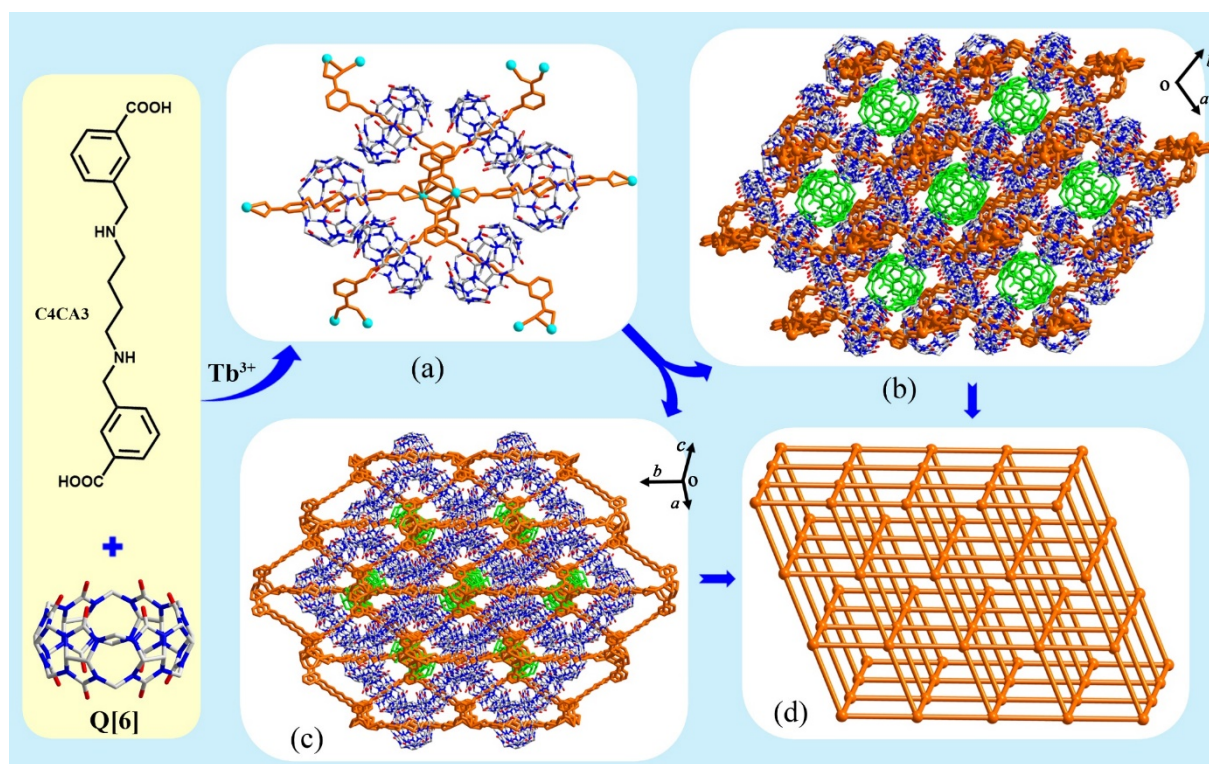


Figure 50. (a) The hexameric C4CA3@Q[6]/Tb³⁺ polyrotaxane; (b, c) the 3D C4CA3@Q[6]/Tb³⁺ polyrotaxane framework viewed from different directions; (d) a schematic representation of the 3D C4CA3@Q[6]/Tb³⁺ polyrotaxane framework.

Wang *et al.* reported the use of dynamic combinatorial coordination chemistry to prepare three isostructural Q[6]-based polyrotaxane frameworks: C6CA4@Q[6]/Mⁿ⁺ (M=Cu²⁺, Zn²⁺, Cd²⁺).^[114] The structures were confirmed using X-ray crystallography and PXRD. The Cu²⁺ case was used as a representative example to illustrate the novelty of the framework structures. Each Cu²⁺ cation coordinates with four protruding carboxyl groups from four adjacent C6CA4@Q[6]/Cu²⁺ pseudorotaxanes (Figure 51a), which can form a 3D C6CA4@Q[6]/Cu²⁺-based pseudorotaxane framework (Figure 51e, Q[6] molecules omitted for clarity). Close inspection revealed that each channel in the framework was formed by a C6CA4@Q[6]/Cu²⁺ helical polyrotaxane (Figure 51c), in which the adjacent helical polyrotaxanes have opposite chirality, as for the system in ref [143] (Figure 33). It is interesting that there are three sets of 3D C6CA4@Q[6]/Cu²⁺ polyrotaxane frameworks which interlock with each other. Figures 51d and e show the frameworks with and without the Q[6] molecules present.

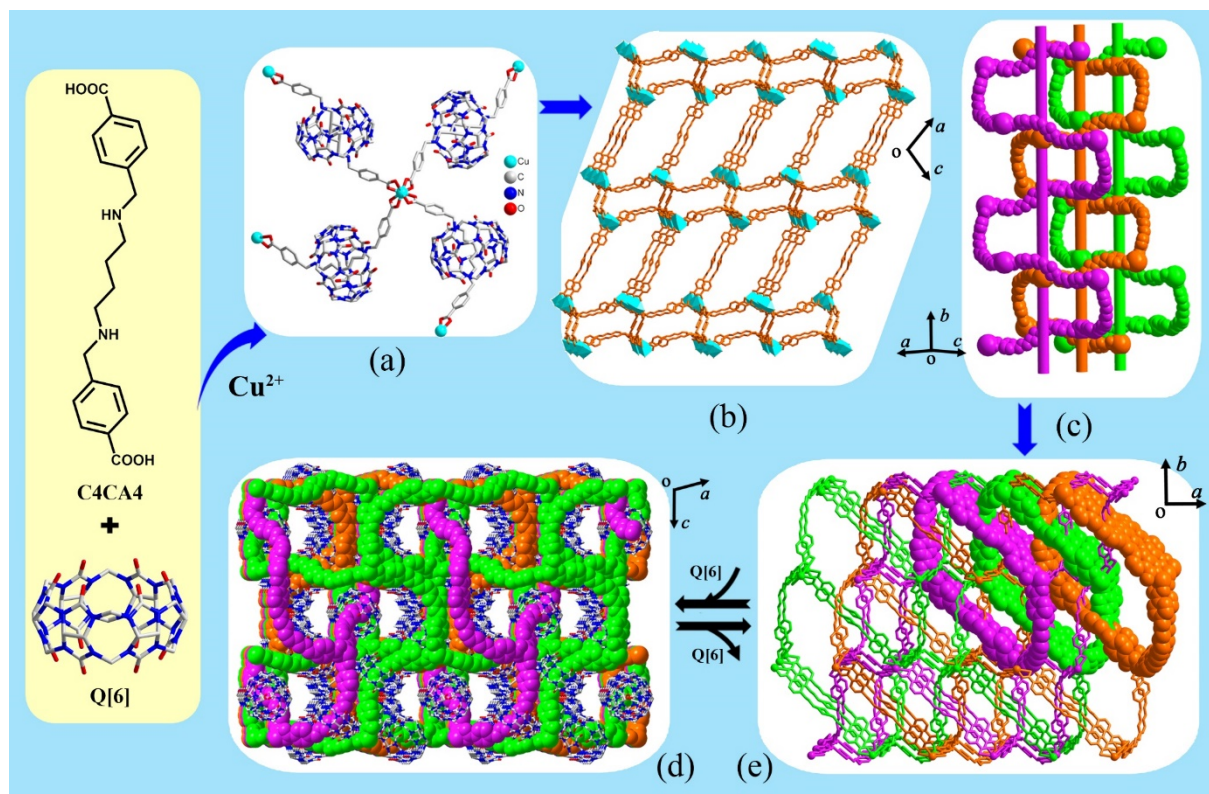


Figure 51. (a) Crystal structure of the basic building block constructed by Cu²⁺ and four C4CA3@Q[6] pseudorotaxanes; (b) a single 3D C4CA3@Q[6] polyrotaxane framework (Q[6] molecules omitted for clarity); (c) the three isolated helices in the framework are mutually

interwoven; the 3D C4CA4@Q[6]/Cu²⁺ polyrotaxane framework (d) with and (e) without Q[6] molecules from different direction.

We have previously mentioned that when Wang and Su introduced 4,4'-biphenyldicarboxylic acid (H₂BPDC) into a C₆N₄@Q[6]/Cd²⁺ system and 1,3-benzenedicarboxylic acid (*m*-H₂BDC) to C₆N₄@Q[6]/Zn²⁺ systems, respectively, they obtained two frameworks constructed from 2D C₆N₄@Q[6]/Cd²⁺- and Zn²⁺-based polyrotaxane frameworks (Figures 49b and e).^[155] Here, we will further introduce their work on the construction of Q[*n*]-based frameworks derived from 3D C₆N₄@Q[6]/Cd²⁺-based polyrotaxanes using the same strategy. For example, introducing 1,4'-benzenedicarboxylic acid (H₂BDC) into the C₆N₄@Q[6]/Cd²⁺ system resulted in the formation of a 3D C₆N₄@Q[6]/Cd²⁺-based polyrotaxane framework (Figure 52e), in which each Cd²⁺ cation coordinated with a protruding pyridyl nitrogen atom of a C₆N₄@Q[6] pseudorotaxane, and two H₂BDC molecules (Figure 52a). In turn, each H₂BDC molecule coordinates to two such Cd²⁺ cations, which resulted in the formation of a 3D C₆N₄@Q[6]/Cd²⁺-based polyrotaxane framework (Figure 52d, Q[6] molecules omitted for clarity). This can also be viewed as the coordination of Cd²⁺/H₂BDC-based 2D frameworks (Figure 52c) and C₆N₄@Q[6] pseudorotaxanes. Similar to the 3D C₆CA₄@Q[6]/Cu²⁺ polyrotaxane framework (Figure 51), there are also three isolated sets of the 3D C₆N₄@Q[6]/Cd²⁺-based polyrotaxane frameworks (shown in original, orange and green, respectively), which are mutually interlocked with one another (Figures 52d and e without and with Q[6] molecules present).

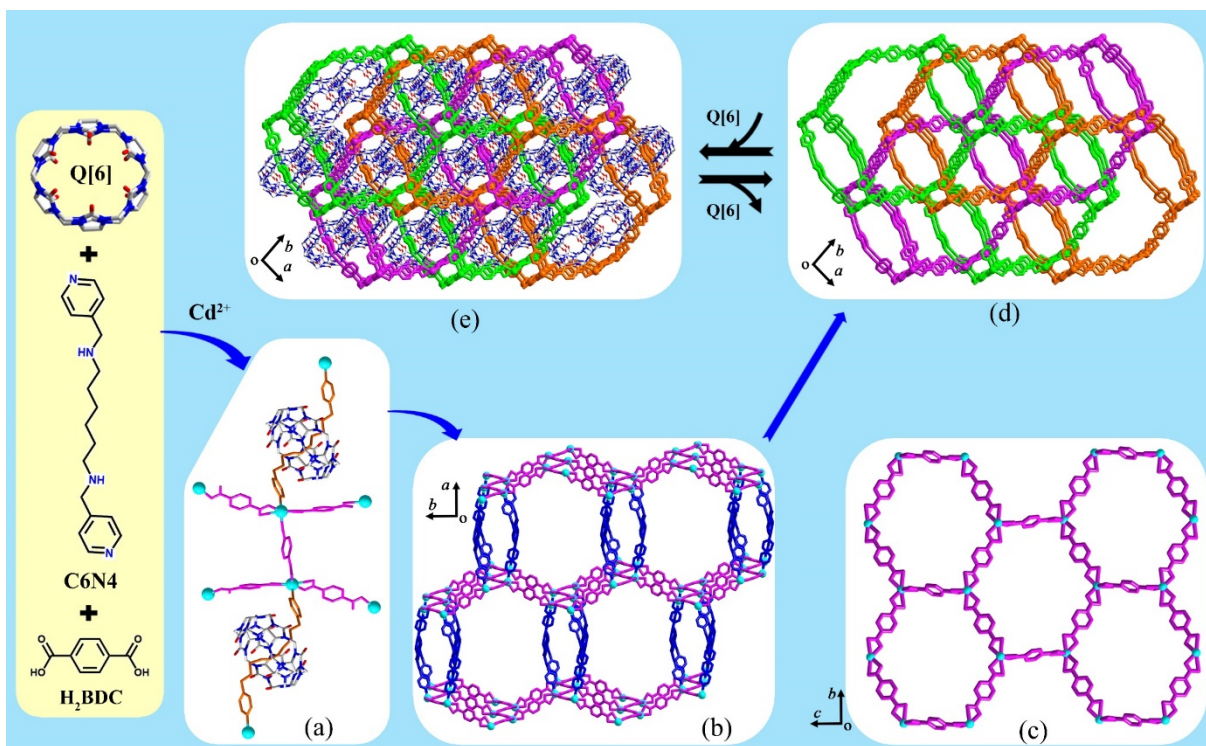


Figure 52. (a) Crystal structure of the C6N4@Q[6]/Cd²⁺/H₂BDC building block; (b) the 3D framework formed by the C6N4@Q[6]/Cd²⁺/H₂BDC building blocks (Q[6] molecules omitted for clarity); (c) the 2D framework formed via the coordination of Cd²⁺ and H₂BDC; the three interlocked 3D frameworks constructed by the C6N4@Q[6]/Cd²⁺/H₂BDC building blocks (d) without and (e) with Q[6] molecules present.

By introducing *m*-H₂BDC into the C6N3@Q[6]/Cd²⁺ system, a 3D C6N3@Q[6]/Cd²⁺/*m*-H₂BDC-based polyrotaxane framework was obtained (Figures 53a and b, with and without the Q[6] molecules present), in which there are two different Cd-complexes. The Cd1 cation coordinates with the protruding carboxyl group of the C6N3@Q[6] pseudorotaxane, and three *m*-H₂BDC molecules, whereas the Cd2 cation is only coordinated to two *m*-H₂BDC molecules (Figure 53c). Figure 53d shows a schematic representation of the 3D C6N3@Q[6]/Cd²⁺/*m*-H₂BDC-based polyrotaxane framework.

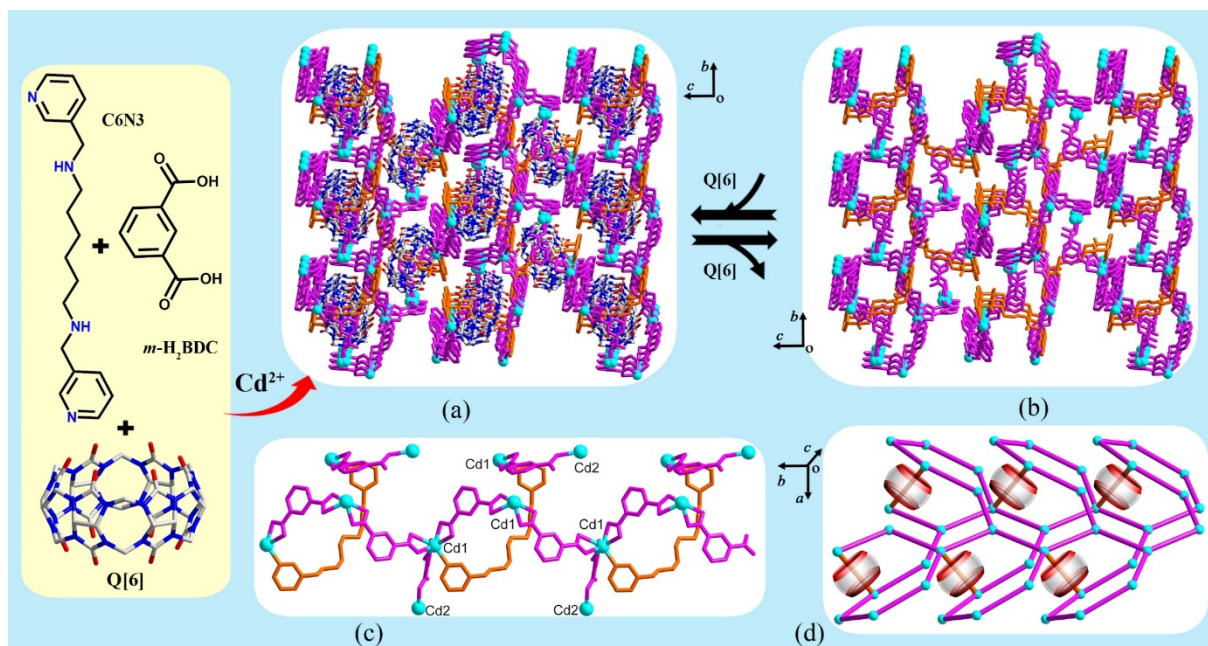


Figure 53. The 3D framework constructed by C6N3@Q[6]/Cd²⁺/*m*-H₂BDC (a) with and (b) without Q[6] molecules; (c) the two different Cd/*m*-H₂BDC complexes; (d) a schematic representation of the C6N3@Q[6]/Cd²⁺/*m*-H₂BDC-based 3D framework.

Upon introducing 1,3,5-benzenetricarboxylic acid (H₃BTC) into a C6N3@Q[6]/Cd²⁺ system, a 3D C6N3@Q[6]/Cd²⁺-based polyrotaxane framework was obtained (Figures 54a and b, without and with the Q[6] molecules present), in which there are three different Cd-complexes. The Cd1 cation coordinates with two protruding carboxyl groups in two C6N3@Q[6] pseudorotaxanes, and two H₃BTC molecules. The Cd2 cation coordinates with a protruding carboxyl group of a C6N3@Q[6] pseudorotaxane, and two H₃BTC molecules. The Cd3 cation coordinates to three H₃BTC molecules and a nitrate anion. This results in the formation of a 2D Cd/H₃BTC-based framework (Figures 54c), which are connected to the C6N3@Q[6] pseudorotaxanes to form a 3D C6N3@Q[6]/Cd²⁺/H₃BTC-based polyrotaxane framework (Figure 54d).^[114]

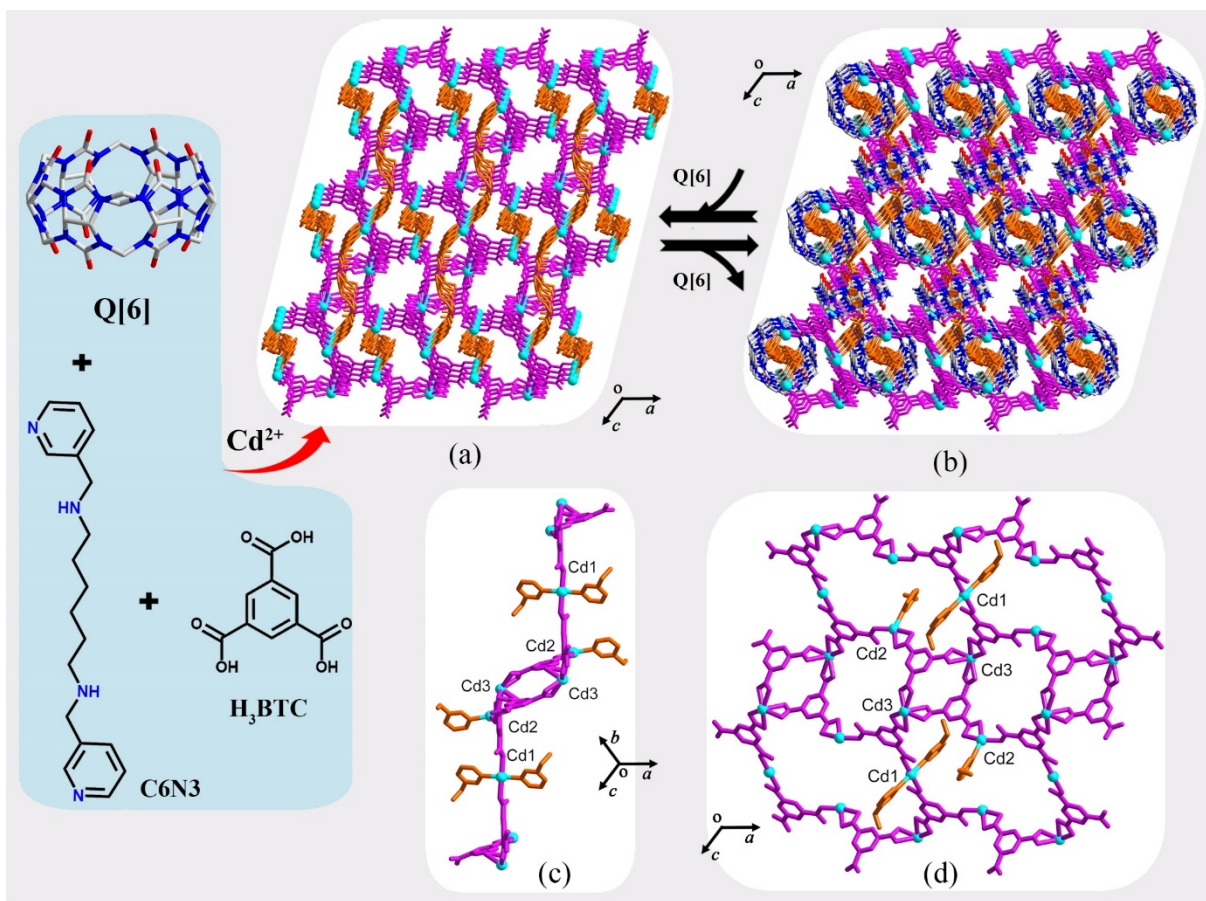


Figure 54. The 3D framework constructed by C₆N₃@Q[6]/Cd²⁺/H₃BTC (a) without and (b) with Q[6] molecules present; (c, d) the three different Cd/H₃BTC complexes observed in the Cd²⁺/*m*-H₂BDC-based 2D framework.

Using the same strategy, Wang *et al.* introduced 1,4-benzenedicarboxylic acid (H₂BDC) into the C₄N₄@Q[6]/Cu²⁺ system, and obtained a framework constructed from 3D C₄N₄@Q[6]/Cu²⁺ polyrotaxanes (Figures 55b and c without and with the Q[6] molecules present).^[156] Every Cu²⁺ cation pair (Cu1-Cu2) is coordinated to four H₂BDC molecules, and in addition to a protruding carboxyl group in an adjacent C₄N₄@Q[6] pseudorotaxane as well as a chloride anion (Figure 55a). In turn, each H₂BDC molecule is coordinated to two Cu²⁺ cation pairs, resulting in the formation of a Cu₂BDC₂-based 2D framework (Figures 55d and e). Indeed, the 3D C₄N₄@Q[6]/Cu²⁺ polyrotaxane framework is constructed by the coordination between the [Cu₂BDC₄] complexes and C₄N₄@Q[6] pseudorotaxanes.

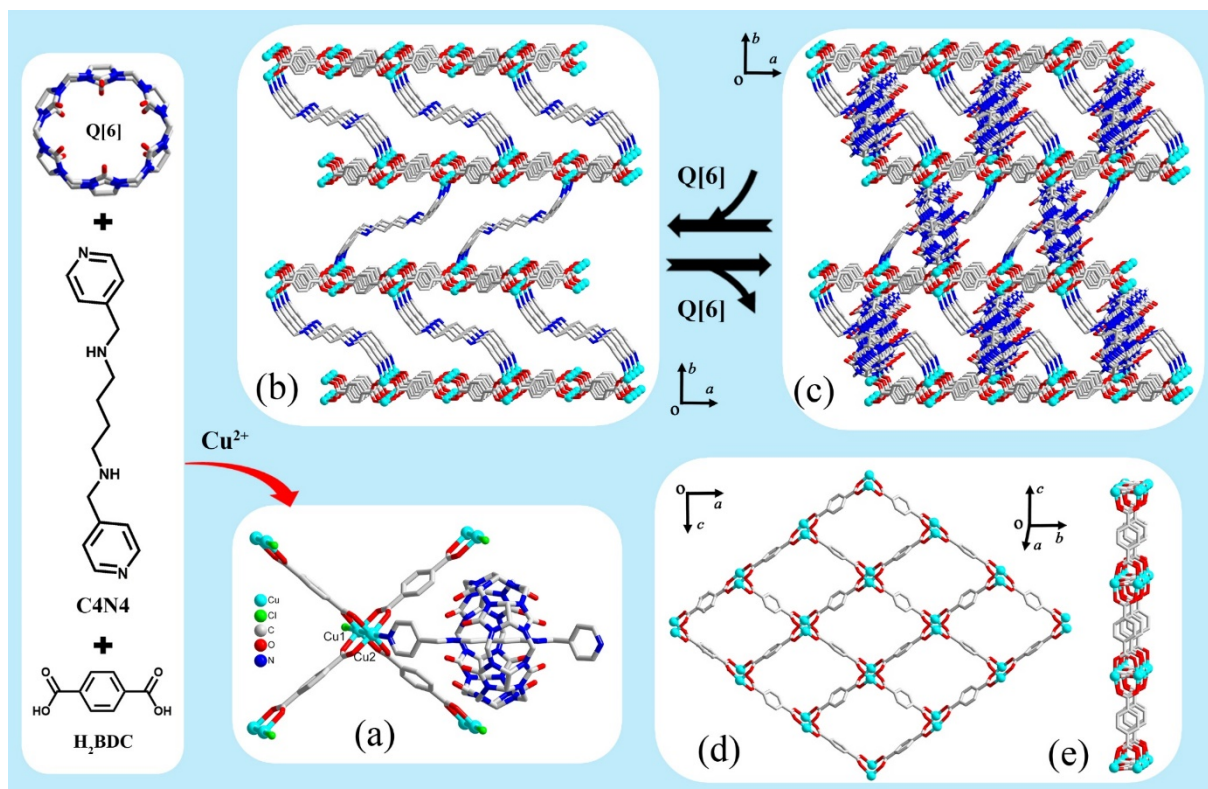


Figure 55. (a) The basic building block constructed by the C4N4@Q[6] pseudorotaxanes, Cu²⁺ cations and BDC²⁻ anions; crystal structure of the 3D C4N4@Q[6]/Cu²⁺-based polyrotaxane framework (b) without and (c) with the Q[6] molecules present; the Cu₂BDC₂-based 2D framework viewed along the (d) *b*- and (e) *c*-axis, respectively.

3. Potential applications of guest@Q[*n*]-based frameworks

This review originated from a series of SOFs based on Q[8] and certain special structural guests reported by Li *et al.*^[98-109] In the process of collecting relevant literature material, it was found that Q[*n*]-based frameworks constructed using Q[*n*]-guest inclusion complexes, especially those supplemented by OSIQs and/or coordination to metal ions, are very common in Q[*n*]-based host-guest chemistry. However, because researchers have tended to focus on other aspects of such Q[*n*]-guest systems, the structural characteristics of many of these frameworks have often been overlooked. Therefore, their potential applications have also gone under the radar. For example, for Q[*n*]-based SOFs constructed by Q[*n*]-guest inclusion complexes, the research purpose usually focuses on the change of the guest properties after inclusion or the properties of the resulting Q[*n*]-guest inclusion complexes. For the Q[*n*]-based

frameworks constructed via the coordination of host-guest inclusion complexes with metal ions, the research purpose usually focuses on the construction strategy and the structural characteristics of the Q[n]-based frameworks. Although the potential applications of these frameworks are yet to be realized, there are emerging some interesting reports, and these are detailed in the sections below.

3.1. Adsorption characteristics

It is well known that extended porous structures and ordered multi-channels are common structural characteristic of all framework materials, and that the selective adsorption of different materials is a common characteristic of such framework materials. Like conventional framework materials, the frameworks constructed using Q[n]-guest inclusion complexes show their own adsorption characteristics for different adsorbates via OSIQs, $\pi \cdots \pi$ stacking, C-H $\cdots\pi$, and hydrogen bonding interactions. The resulting adsorbate@Q[n]-based framework systems exhibit properties such as selective adsorption, sensing, and fluorescence, and thus have extensive potential applications.

3.1.1. Exchange

Kim *et al.* first established the strategy of constructing frameworks via coordinating Q[n]-based host-guest inclusion complexes with metal ions. They introduced oxalates ($\text{Na}_2\text{C}_2\text{O}_4$) into the $\text{C}_5\text{N}_3\text{@Q}[6]/\text{Cu}^{2+}(\text{NO}_3)$ system, and obtained a honeycomb-like polyrotaxane-based 2D cationic framework (Figure 43c).^[153] Stirring a suspension of this Q[6]-based framework in an aqueous solution containing a slight excess of NaPF_6 at room temperature results in exchange of NO_3^- with PF_6^- . The larger tosylate anion can also be exchanged with NO_3^- anions, but the exchange rate is slower than that observed for PF_6^- anions; only ~20% of the anion is exchanged after 6 h. Larger anions such as tetraphenylborate, cannot be exchanged with NO_3^- anions. These results demonstrated the size selectivity of the anion exchange process in this Q[6]-based framework.^[153]

Wang *et al.* have carried out similar work by introducing 1,4-benzenedicarboxylic acid

(H₂BDC) into the C₄N₄@Q[6]/Cu²⁺(NO₃) system, and obtained a Q[6]-based framework (Figure 55d),^[156] which exhibited a pillared-layer structure with a 5-connected *sqp* topology and 45.4% effective free volume. The framework contained a large amount of high boiling point solvent molecules (DMF), which were hard to remove by direct evacuation only. A good solution was to exchange the high boiling point solvent with a low boiling point solvent. The exchange experiment using benzene to exchange with DMF in the solid framework showed that the solvent exchange process was completed over 10 h and the driving force changed from π -interactions between C=O_{portal} and C=O_{DMF} to aromatic-induced OSIQs (Figure 56a). Thus, guest molecule exchange can be used in a single-crystal-to-single-crystal fashion (Figure 56b).

the

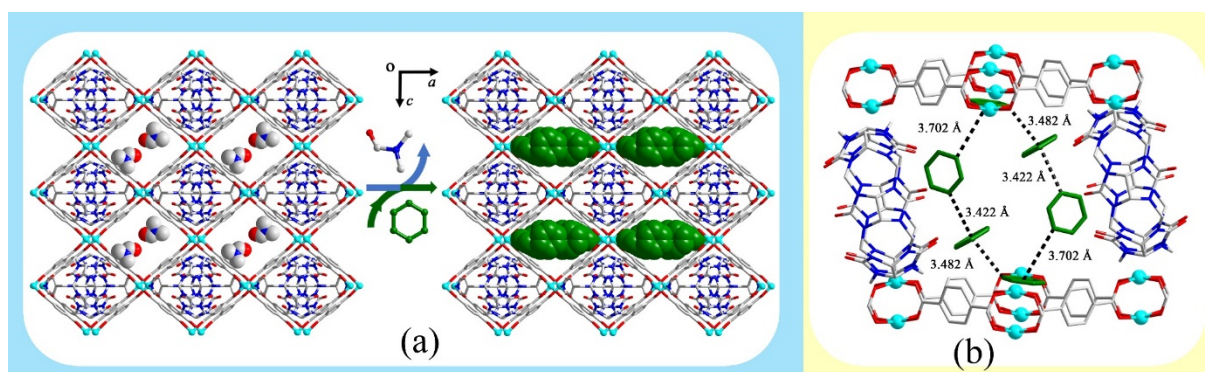


Figure 56. (a) A schematic illustration of the guest exchange process from the Q[6]-based framework to benzene-Q[6]-based framework; (b) the arrangement and interactions of the benzene molecules within the cavity of the Q[6]-based framework.

3.1.2. Selective adsorption and release

Li *et al.* used a tetratopic guest bearing four 4-(4-methoxyphenyl)pyridin-1-ium units to prepare a periodic 3D SOF in both the solid-state and in water (Figure 22b).^[104] This framework exhibited different adsorption abilities for 20 different anionic guests of varying shape and size, including dyes, drugs, peptides, DNA and dendrimers (Figure 57). Indeed, this SOF can act as a supramolecular ‘ion sponge’. Figure 58a shows the amount of 20 guests absorbed by the microcrystals of this SOF after 60 h when the adsorption process reached equilibrium. Figures 58b and c show that the drugs absorbed in microcrystals can be selectively released into

different aqueous solutions.^[104]

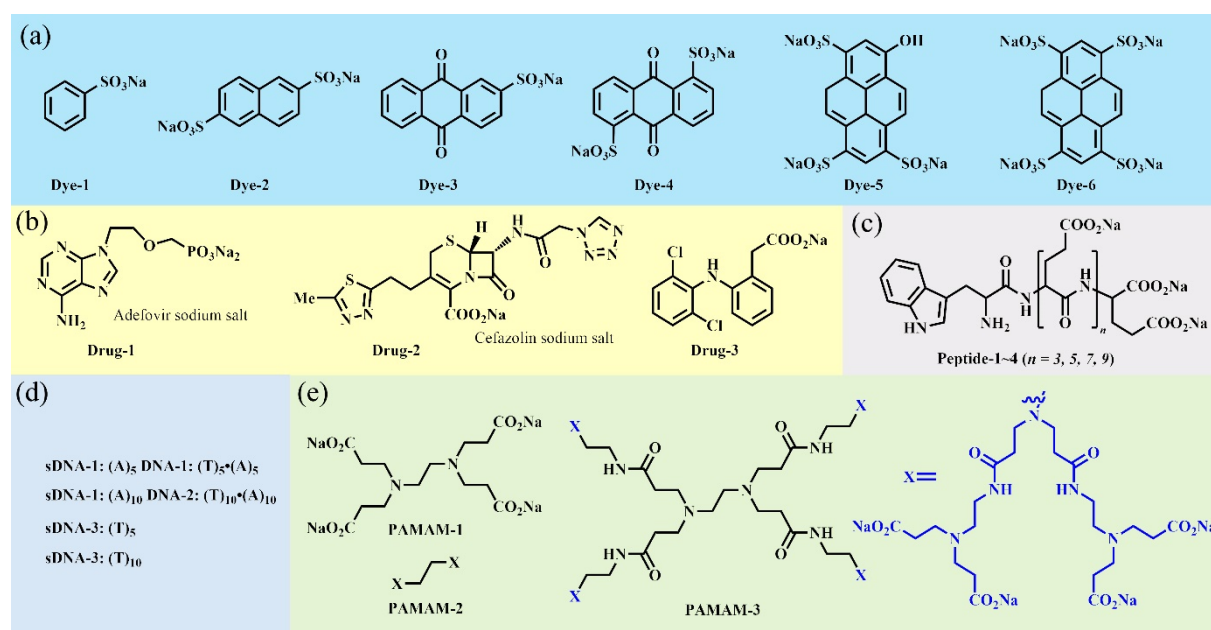


Figure 57. Structures of the guest molecules: (a) Dye-1–6, (b) Drug-1–3, (c) Peptide-1–4, (d) sDNA-1–4, DNA-1–2 and (e) dendrimers PAMAM-1–3.

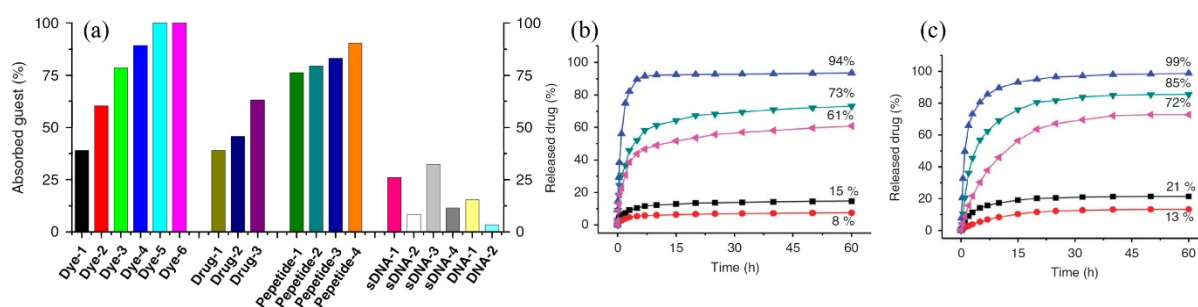


Figure 58. (a) Amount of guest molecules absorbed by the microcrystals of the SOF after 60 h. The release of microcrystal (1 mg)-adsorbed drugs observed at 37 °C vs. time in (b) 1.0 mL of water containing 1.0 equivalent of hydrochloric acid relative to the molar amount of the Na⁺ ion of the attracted guests and (c) 1.0 mL of CH₃CO₂H/CH₃CO₂Na buffer (pH = 4.5). The experiments were conducted with samples in a static state (blue triangles: Drug-3, black squares: Drug-1 and red circles: Drug-2) or on an orbital shaker (green triangles: Drug-1 and purple triangles: Drug-2).^[104]

Again, Li *et al.* prepared a 3D SOF with hexagonal pores constructed from a TPE derivative bearing four 4,4'-bipyridin-1-ium ends at the TPE core and the host Q[8] (Figure 22g). Moreover, adsorption experiments revealed that this ionic framework exhibited affinity toward

photosensitizers in water, such as $[\text{Ru}(\text{BDC})_3]^{4-}$ (K^+ salt) and $\text{Ru}(\text{BPY})_2(\text{BDC})$ (Figures 59a and b), and polyoxometalate (POM) catalysts (redox-active Wells–Dawson-type- $[\text{P}_2\text{W}_{18}\text{O}_{62}]^{6-}$ (K^+ salt, WD-POM) and Keggin-type $\text{PW}_{12}\text{O}_{40}^{3-}$ (Na^+ salt, K-POM-a) (Figures 59c and d) via fluorescence quenching. These two categories of guest molecules have a size of 1.1–1.3 nm and represent important components used in integrated photocatalytic systems (Figure 59e).^[99] Thus, SOFs could be used for the enrichment of molecular photosensitizers and catalysts in a confined nanospace, which are conducive for photocatalytic reactions due to improved photoexcited electron transfer from the photosensitizers to catalysts.

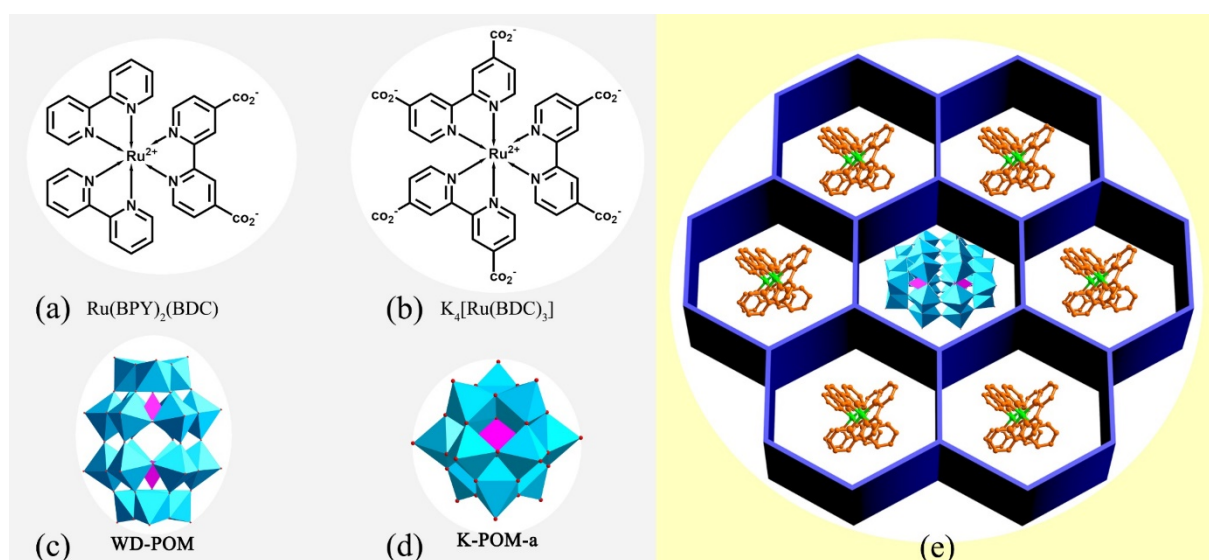


Figure 59. (a-d) Structures of the two Ru-based photosensitizers and two polyoxometalate catalysts; (e) the 3D SOF adsorbed photosensitizer and POM.

3.1.3. Sensor

Zhao *et al.* synthesized two 2D SOFs, one was constructed from a TPE derivative bearing four 4,4'-bipyridin-1-ium ends on the periphery of the TPE core (Figure 23d) and the host Q[8],^[132] whilst the other was constructed from a guest by incorporating three 4-(p-methoxyphenyl)-1-pyridinium units at the periphery of a triphenylamine skeleton (Figure 23e) and the Q[8] host.^[133] The first single-layered 2D SOF with parallelogram pores was prone to aggregation forming layered structures, as a result of the large surface areas of its sheet-like

structure. Moreover, solvophobic interactions can arise between the SOF and organic solvents, in which the SOF cannot be readily solvated due to its ionic nature. Thus, the addition of water-miscible organic solvents such as acetone, acetonitrile, dioxane, and tetrahydrofuran (THF) to an aqueous solution of the SOF resulted in an enhancement of its fluorescence emission at different levels. Figure 60 shows representative fluorescence spectra obtained for the SOF in water-THF at different water/THF ratios, indicating that the aggregation of the 2D SOF results in enhancement of the fluorescence emission of the system.^[132] This property allows these assembled systems to be used as sensors to detect certain solvents or organic compounds. Indeed, the second 2D SOF exhibited a fluorescence turn-on effect upon self-assembly of its components, and displays highly selective and sensitive recognition of picric acid over a variety of other nitroaromatic compounds (Figure 60b).^[133]

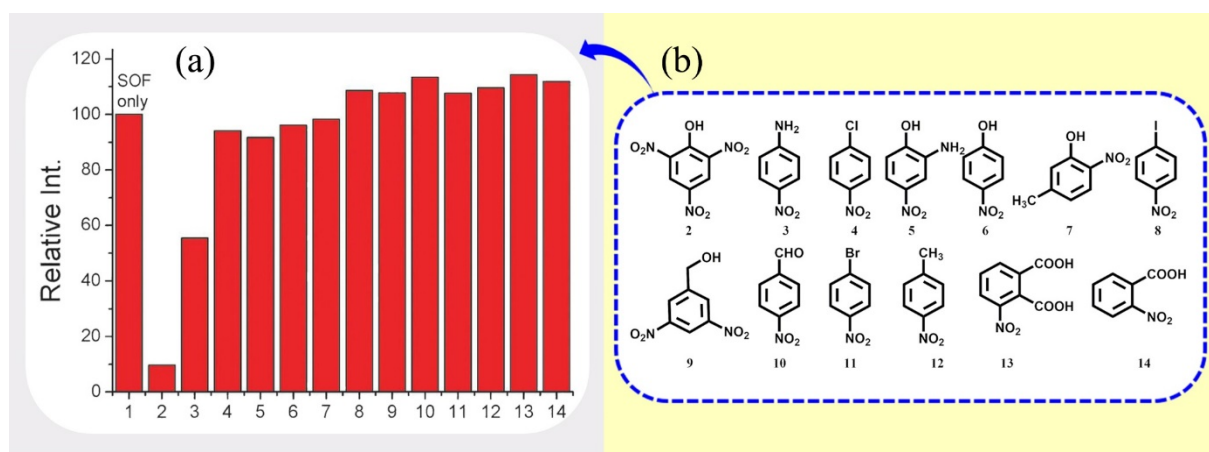


Figure 60. (a) Changes in the fluorescence intensity of the second 2D SOF upon addition of (b) different nitroaromatic compounds.

Using Kim's strategy, namely constructing the frameworks via the coordination of Q[n]-based host-guest inclusion complexes with metal ions, Wang and Su synthesized a 2D C₆N₄@Q[6]/Cd²⁺/H₂BPDC-based polyrotaxane framework and C₆N₄@Q[6]/Zn²⁺/*m*-H₂BDC-based polyrotaxane framework, as shown in Figure 49, as well as a 3D C₆N₄@Q[6]/Cd²⁺/H₂BDC-based polyrotaxane framework (Figure 52), a C₆N₃@Q[6]/Cd²⁺/*m*-H₂BDC -based polyrotaxane framework (Figure 53) and a

C6N3@Q[6]/Cd²⁺ /H₃BTC-based polyrotaxane framework (Figure 54).^[155] Considering the enormous amount of portal carbonyl groups available to the Q[6] molecules at the surfaces of these crystals, the sensitization ability toward visible emitting lanthanide cations was investigated and the experimental results showed that the solid samples maintained their full crystallinity. Figure 61 shows the photographs of these composites excited using a standard laboratory ultraviolet lamp (254 nm), which indicated that (H₂BDC)C6N4@Q[6]/Cd²⁺⊂Eu and (*m*-H₂BDC)C6N4@Q[6]/Zn²⁺⊂Eu were better emitters than (*m*-H₂BDC)C6N3@Q[6]/Cd²⁺⊂Eu and (H₃BTC)C6N3@Q[6]/Cd²⁺⊂Eu (pink colour). They emitted a distinctive red colour, which was readily observed by the naked eye as a qualitative indication of europium sensitization.^[155]

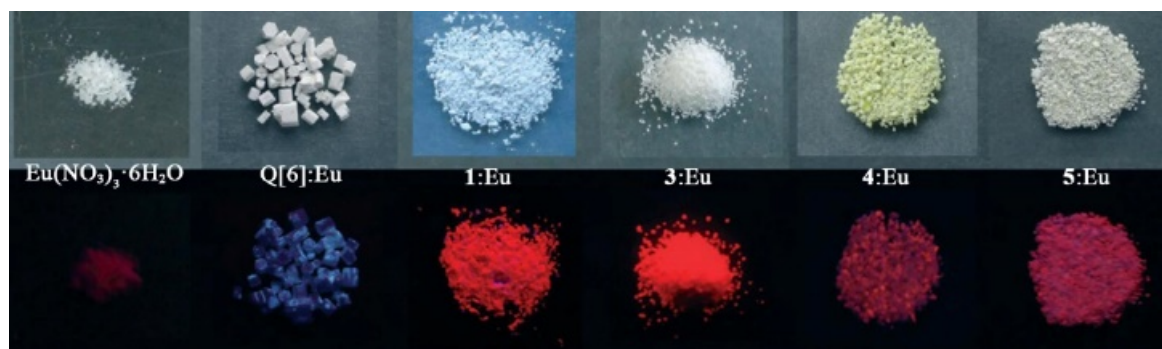


Figure 61. Samples illuminated using daylight (top) and a 254 nm laboratory UV light (bottom). From left to right: Eu(NO₃)₃·6H₂O and **X**: Eu (**X** = Q[6] powder, **1**: (H₂BDC)C6N4@Q[6]/Cd²⁺ ; **3**: (*m*-H₂BDC)C6N4@Q[6]/Zn²⁺; **4**: (*m*-H₂BDC)C6N3@Q[6]/Cd²⁺; **5**: (H₃BTC)C6N3@Q[6]/Cd²⁺⊂Eu).

3.2. Catalysis

Li *et al.* reported a self-assembly strategy for the generation of the first homogeneous supramolecular metal-organic framework in water at room temperature from a hexa-armed [Ru(bpy)₃]²⁺-based precursor and a Q[8] host (Figure 22b).^[102] The framework adsorbs anionic WD-POMs to form a photocatalyst. Upon visible-light (500 nm) irradiation, such hybrids enable fast multi-electron injection from the photosensitive [Ru(bpy)₃]²⁺ units to the redox-active WD-POM units, leading to efficient H₂ production in both aqueous and organic media.

The demonstrated strategy opens the door for the development of new classes of liquid-phase and solid-phase ordered porous materials.

Li *et al.* also modified a $[\text{Ru}(\text{byp})_3]^{2+}$ -attached acylhydrazine moiety to a 3D diamond SOF-CHO to obtain an efficient recyclable heterogeneous catalyst, as shown in (Figure 22e).^[101] The resulting SOF-CH=N- $[\text{Ru}(\text{byp})_3]$ can act as the heterogeneous photocatalyst which allowed the reduction of aromatic azides to related amines under visible light.

3.3. Bioapplications

Li *et al.* synthesized a series of 2D and 3D SOFs, among them two 2D single-layered SOFs were constructed from a 1,3,5-triphenylbenzene derivative bearing three viologen units at the peripheral benzene rings and three hydrophilic bis(2-hydroxy-ethyl)carbamoyl groups in an aqueous medium, respectively (Figure 21a).^[105] The 2D SOFs may be regarded as layered cationic supramolecular polyelectrolytes and their antimicrobial activity was studied using agar diffusion assays of methicillin-resistant *Staphylococcus aureus* (MRSA) as a test strain. The assays showed that both SOFs exhibited moderate activity against MRSA in a dose-dependent manner. In contrast, the guests (Figures 22a and 23b) and Q[8] at an identical concentration did not show any detectable activity. Thus, the activity exhibited by the two SOFs was tentatively attributed to their increased cation concentration in the 2D space on the surface of MRSA. ^[157]
^[158]

4. Conclusion

This paper reviews research progress on guest@Q[n]-based frameworks in Q[n]-chemistry. Although it focuses on those frameworks based on the interaction between Q[n]s and guest molecules, these are inevitably related to the OSIQs and coordination with metal ions. Therefore, this review represents a comprehensive study of integrating Q[n]-based host-guest chemistry, Q[n]-based coordination chemistry and OSIQ chemistry. According to the structural characteristics of the guest@Q[n] inclusion complexes, their guest@Q[n]-based frameworks can be divided into four categories, namely, those constructed through (1) simple host-guest

inclusion complexes; (2) host–guest inclusion supramolecular polymers or frameworks; (3) host-guest exclusion complexes or supramolecular polymers; and (4) coordination complexes of the host–guest inclusion complexes with metal ions. For guest@Q[n]-based frameworks composed of simple host-guest inclusion complexes, other interactions are usually present. The most common are OSIQs, including self-induced OSIQ, anion-induced OSIQ and aromatic-induced OSIQ. Similar situations can be observed in the case of the construction via 1D or even 2D polyrotaxanes and host–guest inclusion supramolecular polymers or frameworks. This is attributed to the electrostatic positive potential of the outer surface of Q[n]s.

Like any other framework material, Q[n]-based frameworks constructed from Q[n]-based host–guest inclusion complexes also have various channels and holes. Therefore, they also have the adsorption characteristics common to all framework materials, such as adsorption-desorption characteristics, molecular recognition functions, special molecular containers, sensors, molecule delivery and other characteristics derived from their adsorption characteristics. Some investigations on functional properties have shown that guest@Q[n]-based frameworks are outstanding in molecular exchanges, selective adsorption and release, sensors, catalytic processes.

However, it is a new proposition to take Q[n]-based frameworks constructed from Q[n]-based host-guest inclusion complexes as a research direction of Q[n]-chemistry, because the mainstream research direction based on Q[n]-based host-guest chemistry is usually concerned with interactions formed between Q[n]s and guest molecules and the characteristics of the Q[n]-guests interaction system. However, the architectural problems of Q[n]-based host–guest inclusion complexes are often ignored. Indeed, to our knowledge, there is limited research on the functional properties of these framework structures or their application prospects. Therefore, in the next stage of research, we should not only develop more updated guest@Q[n]-based framework systems, but also strengthen the research on the characteristics of these new systems, especially their functional properties and the application prospects thereof.

Acknowledgements

We acknowledge the support of National Natural Science Foundation of China (No. 21601090, 21761007 and 21871064), and the Natural Science Foundation of Jiangsu Province (Grant No. BK20160943). Dr. J.-L. Zhao thanks the Basic Research Program of Shenzhen (JCYJ20190812151405298); CR thanks the EPSRC for an Overseas Travel Grant.

Received: ((will be filled in by the editorial staff))

Revised: ((will be filled in by the editorial staff))

Published online: ((will be filled in by the editorial staff))

References

- [1] A. A. Siyal, M. R. Shamsuddin, A. Low, N. E. Rabat, A review on recent developments in the adsorption of surfactants from wastewater, *J. Environ. Manage.*, 2020, **254**, 109797.
- [2] D. Schwalbe-Koda, Z. Jensen, E. Olivetti, R. Gómez-Bombarelli, Graph similarity drives zeolite diffusionless transformations and intergrowth, *Nat. Mater.*, **2019**, *18*, 1177-1181.
- [3] M. Moliner, Y. Román-Leshkov, A. Corma, Machine Learning Applied to Zeolite Synthesis: The Missing Link for Realizing High-Throughput Discovery, *Acc. Chem. Res.*, 2019, **52**, 2971-2980.
- [4] B. C. Knott, C. T. Nimlos, D. J. Robichaud, M. R. Nimlos, S. Kim, R. Gounder, Consideration of the Aluminum Distribution in Zeolites in Theoretical and Experimental Catalysis Research, *ACS Catal.*, 2018, **8**, 770-784.
- [5] I. I. Ivanova, E. E. Knyazeva, Micro-mesoporous materials obtained by zeolite recrystallization: synthesis, characterization and catalytic applications, *Chem. Soc. Rev.*, 2013, **42**, 3671-3688.

- [6] E. Garrone, C. O. Areán, Variable temperature infrared spectroscopy: A convenient tool for studying the thermodynamics of weak solid–gas interactions, *Chem. Soc. Rev.*, 2005, **34**, 846.
- [7] C. Tung, L. Wu, L. Zhang, B. Chen, Supramolecular Systems as Microreactors: Control of Product Selectivity in Organic Phototransformation, *Acc. Chem. Res.*, 2003, **36**, 39.
- [8] M. Fujita, Y. J. Kwon, S. Washizu, K. Ogura, Preparation, clathration ability, and catalysis of a two-dimensional square network material composed of cadmium (II) and 4,4'-bipyridine, *J. Am. Chem. Soc.*, 1994, **114**, 1151-1152.
- [9] K. Kasai, M. Aoyagi, M. Fujita, Flexible coordination networks with fluorinated backbones. Remarkable ability for induced-fit enclathration of organic molecules, *J. Am. Chem. Soc.*, 2000, **122**, 2140-2141.
- [10] O. M. Yaghi, G. Li, H. Li, Selective binding and removal of guests in a microporous metal-organic framework, *Nature*, 1995, **378**, 703-706.
- [11] M. Kondo, T. Yoshitomi, K. Seki, H. Matsuzaka, S. Kitagawa, Three-Dimensional Framework with Channeling Cavities for Small Molecules: $\{[M_2(4,4'-bpy)_3(NO_3)_4] \cdot xH_2O\}_n$ (M=Co, Ni, Zn), *Angew. Chem. Int. Ed.*, 1997, **36**, 1725-1727.
- [12] M. Eddaoudi, D. B. Moler, H. Li, B. Chen, T. M. Reineke, M. O'keeffe, O. M. Yaghi, *Acc. Chem. Res.* **2001**, *34*, 319-330.
- [13] K. Biradha, M. Fujita, A Springlike 3D - Coordination Network That Shrinks or Swells in a Crystal - to - Crystal Manner upon Guest Removal or Readsorption, *Angew. Chem. Int. Ed.*, 2002, **41**, 3392-3395.
- [14] O. M. Yaghi, M. O'Keeffe, N. W. Ockwig, H. K. Chae, M. Eddaoudi, J. Kim, Reticular synthesis and the design of new materials, *Nature*, 2003, **423**, 705-714.
- [15] S. Kitagawa, R. Kitaura, S.-i. Noro, Functional porous coordination polymers, *Angew. Chem. Int. Ed.*, 2004, **43**, 2334-2375.

- [16] M. Kawano, M. Fujita, Direct observation of crystalline-state guest exchange in coordination networks, *Coord. Chem. Rev.*, 2007, **251**, 2592-2605.
- [17] A. Helal, Z. H. Yamani, K. E. Cordova, O. M. Yaghi, Multivariate metal-organic frameworks, *Natl. Sci. Rev.*, 2017, **4**, 296.-298
- [18] Q. Wang, D. Astruc, State of the Art and Prospects in Metal–Organic Framework (MOF)-Based and MOF-Derived Nanocatalysis, *Chem. Rev.*, 2020, **120**, 1438-1511.
- [19] T. J. Greenfield, M. Julve, R. P. Doyle, Exploring the biological, catalytic, and magnetic properties of transition metal coordination complexes incorporating pyrophosphate, *Coord. Chem. Rev.* 2019, **384**, 37-64.
- [20] D. Li, P. Ma, J. Niu, J. Wang, Recent advances in transition-metal-containing Keggin-type polyoxometalate-based coordination polymers, *Coord. Chem. Rev.*, 2019, **392**, 49-80.
- [21] Q. Yue, E. Gao, Azide and carboxylate as simultaneous coupler for magnetic coordination polymers, *Coord. Chem. Rev.*, **2019**, 382, 1-31.
- [22] S. Kitagawa, R. Kitaura, S. Noro, Functional Porous Coordination Polymers, *Angew. Chem. Int. Ed.*, 2004, **43**, 2334-2375.
- [23] X. Feng, X. S. Ding, D. L. Jiang, Covalent organic frameworks, *Chem. Soc. Rev.*, 2012, **41**, 6010-6022.
- [24] S.-Y. Ding, W. Wang, Covalent organic frameworks (COFs): from design to applications, *Chem. Soc. Rev.*, 2013, **42**, 548-568.
- [25] P. J. Waller, F. Gándara, O. M. Yaghi, Chemistry of Covalent Organic Frameworks, *Acc. Chem. Res.*, 2015, **48**, 3053-3063.
- [26] H. Wang, Z. Zeng, P. Xu, L. Li, G. Zeng, R. Xiao, Z. Tang, D. Huang, L. Tang, C. Lai, D. Jiang, Y. Liu, H. Yi, L. Qin, S. Ye, X. Ren, W. Tang, Recent progress in covalent organic framework thin films: fabrications, applications and perspectives, *Chem. Soc. Rev.*, 2019, **48**, 488-516.

- [27] J. Zhang, J. Chen, S. Peng, S. Peng, Z. Zhang, Y. Tong, P. W. Miller, Emerging porous materials in confined spaces: from chromatographic applications to flow chemistry, X. Yan, *Chem. Soc. Rev.*, 2019, **48**, 2566-2595.
- [28] Z. Li, X. Zhang, H. Cheng, J. Liu, M. Shao, M. Wei, D. G. Evans, H. Zhang, X. Duan, Confined Synthesis of 2D Nanostructured Materials toward Electrocatalysis, *Adv. Energy Mater.*, 2020, **10**, 1900486.
- [29] W. Xie, D. Cui, S. Zhang, Y. Xu, D. Jiang, Iodine capture in porous organic polymers and metal–organic frameworks materials, *Mater. Horiz.*, 2019, **6**, 1571.
- [30] J. Zhu, C. Yang, C. Lu, F. Zhang, Z. Yuan, X. Zhuang, Two-Dimensional Porous Polymers: From Sandwich-like Structure to Layered Skeleton, *Acc. Chem. Res.*, 2018, **51**, 3191.
- [31] C. W. Abney, R. T. Mayes, T. Saito, S. Da, Materials for the Recovery of Uranium from Seawater, *Chem. Rev.*, 2017, **117**, 13935.
- [32] E. Moulin, J. J. Armao IV, N. Giuseppone, Triarylamine-Based Supramolecular Polymers: Structures, Dynamics, and Functions, *Acc. Chem. Res.*, 2019, **52**, 975.
- [33] B. M. Rambo, H. Gong, M. Oh, J. L. Sessler, The “Texas-Sized” Molecular Box: A Versatile Building Block for the Construction of Anion-Directed Mechanically Interlocked Structures, *Acc. Chem. Res.*, 2012, **45**, 1390.
- [34] S. J. Loeb, Rotaxanes as ligands: from molecules to materials, *Chem. Soc. Rev.*, 2007, **36**, 226.
- [35] S. M. Cohen, Molecular crystal balls, *Nature*, 2009, **461**, 602.
- [36] A. S. Tayi, A. Kaeser, M. Matsumoto, T. Aida, S. I. Stupp, Supramolecular ferroelectrics, *Nat. Chem.*, 2015, **7**, 281.
- [37] L. Brammer, Developments in inorganic crystal engineering, *Chem. Soc. Rev.*, 2004, **33**, 476.

- [38] L. Cao, P. Wang, X. Miao, Y. Dong, H. Wang, H. Duan, Y. Yu, X. Li, P. J. Stang, Diamondoid Supramolecular Coordination Frameworks from Discrete Adamantanoid Platinum(II) Cages, *J. Am. Chem. Soc.*, 2018, **140**, 7005.
- [39] T. R. Cook, Y. Zheng, P. J. Stang, Metal–Organic Frameworks and Self-Assembled Supramolecular Coordination Complexes: Comparing and Contrasting the Design, Synthesis, and Functionality of Metal–Organic Materials, *Chem. Rev.*, 2013, **113**, 734.
- [40] L. Chen, Q. Chen, M. Wu, F. Jiang, M. Hong, Controllable Coordination-Driven Self-Assembly: From Discrete Metallocages to Infinite Cage-Based Frameworks, *Acc. Chem. Res.*, 2015, **48**, 201.
- [41] J. Teyssandier, S. D. Feyter, K. S. Mali, Host–guest chemistry in two-dimensional supramolecular networks, *Chem. Commun.*, 2016, **52**, 11465.
- [42] T. Friščić, Supramolecular concepts and new techniques in mechanochemistry: cocrystals, cages, rotaxanes, open metal–organic frameworks, *Chem. Soc. Rev.*, 2012, **41**, 3493.
- [43] Y. Inokuma, S. Yoshioka, J. Ariyoshi, T. Arai, Y. Hitora, K. Takada, S. Matsunaga, K. Rissanen, M. Fujita, *Nature*, 2013, **495**, 461.
- [44] M. Fujita, D. Oguro, M. Miyazawa, H. Oka, K. Yamaguchi, K. Ogura, *Nature*, 1995, **378**, 469.
- [45] M. Yoshizawa, M. Tamura, M. Fujita, Diels–Alder in aqueous molecular hosts: unusual regioselectivity and efficient catalysis, *Science*, 2006, **312**, 251.
- [46] T. Murase, Y. Nishijima, M. Fujita, Cage-catalyzed Knoevenagel condensation under neutral conditions in water, *J. Am. Chem. Soc.*, 2012, **134**, 162.
- [47] Q.-F. Sun, J. Iwasa, D. Ogawa, Y. Ishido, S. Sato, T. Ozeki, Y. Sei, K. Yamaguchi, M. Fujita, Self-assembled M24L48 polyhedra and their sharp structural switch upon subtle ligand variation, *Science*, 2010, **328**, 1144.

- [48] D. Fujita, Y. Ueda, S. Sato, H. Yokoyama, N. Mizuno, T. Kumasaka, M. Fujita, Self-assembly of M30L60 icosidodecahedron, *Chem*, 2016, **1**, 91.
- [49] D. Fujita, K. Suzuki, S. Sato, M. Yagi-Utsumi, Y. Yamaguchi, N. Mizuno, T. Kumasaka, M. Takata, M. Noda, S. Uchiyama, K. Kato, M. Fujita, Protein encapsulation within synthetic molecular hosts, *Nat. Commun.*, 2012, **3**, 1093.
- [50] M. Eddaoudi, J. Kim, N. Rosi, D. Vodak, J. Wachter, M. O'Keeffe, O. M. Yaghi, Systematic Design of Pore Size and Functionality in Isoreticular MOFs and Their Application in Methane Storage, *Science*, 2002, **295**, 469.
- [51] J. Zhang, J. Chen, S. Peng, S. Peng, Z. Zhang, Y. Tong, P. W. Miller, X. P. Yan, Emerging porous materials in confined spaces: from chromatographic applications to flow chemistry, *Chem. Soc. Rev.*, 2019, **38**, 1460.
- [52] Y. Wen, J. Zhang, Q. Xu, X. T. Wu, Q. L. Zhu, Pore surface engineering of metal–organic frameworks for heterogeneous catalysis, *Coord. Chem. Rev.*, 2018, **376**, 248.
- [53] X. Liu, D. Huang, C. Lai, G. Zeng, L. Qin, H. Wang, H. Yi, B. Li, S. Liu, M. Zhang, R. Deng, Y. Fu, L. Li, W. Xue, S. Chen, Recent advances in covalent organic frameworks (COFs) as a smart sensing material, *Chem. Soc. Rev.*, 2019, **48**, 5266.
- [54] D. Rodríguez-San-Miguel, F. Zamora, Processing of covalent organic frameworks: an ingredient for a material to succeed, *Chem. Soc. Rev.*, 2019, **48**, 4375.
- [55] C. Zhang, B. Wu, M. Ma, Z. Wang, Z. Xu, Ultrathin metal/covalent–organic framework membranes towards ultimate separation, *Chem. Soc. Rev.*, 2019, **48**, 3811.
- [56] R. Lin, Y. He, P. Li, H. Wang, W. Zhou, B. Chen, Multifunctional porous hydrogen-bonded organic framework materials, *Chem. Soc. Rev.*, **2019**, *48*, 1362.
- [57] H. Cong, X. L. Ni, X. Xiao, Y. Huang, Q. J. Zhu, S. F. Xue, Z. Tao, L. F. Lindoy, G. Wei, Synthesis and separation of cucurbit[n]urils and their derivatives, *Org. Biomol. Chem.*, 2016, **14**, 4335.

- [58] Y. Yu, J. Rebek, Reactions of folded molecules in water. *Acc. Chem. Res.*, 2018, **51**, 3031.
- [59] K. Kim, N. Selvapalam, Y. H. Ko, K. M. Park, D. Kim, J. Kim, Functionalized cucurbiturils and their applications, *Chem. Soc. Rev.*, 2007, **36**, 267.
- [60] K. I. Assaf, W. M. Nau, Cucurbiturils: from synthesis to high-affinity binding and catalysis, *Chem. Soc. Rev.*, 2015, **44**, 394.
- [61] W. Liu, S. K. Samanta, B. D. Smith, L. Isaacs, Synthetic mimics of biotin/(strept) avidin, *Chem. Soc. Rev.*, 2017, **46**, 2391.
- [62] J. Mosquera, Y. Zhao, H. Jang, N. Xie, C. Xu, N. A. Kotov, L. M. Liz-Marzán, Plasmonic Nanoparticles with Supramolecular Recognition, *Adv. Funct. Mater.*, 2020, **30**, 190208.
- [63] R. Pinalli, A. Pedrini, E. Dalcanale, Biochemical sensing with macrocyclic receptors, *Chem. Soc. Rev.*, 2018, **47**, 7006.
- [64] S. Gadde, A. E. Kaifer, Cucurbituril complexes of redox active guests, *Curr. Org. Chem.*, 2011, **15**, 27.
- [65] J. Murray, K. Kim, T. Ogoshi, W. Yao, B. C. Gibb, The aqueous supramolecular chemistry of cucurbit[n]urils, pillar[n]arenes and deep-cavity cavitands, *Chem. Soc. Rev.*, 2017, **46**, 2479.
- [66] O. A. Gerasko, M. N. Sokolov, V. P. Fedin, Mono- and polynuclear aqua complexes and cucurbit[6]uril: Versatile building blocks for supramolecular chemistry, *Pure Appl. Chem.*, 2004, **76**, 1633.
- [67] J. Lü, J. X. Lin, M. N. Cao, R. Cao, Cucurbituril: A promising organic building block for the design of coordination compounds and beyond, *Coord. Chem. Rev.*, 2013, **257**, 1334.
- [68] X. L. Ni, X. Xiao, H. Cong, L. L. Liang, K. Chen, X. J. Cheng, N. N. Ji, Q. J. Zhu, S. F. Xue, Z. Tao, Cucurbit[n]uril-based coordination chemistry: from simple coordination

- complexes to novel poly-dimensional coordination polymers, *Chem. Soc. Rev.*, 2013, **42**, 9480.
- [69] X. L. Ni, S. F. Xue, Z. Tao, Q. J. Zhu, L. F. Lindoy, G. Wei, Advances in the lanthanide metallosupramolecular chemistry of the cucurbit[n]urils, *Coord. Chem. Rev.*, 2015, **287**, 89.
- [70] X. L. Ni, X. Xiao, H. Cong, Q. J. Zhu, S. F. Xue, Z. Tao, Self-assemblies based on the “outer-surface interactions” of cucurbit[n]urils: new opportunities for supramolecular architectures and materials, *Acc. Chem. Res.*, 2014, **47**, 1386.
- [71] Y. Huang, R. H. Gao, X. L. Ni, X. Xiao, H. Cong, Q. J. Zhu, K. Chen, Z. Tao, Cucurbit[n]uril-based supramolecular frameworks assembled through the outer surface interactions and their functional properties, *Angew. Chem. Int. Ed.*, 2021, **60**, 15166.
- [72] Y. Shen, L. Zou, Q. Wang, *New J. Chem.*, 2017, **41**, 7857.
- [73] Y. Wu, L. Xu, Y. Shen, Y. Wang, L. Zou, Q. Wang, X. Jiang, J. Liu, H. Tian, Template-directed synthesis of cucurbituril analogues using propanediurea as a building block, *Chem. Commun.*, 2017, **53**, 4070.
- [74] W. A. Freeman, W. L. Mock, N. Y. Shih, Cucurbituril, *J. Am. Chem. Soc.*, 1981, **103**, 7367.
- [75] A. I. Day, A. P. Arnold, R. J. Blanch, “Method for synthesis of cucurbiturils”, PCT Int. Appl., WO 2000068232A1, 20001116, 2000.
- [76] J. Kim, I. S. Jung, S. Y. Kim, E. Lee, J. K. Kang, S. Sakamoto, K. Yamaguchi, K. Kim, New Cucurbituril Homologues: Syntheses, Isolation, Characterization, and X-ray Crystal Structures of Cucurbit[n]uril (n = 5, 7, and 8), *J. Am. Chem. Soc.*, 2000, **122**, 540.

- [77] A. I. Day, R. J. Blanch, A. P. Arnold, S. Lorenzo, G. R. Lewis, I. Dance, A cucurbituril - based gyroscane: a new supramolecular form, *Angew. Chem. Int. Ed.*, 2002, **41**, 275.
- [78] X. J. Cheng, L. L. Liang, K. Chen, N. N. Ji, X. Xiao, J. X. Zhang, Y. Q. Zhang, S. F. Xue, Q. J. Zhu, X. L. Ni, Z. Tao, Twisted cucurbit[14]uril, *Angew. Chem., Int. Ed.*, 2013, **52**, 7252.
- [79] Q. Li, S. C. Qiu, J. Zhang, K. Chen, Y. Huang, X. Xiao, Y. Zhang, F. Li, Y. Q. Zhang, S. F. Xue, Q. J. Zhu, Z. Tao, L. F. Lindoy, G. Wei, Twisted cucurbit[n]urils, *Org. Lett.*, 2016, **18**, 4020.
- [80] J. Z. Zhao, H. J. Kim, J. Oh, S. Y. Kim, J. W. Lee, S. Sakamoto, K. Yamaguchi, K. Kim, Cucurbit[n]uril Derivatives Soluble in Water and Organic Solvents, *Angew. Chem. Int. Ed.*, 2001, **40**, 4233.
- [81] S. Sasmal, M. K. Sinha, E. Keinan, Facile purification of rare cucurbiturils by affinity chromatography, *Org. Lett.*, 2004, **6**, 1225.
- [82] L. B. Lu, Y. Q. Zhang, Q. J. Zhu, S. F. Xue, Z. Tao, Synthesis and X-ray Structure of the Inclusion Complex of Dodecamethylcucurbit[6]uril with 1, 4-Dihydroxybenzene, *Molecules*, 2007, **12**, 716.
- [83] F. Wu, L. H. Wu, X. Xiao, Y. Q. Zhang, S. F. Xue, Z. Tao, A. I. Day, Locating the Cyclopentano Cousins of the Cucurbit[n]uril Family, *J. Org. Chem.*, 2012, **77**, 606.
- [84] H. Isobe, S. Sato, E. Nakamura, Synthesis of disubstituted cucurbit [6] uril and its rotaxane derivative, *Org. Lett.*, 2002, **4**, 1287.
- [85] A. I. Day, A. P. Arnold, R. J. Blanch, A method for synthesizing partially substituted cucurbit[n]uril, *Molecules*, 2003, **8**, 74.

- [87] Y. J. Zhao, S. F. Xue, Q. J. Zhu, Z. Tao, J. X. Zhang, Z. B. Wei, L. S. Long, M. L. Hu, H. P. Xiao, A. I. Day, Synthesis of a symmetrical tetrasubstituted cucurbit[6]uril and its host-guest inclusion complex with 2,2'-bipyridine, *Chin. Sci. Bull.*, 2004, **49**, 1111.
- [87] L. M. Zheng, Q. J. Zhu, J. N. Zhu, Y. Q. Zhang, Z. Tao, S. F. Xue, Z. B. Wei, L. S. Long, *Chin. J. Inorg. Chem.*, 2005, **21**, 1583.
- [88] N. Zhao, G. O. Lloyd, O. A. Scherman, Monofunctionalised cucurbit[6]uril synthesis using imidazolium host-guest complexation, *Chem. Commun.*, 2012, **48**, 3070.
- [89] W. H. Huang, P. Y. Zavalij, L. Isaacs, Folding of long-chain alkanediammonium ions promoted by a cucurbituril derivative, *Org. Lett.*, 2008, **10**, 2577.
- [90] D. Lucas, T. Minami, G. Iannuzzi, L. Cao, J. B. Wittenberg, Jr. P. Anzenbacher, L. Isaacs, Templated synthesis of glycoluril hexamer and monofunctionalized cucurbit[6]uril derivatives, *J. Am. Chem. Soc.*, 2011, **133**, 17966.
- [91] B. Vinciguerra, L. Cao, J. R. Cannon, P. Y. Zavalij, C. Fenselau, L. Isaacs, Synthesis and self-assembly processes of monofunctionalized cucurbit[7]uril, *J. Am. Chem. Soc.*, 2012, **134**, 13133.
- [92] L. Cao, L. Isaacs, Daisy chain assembly formed from a cucurbit [6] uril derivative, *Org. Lett.*, 2012, **14**, 3072.
- [93] L. Isaacs, S. K. Park, S. Liu, Y. H. Ko, N. Selvapalam, Y. Kim, H. Kim, P.Y. Zavalij, G-H. Kim, H-S. Lee, K. Kim, The Inverted Cucurbit[n]uril Family, *J. Am. Chem. Soc.*, 2005, **127**, 18000.
- [94] W. H. Huang, S. Liu, P. Y. Zavalij, L. Isaacs, Nor-seco-cucurbit[10]uril exhibits homotropic allostereism, *J. Am. Chem. Soc.*, 2006, **128**, 14744.
- [95] W. H. Huang, P. Y. Zavalij, L. Isaacs, Chiral recognition inside a chiral cucurbituril, *Angew. Chem. Int. Ed.*, 2007, **46**, 7425.
- [96] W. H. Huang, P. Y. Zavalij, L. Isaacs, Cucurbit[n]uril Formation Proceeds by Step-Growth Cyclo-oligomerization, *J. Am. Chem. Soc.*, 2008, **130**, 8446.

- [97] R. H. Gao, Y. Huang, K. Chen, Z. Tao, Cucurbit[n]uril-based frameworks constructed through coordination interaction and their functional properties, *Coord. Chem. Rev.*, 2021, **437**, 213741.
- [98] M. Yan, X. B. Liu, Z. Z. Gao, Y. P. Wu, J. L. Hou, H. Wang, D. W. Zhang, Y. Liu, Z. T. Li, A pore-expanded supramolecular organic framework and its enrichment of photosensitizers and catalysts for visible-light-induced hydrogen production, *Org. Chem. Front.*, 2019, **6**, 1698.
- [99] S. B. Yu, Q. Qi, B. Yang, H. Wang, D. W. Zhang, Y. Liu, Z. T. Li, Enhancing Hydrogen Generation Through Nanoconfinement of Sensitizers and Catalysts in Homogeneous Supramolecular Organic Framework, *Small*, 2018, **14**, 1801037.
- [100] X. F. Li, S. B. Yu, B. Yang, J. Tian, H. Wang, D. W. Zhang, Y. Liu, Z. T. Li, A stable metal-covalent-supramolecular organic framework hybrid: enrichment of catalysts for visible light-induced hydrogen production, *Sci. China Chem.*, 2018, **61**, 830.
- [101] Y. P. Wu, B. Yang, J. Tian, S. B. Yu, H. Wang, D. W. Zhang, Y. Liu, Z. T. Li, Postmodification of supramolecular organic framework: visible-light-induced recyclable heterogeneous photocatalysis for reduction of azides to amines, *Chem. Commun.*, 2017, **53**, 13367.
- [102] J. Tian, Z. Y. Xu, D. W. Zhang, H. Wang, S. H. Xie, D. W. Xu, Y. H. Ren, H. Wang, Y. Liu, Z. T. Li, Supramolecular metal-organic frameworks that display high homogeneous and heterogeneous photocatalytic activity for H₂ production, *Nat. Commun.*, 2016, **7**, 11580.
- [103] L. Zhang, Y. L. Jia, H. Wang, D. W. Zhang, Q. Zhang, Y. Liu, Z. T. Li, pH-Responsive single-layer honeycomb supramolecular organic frameworks that exhibit antimicrobial activity, *Polym. Chem.*, 2016, **7**, 1861.

- [104] J. Tian, T. Y. Zhou, S. C. Zhang, S. Aloni, M. V. Altoe, S. H. Xie, H. Wang, D. W. Zhang, X. Zhao, Y. Liu, Z. T. Li, Three-dimensional periodic supramolecular organic framework ion sponge in water and microcrystals, *Nat. Commun.*, 2014, **5**, 5574.
- [105] L. Zhang, T. Y. Zhou, J. Tian, H. Wang, D. W. Zhang, X. Zhao, Y. Liu, Z. T. Li, A two-dimensional single-layer supramolecular organic framework that is driven by viologen radical cation dimerization and further promoted by cucurbit[8]uril, *Polym. Chem.*, 2014, **5**, 4715.
- [106] K. D. Zhang, J. Tian, D. Hanifi, Y. B. Zhang, A. C. Sue, T. Y. Zhou, L. Zhang, X. Zhao, Y. Liu, Z. T. Li, Toward a Single-Layer Two-Dimensional Honeycomb Supramolecular Organic Framework in Water, *J. Am. Chem. Soc.*, 2013, **135**, 17913.
- [107] J. Tian, L. Chen, D. W. Zhang, Y. Liu, Z. T. Li, Supramolecular organic frameworks: engineering periodicity in water through host-guest chemistry, *Chem. Commun.*, 2016, **52**, 6351.
- [108] J. Tian, H. Wang, D. W. Zhang, Y. Liu, Z. T. Li, Supramolecular organic frameworks (SOFs): homogeneous regular 2D and 3D pores in water, *Natl. Sci. Rev.* **2017**, *4*, 426.
- [109] L. He, J. P. Zeng, D. H. Yu, H. Cong, Y. Q. Zhang, Q. J. Zhu, S. F. Xue, Z. Tao, Kinetic and thermo dynamic inclusion complexes of symmetric teramethyl-substituted cucurbit[6]uril with HCl salts of N,N'-bis(pyridylmethyl)-1,6-hexanediamine, *Supramol. Chem.*, 2010, **22**, 619.
- [110] F. Zhang, T. Yajima, Y. Z. Li, G. Z. Xu, H. L. Chen, Q. T. Liu, O. Yamauchi, Iodine-Assisted Assembly of Helical Coordination Polymers of Cucurbituril and Asymmetric Copper (II) Complexes. *Angew. Chem. Int. Ed.*, 2005, **44**, 3402–3407.
- [111] M. V. S. N. Maddipatla, M. Pattabiraman, A. Natarajan, K. Srivastava, J. T. Mague, V. Ramamurthy, Regioselective photodimerization of pyridyl-butadienes within cucurbit[8]uril cavities, *Org. Biomol. Chem.*, 2012, **10**, 9219.

- [112] Z. F. Fan, J. Wang, Y. Huang, S. F. Xue, X. Xiao, Y. Q. Zhang, Q. J. Zhu, Z. Tao, Host–guest complexes of various cucurbit[n]urils with the hydrochloride salt of 2,4-diaminoazobenzene, *J. Incl. Phenom. Macrocycl. Chem.*, 2012, **72**, 213.
- [113] K. J. Hartlieb, A. N. Basuray, C. Ke, A. A. Sarjeant, H.-P. J. de Rouville, T. Kikuchi, R. S. Forgan, J. W. Kurutz, J. F. Stoddart, Chameleonic Binding of the Dimethyldiazaperopyrenium Dication by Cucurbit[8]uril, *Asian J. Org. Chem.*, 2013, **2**, 225.
- [114] J. Liang, X. L. Wang, Y. Q. Jiao, C. Qin, K. Z. Shao, Z. M. Su, Q. Y. Wu, Metal ion directed metal–organic rotaxane frameworks with intrinsic features of self-penetration and interpenetration, *Chem. Commun.*, 2013, **49**, 8555.
- [115] O. Danylyuk, V. P. Fedin, V. Sashuk, Host–guest complexes of cucurbit[6]uril with isoprenaline: the effect of the metal ion on the crystallization pathway and supramolecular architecture, *CrystEngComm*, 2013, **15**, 7414.
- [116] W. J. Ma, J. M. Chen, L. Jiang, J. Yao, T. B. Lu, The Delivery of Triamterene by Cucurbit[7]uril: Synthesis, Structures and Pharmacokinetics Study, *Mol. Pharmaceutics*, 2013, **10**, 4698.
- [117] L. Gilberg, M. S. A. Khan, M. Enderesova, V. Sindelar, Cucurbiturils Substituted on the Methylene Bridge, *Org. Lett.*, 2014, **16**, 2446.
- [118] C. L. Shan, B. Yang, W. Q. Sun, X. Xiao, Z. Tao, J. X. Liu, 1,3-Propanediammonium and 1,12-dodecanediammonium encapsulated in the cavity of symmetrical $\alpha,\alpha',\delta,\delta'$ -tetramethyl-cucurbit[6]uril, *Supramol. Chem.*, 2015, **27**, 606.
- [119] J. Li, Y. Zhao, Y. Dong, Y. Yu, L. Cao, B. Wu, Supramolecular organic frameworks of cucurbit[n]uril-based [2]pseudorotaxanes in the crystalline state, *CrystEngComm*, 2016, **18**, 7929.
- [120] Z. F. Fan, R. L. Lin, W. Q. Sun, Z. Tao, J. X. Liu, Encapsulation of 2,2'-(decane-1,10-diy)-diisoquinoline into cucurbit[6]uril and $\alpha,\alpha',\delta,\delta'$ -tetramethyl-cucurbit[6]uril:

- formation of pseudorotaxanes and polypseudorotaxanes, *Supramol. Chem.*, 2017, **29**, 323.
- [121] X. Cui, W. Zhao, K. Chen, X. L. Ni, Y. Q. Zhang, Z. Tao, Outer Surface Interactions of Cucurbit[6]uril That Trigger the Assembly of Supramolecular Three-Dimensional Polycatenanes, *Chem. Eur. J.*, 2017, **23**, 2759.
- [122] Z. Y. Xiao, R. L. Lin, Z. Tao, Q. Y. Liu, J. X. Liu, X. Xiao, Multiple noncovalent interaction constructed polymeric supramolecular crystals: recognition of butyl viologen by para-dicyclohexanocucurbit[6]uril and $\alpha,\alpha',\delta,\delta'$ -tetramethylcucurbit[6]uril, *Org. Chem. Front.*, 2017, **4**, 2422.
- [123] T. H. Meng, Y. Zhou, Z. Z. Gao, Q. Y. Liu, Z. Tao, X. Xiao, A study of the inclusion of 1-hexyl-4-(4-pyridyl)pyridinium bromide in cucurbit[6]uril, *J. Incl. Phenom. Macrocycl. Chem.*, 2018, **90**, 357.
- [124] D. Bai, Z. Gao, Z. Tao, X. Xiao, T. J. Prior, G. Wei, Q. Liu, C. Redshaw, A study of the interaction between inverted cucurbit[6]uril and symmetric viologens, *New J. Chem.*, 2018, **42**, 11085.
- [125] D. W. Zhang, H. Wang, Z. T. Li, Porous organic frameworks for drug delivery, *Polym. Bull.*, 2018, **6**, 243.
- [126] J. Tian, L. Zhang, H. Wang, D. W. Zhang, Z. T. Li, Supramolecular polymers and networks driven by cucurbit[8]uril-guest pair encapsulation in water, *Supramol. Chem.*, 2016, **28**, 769.
- [127] H. Wang, D. W. Zhang, X. Zhao, Z. T. Li, Supramolecular organic frameworks (SOFs): water-phase periodic porous self-assembled architectures, *Acta Chim. Sinica*, 2015, **73**, 471.
- [128] L. Chen, Y. C. Zhang, W. K. Wang, J. Tian, L. Zhang, H. Wang, D. W. Zhang, Z. T. Li, Conjugated radical cation dimerization-driven generation of supramolecular architectures, *Chinese Chem. Lett.*, 2015, **26**, 811.

- [129] B. Yang, S. B. Yu, H. Wang, D. W. Zhang, Z. T. Li, 2:2 complexes from diphenylpyridiniums and cucurbit[8]uril: encapsulation-promoted dimerization of electrostatically repulsing pyridiniums, *Chem. Asian J.*, 2018, **13**, 1312.
- [130] X. Xiao, J. S. Sun, J. Z. Jiang, X-ray Structure of a Porphyrin–Tetramethylcucurbit[6]uril Supramolecular Polymer, *Chem. Eur. J.*, 2013, **19**, 16891.
- [131] M. Pfeiffermann, R. Dong, R. Graf, W. Zajaczkowski, T. Gorelik, W. Pisula, A. Narita, K. Müllen, X. Feng, Free-Standing Monolayer Two-Dimensional Supramolecular Organic Framework with Good Internal Order, *J. Am. Chem. Soc.*, 2015, **137**, 14525.
- [132] S. Q. Xu, X. Zhang, C. B. Nie, Z. F. Pang, X. N. Xu, X. Zhao, The construction of a two-dimensional supramolecular organic framework with parallelogram pores and stepwise fluorescence enhancement, *Chem. Commun.*, 2015, **51**, 16417.
- [133] Y. Zhang, T. G. Zhan, T. Y. Zhou, Q. Y. Qi, X. N. Xu, X. Zhao, Fluorescence enhancement through the formation of a single-layer two-dimensional supramolecular organic framework and its application in highly selective recognition of picric acid, *Chem. Commun.*, 2016, **52**, 7588.
- [134] L. Wang, Z. Sun, M. Ye, Y. Shao, L. Fang, X. Liu, Fabrication of a cross-linked supramolecular polymer on the basis of cucurbit[8]uril-based host–guest recognition with tunable AIE behaviors, *Polym. Chem.*, 2016, **7**, 3669.
- [135] Z. Gao, J. Zhang, N. Sun, Huang, Z. Tao, X. Xiao, J. Jiang, Hyperbranched supramolecular polymer constructed from twisted cucurbit[14]uril and porphyrin via host-guest interactions, *Org. Chem. Front.*, 2016, **3**, 1144.
- [136] X. Xiao, W. Li, J. Jiang, Porphyrin-cucurbituril organic molecular porous material: Structure and iodine adsorption properties, *Inorg. Chem. Commun.*, 2013, **35**, 156.
- [137] X. Jiang, X. Yao, X. Huang, Q. Wang, H. Tian, A cucurbit[5]uril analogue from dimethylpropanediurea–formaldehyde condensation, *Chem. Commun.*, 2015, **51**, 2890.

- [138] O. Danylyuk, H. Butkiewicz, V. Sashuk, Host–guest complexes of cucurbit[6]uril with the trypanocide drug diminazene and its degradation product 4-aminobenzamidine, *CrystEngComm*, 2016, **18**, 4905.
- [139] Z. Qian, T. Yuan, Q. Wang, Supramolecular hexagonal network based on a tritopic amine hydrochloride and a cucurbit[5]uril analogue, *Res. Chem. Intermed.*, 2018, **44**, 6445.
- [140] Y. Wu, H. Hua, Q. Wang, A CB[5] analogue based supramolecular polymer with AIE behaviors, *New J. Chem.*, 2018, **42**, 8320.
- [141] D. Whang, K. Kim, Polycatenated Two-Dimensional Polyrotaxane Net, Use of Silver(I) and Copper (II) Ions to Assist the Self-Assembly of Polyrotaxanes Incorporating Symmetrical $\alpha,\alpha'\delta,\delta'$ -Tetramethyl-cucurbit[6]uril, *J. Am. Chem. Soc.*, 1997, **119**, 451.
- [142] J. P. Zeng, S. M. Zhang, Y. Q. Zhang, Z. Tao, Q. J. Zhu, S. F. Xue, G. Wei, A Novel Strategy to Assemble Achiral Ligands to Chiral Helical Polyrotaxane Structures, *Cryst. Growth Des.*, 2010, **10**, 4511.
- [143] J. P. Zeng, H. Cong, K. Chen, S. F. Xue, Y. Q. Zhang, Q. J. Zhu, J. X. Liu, Z. Tao, A Novel Strategy to Assemble Achiral Ligands to Chiral Helical Polyrotaxane Structures, *Inorg. Chem.*, 2011, **50**, 6521.
- [144] X. Wei, J. P. Zeng, H. Cong, Y. Q. Zhang, Z. Tao, Q. J. Zhu, S. F. Xue, Synthesis of supramolecular polyrotaxanes assemblies incorporating symmetrical $\alpha,\alpha'\delta,\delta'$ -tetramethyl-cucurbit[6]uril moieties using polychloride zinc(II) and cadmium(II) anions, *Supramol. Chem.*, 2014, **26**, 692.
- [145] L. Mei, Q. Y. Wu, C. M. Liu, Y. L. Zhao, Z. F. Chai, W. Q. Shi, The first case of an actinide polyrotaxane incorporating cucurbituril: a unique ‘dragon-like’ twist induced by a specific coordination pattern of uranium, *Chem. Commun.*, 2014, **50**, 3612.
- [146] L. Mei, L. Wu, C. M. Liu, Y. L. Zhao, Z. F. Chai, W. Q. Shi, Tetranuclear Uranyl Polyrotaxanes: Preferred Selectivity toward Uranyl Tetramer for Stabilizing a Flexible

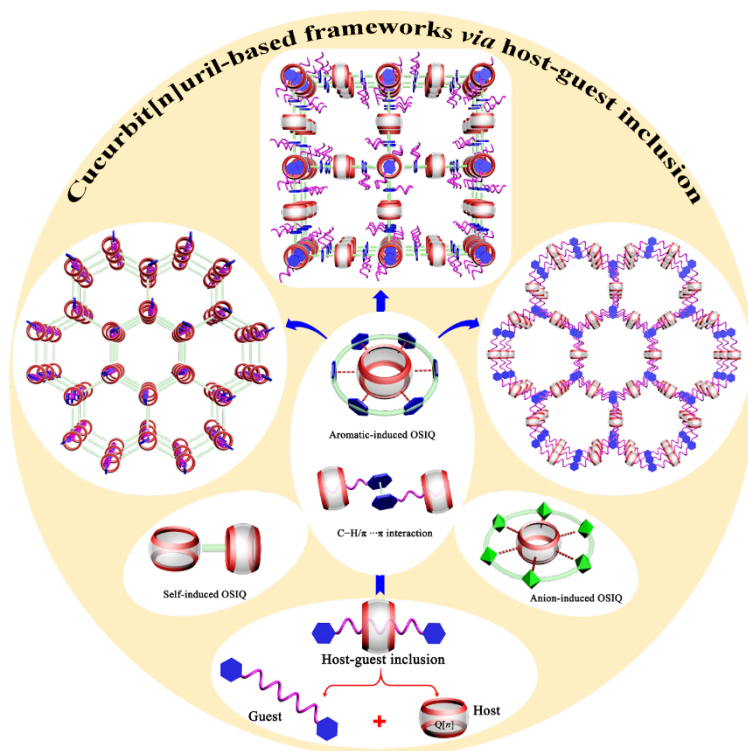
- Polyrotaxane Chain Exhibiting Weakened Supramolecular Inclusion, *Chem. Eur. J.* 2015, **21**, 10226.
- [147] L. Mei, L. Wu, L. Y. Yuan, S. W. An, Y. L. Zhao, Z. F. Chai, P. C. Burns, W. Q. Shi, Supramolecular inclusion-based molecular integral rigidity: a feasible strategy for controlling the structural connectivity of uranyl polyrotaxane networks, *Chem. Commun.*, 2015, **51**, 11990.
- [148] Z. N. Xie, L. Mei, K. Q. Hu, L. S. Xia, Z. F. Chai, W. Q. Shi, Mixed-Ligand Uranyl Polyrotaxanes Incorporating a Sulfate/Oxalate Coligand: Achieving Structural Diversity via pH-Dependent Competitive Effect, *Inorg. Chem.*, 2017, **56**, 3227.
- [149] Y. C. Ge, L. Mei, F. Z. Li, K. Q. Hu, C. Q. Xia, Z. F. Chai, W. Q. Shi, Template-Driven Assembly of Rare Hexameric Uranyl-Organic Rotaxane Networks Threaded on Dimeric Uranyl Chains, *Cryst. Growth Des.*, 2018, **18**, 3073.
- [150] F. Z. Li, L. Mei, K. Q. Hu, J. P. Yu, S. W. An, K. Liu, Z. F. Chai, N. Liu, W. Q. Shi, Releasing Metal-Coordination Capacity of Cucurbit[6]uril Macrocycle in Pseudorotaxane Ligands for the Construction of Interwoven Uranyl-Rotaxane Coordination Polymers, *Inorg. Chem.*, 2018, **57**, 13513-13523.
- [151] K. Kim, Mechanically interlocked molecules incorporating cucurbituril and their supramolecular assemblies, *Chem. Soc. Rev.*, 2002, **31**, 96.
- [152] E. Lee, J. Heo, K. Kim, A three-dimensional polyrotaxane network, *Angew. Chem. Int. Ed.*, 2000, **39**, 2699.
- [153] E. Lee, J. Kim, J. Heo, D. Whang, K. Kim, A Two-Dimensional Polyrotaxane with Large Cavities and Channels: A Novel Approach to Metal-Organic Open-Frameworks by Using Supramolecular Building Blocks, *Angew. Chem. Int. Ed.*, 2001, **40**, 399.
- [154] L. Mei, C. Xu, Q. Y. Wu, K. Q. Hu, L. Y. Yuan, J. Chen, C. L. Xiao, S. A. Wang, Z. F. Chai, W. Q. Shi, A neptunium(v)-mediated interwoven transuranium-rotaxane network

- incorporating a mechanically interlocked [c2]daisy chain unit, *Chem. Commun.*, 2018, **54**, 8645.
- [155] J. Liang, X. S. Wu, X. L. Wang, C. Qin, K. Z. Shao, Z. M. Su, R. Cao, Syntheses, crystal structures and properties of metal–organic rotaxane frameworks with cucurbit[6]uril, *CrystEngComm*, 2016, **18**, 2327.
- [156] X. S. Wu, X. L. Wang, F. L. Zhu, H. F. Bao, C. Qin, Z. M. Su, Guest exchange in a porous cucurbit[6]uril-based metal–organic rotaxane framework probed by NMR and X-ray crystallography, *Chem. Commun.*, 2018, **54**, 5474.
- [157] R. Tejero, D. Lopez, F. Lopez-Fabal, J. L. Gomez-Garces, M. Fernandez-Garcia, Antimicrobial polymethacrylates based on quaternized 1, 3-thiazole and 1, 2, 3-triazole side-chain groups, *Polym. Chem.*, 2015, **6**, 3449-3459.
- [158] L. D. de Melo Carrasco, J. L. M. Sampaio, A. M. Carmona-Ribeiro, Supramolecular Cationic Assemblies against Multidrug-Resistant Microorganisms: Activity and Mechanism of Action, *Int. J. Mol. Sci.*, 2015, **16**, 6337-6352.
- [159] K. I. Assaf, W. M. Nau, Cucurbiturils: from synthesis to high-affinity binding and catalysis, *Chem. Soc. Rev.*, 2015, **44**, 394.
- [160] S. J. Barrow, S. Kasera, M. J. Rowland, J. D. Barrio, O. A. Scherman, Cucurbituril-Based Molecular Recognition, *Chem. Rev.*, 2015, **115**, 12320.

TOC

Construction of cucurbit[*n*]uril-based supramolecular frameworks via host-guest inclusion and functional properties thereof

Kai Chen*, Zi-Yi Hua, Jiang-Lin Zhao*, Carl Redshaw, and Zhu Tao*



In this review, some useful ideas and strategies are presented on how to construct guest@Q[*n*]-based supramolecular frameworks, including the different uses of these guest@Q[*n*]-based supramolecular frameworks, and also their relationship to other supramolecular building blocks, such as polyoxometalates, calixarenes or pillararenes as well as other macrocyclic compounds.